Telomerase and Cellular Aging: Analysis of Telomerase RNA Structure and the Impact of Telomerase on miRNA Expression

Laura Naomi Bonifacio, PharmD

A dissertation submitted to the faculty of the University of North Carolina at Chapel Hill in partial fulfillment of the requirements for the degree of Doctor of Philosophy in the Department of Pharmaceutical Sciences (Medicinal Chemistry and Natural Products).

Chapel Hill
2010

Approved by: Michael B. Jarstfer, PhD

David Lawrence, PhD

Shawn Ahmed, PhD

Ken Bastow, PhD

Stuart Maxwell, PhD

Abstract

Laura Bonifacio, PharmD

Telomerase and Cellular Aging: Analysis of Telomerase RNA Structure and the Impact of Telomerase on miRNA Expression

(Under the direction of Michael B. Jarstfer, PhD)

Human cellular mortality is exquisitely regulated in order to prevent both premature loss of cellular replicative potential, which can lead to complications of aging, and the aberrant immortalization of somatic cells, which is associated with tumorigenesis. Human somatic cells experience a finite term of replication, measured in part by telomere attrition. As human somatic cells divide, their telomeres erode due to the end replication problem. When telomeres become critically short, cells enter an irreversible growth arrest called senescence, marked by accumulation of inflammatory mediators, which ultimately cause cell death. Occasionally, cells bypass senescence and continue dividing despite having critically short telomeres. These cells will encounter a second growth arrest check point called crisis, characterized by robust inflammation and profuse cell death. Rarely, cells evade the impetus to stop dividing imposed by senescence and crisis by activating telomerase and becoming immortalized.

Telomerase is a ribonucleoprotein reverse transcriptase, minimally comprised of an RNA subunit, TR, and a catalytic protein subunit, TERT. Cells expressing high levels of telomerase (such as germline and embryonic stem

cells) are immortal. In addition, telomerase is activated in and conveys immortality to about 90% of all cancer cells. The most well understood contribution of telomerase to determining cellular mortality is its role in maintaining/extending telomeres, which offsets induction of replicative senescence.

Despite significant advances in senescence and telomerase biology, a complete understanding of the mechanisms regulating senescence and the mechanisms by which telomerase influences cellular mortality is still lacking. Work presented in this dissertation will provide the first evidence confirming a dramatic conformational change within Tetrahymena telomerase RNA (tTR) upon assembly into the telomerase complex that is essential to facilitating telomerase activity. In addition, work described in Chapter 3 provides the first full microRNA profile for replicatively senescent human foreskin fibroblasts. Finally, experiments described in Chapter 4 demonstrate the ability of telomerase to influence expression of miRNAs that undergo regulated expression during senescence and thereby influence a cell's ability to proliferate. A thorough understanding of these miRNA-regulated senescence pathways, and the mechanisms by which telomerase influences these pathways, will facilitate new approaches to treat aging-related disorders and cancer.

Acknowledgements

I have been extremely blessed in my life to receive the opportunities and encouragement that have bolstered by educational aspirations of earning a PharmD and PhD in Medicinal Chemistry. In acknowledging that this educational path has been a long one, I am so thankful to my mother, the strongest person I know, for instilling in me the determination and strength that are requisite for such arduous pursuits. I appreciate the unwavering support and encouragement she has always provided, as evidenced by her belief that in terms of careers, I could do anything I wanted to do. This unearned, but priceless faith in my abilities was my rock of support when this journey seemed long and I could not see the end.

I would also like to thank my husband, Alberto, for not only being patient and supportive, but actually encouraging me to pursue this lengthy education. I believe this educational path required not only significant input from me, but also the pliability of those I love. I can't say how much it means to me that he never pushed me to come home earlier when I needed to work late in the lab, and he never brought to my attention that I was contributing only a student's salary to our household (except in joking). I am so thankful to have this man as my teammate and partner in crime.

Finally, I would like to thank my boss, Michael Jarstfer, for fostering my independence as a scientist and critical thinker. Dr. Jarster has been and continues to be an inspiration to me as a scientist with an incisive mind. I believe that the primary role of graduate school is to teach grad students how to think on a higher level about research. In this respect, Mike has been my role model for the last 8 years. I have so much respect for him as a scientist, academic, and PI, and I hope to successfully employ in my career the lessons I have learned by working with and for him. Over the years, I have grown to consider Mike not just as a boss, but also a friend. I will never forget his support during rough times, both in the lab and personally. I am so thankful for the experience of being a graduate student in Dr. Jarstfer's lab, and I consider these years extremely valuable.

Table of Contents

Contents

List of Tables

List of Figures

List of Abbreviations

AML	acute myelogenous leukemia
ATM	Ataxia telangiectasia mutated kinase
BSA	bovine serum albumin
CDC6	Cell division cycle 6 protein
CDK	Cyclin dependent kinase
CTE	C-terminal extension
DC	Dyskeratosis congenita
ddT	dideoxythymidine
DKC1	Dyskerin gene
DMSO	dimethyl sulfoxide
DNA	deoxyribonucleic acid
DTT	dithiothreitol
EtOH	ethanol
hTERT	human telomerase reverse transcriptase subunit
hTR	human telomerase RNA subunit
miRNA	microRNA
MRE	miRNA recognition element
mRNA	messenger RNA
MS1	tTR mutant I
MS1-2	tTR compensatory mutant
MS2	tTR mutant II

NMIA	*N*-methyl isatoic anhydride
NMR	nuclear magnetic resonance
NT	nucleotide
PAGE	polyacrylamide gel electrophoresis
PBS	phosphate-buffered saline
PCGT	Targets of polycomb group proteins
PCR	polymerase chain reaction
Rb	retinoblastoma protein
RNA	ribonucleic acid
RNP	ribonucleoprotein
ROS	reactive oxygen species
RRL	rabbit reticulocyte lysate
RT	reverse transcriptase
RT-PCR	real time PCR
SA β-gal	senescence associated beta-galactosidase
SASP	senescence-associated secretory phenotype
SHAPE	selective 2’-hydroxyl acylation analyzed by primer extension
SRB	sulforhodamine B
TE	tris-EDTA
TEN	N-terminal extension
TRBD	telomerase RNA binding domain
UTR	untranslated region
WT	wild type

Chapter 1. Introduction

In 1965 Leonard Hayflick discovered that human fibroblasts have a finite ability to divide, due in part to the process of senescence [1]. As somatic cells divide, long G-rich repeats at the 3' terminus of chromosomes called telomeres shorten due to the end replication problem [2] and the absence of telomerase. At some point when the telomeres become "critically short," the cells become senescent, characterized by an irreversible loss of proliferative capacity despite continued metabolic activity. Senescent cells experience a profound up-regulation of inflammatory signaling, and the accumulation of these inflammatory mediators eventually contributes to the death of senescent cells. Occasionally, a cell may bypass senescence by abrogating p53 and continue to divide despite having critically short telomeres. In this case, cells will encounter a second checkpoint called M2, or Crisis. Crisis is characterized by massive cell death and inflammation. Activation (or reactivation) of telomerase allows cells to bypass crisis and become immortal (Figure 1.1).

Clearly, expression of the ribonucleoprotein telomerase is a critical indicator in determining whether a cell is susceptible to senescence. While the RNA component of the telomerase (hTR) is expressed ubiquitously in humans, the catalytic protein reverse transcriptase subunit of telomerase (hTERT) is not expressed in somatic cells. Human embryonic stem cells and germline cells

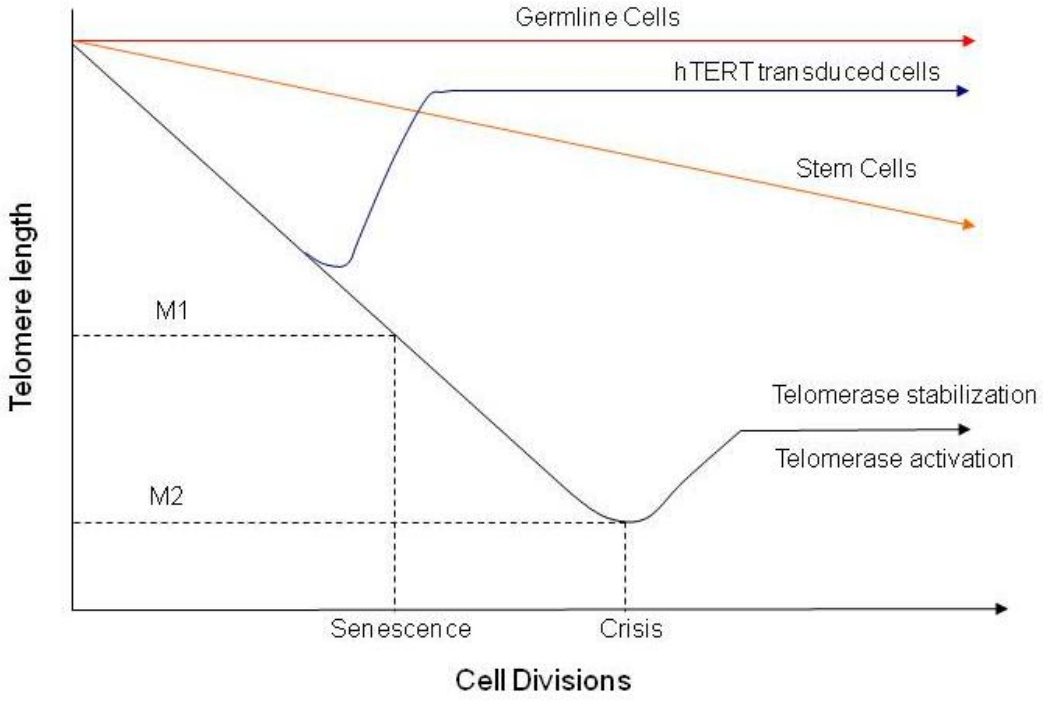

Figure 1.1 Hayflick Limit. In the absence of telomerase expression, telomere length decreases with increased cell divisions. Adapted from Hayflick [1].

express TERT and are therefore able to maintain their telomere lengths throughout indefinite proliferation and without senescing. Tissue stem cells, also known as progenitor cells, reside within post-mitotic tissues and function to replenish cells that have undergone stress and damage associated with aging. While progenitor cells do express telomerase, they express it at lower levels compared to germline cells and are thus susceptible to senescence.

Senescence in stem cells is thought to contribute to the age-associated decline in organ and tissue function because the ability of tissue stem cells to proliferate and replenish lost cells is diminished with age [3]. Since replicative senescence is critically associated with telomere length and expression of

telomerase, accurate and precise information regarding telomere biology and the structural biology of telomerase as well as pathways involved in conveying senescence is fundamental to understanding regulation of senescence. Further, a more detailed knowledge of senescence mechanisms and associated biology will facilitate an informed appreciation of the contribution of senescence to aging and tumorigenesis.

I. Telomeres, Telomerase, and Replicative Senescence

A. Telomere Biology

1. DNA Replication and Telomere Function

The replication of human chromosomes is accomplished by DNA polymerase and occurs in a 5' to 3' manner. Each strand of the double stranded parent DNA chromosome is replicated, beginning at the origin of a replication fork and proceeding to chromosome termini. One strand, known as the leading strand, is replicated in a continuous manner in the 5' to 3' direction. Due to the requirement of DNA polymerase to bind at sites with a 3'-OH, synthesis of the opposite strand, known as the lagging strand, requires the aid of RNA primers. DNA polymerase binds the RNA primer and synthesizes short DNA segments known as Okazaki fragments. When synthesis is complete, the RNA primers are removed and DNA polymerase fills in the gaps. After the terminal RNA primer is removed on the lagging strand, DNA polymerase is incapable of binding to fill in

the gap left by removal of the primer. This is commonly referred to as the end-replication problem. Without a mechanism to circumvent this problem, the 3'-end of the lagging strand would shorten with each round of replication (Figure 1.2a). As a solution to this problem, telomeres mask the ends of chromosomes and undergo attrition with each round of replication. In this way telomeres prevent loss of genomic sequences during cell proliferation and prevent recognition of chromosomal termini by DNA repair machinery. Although theoretically the chromosome generated by synthesis of the leading strand should be blunt ended, replication of each strand of the chromosome generates a new dsDNA chromosome with 3' overhangs. There is some evidence to suggest that leading strand replication incorporates a mechanism for generating a short 3' overhang, possibly by utilization of exonucleases that facilitate recognition and processing by the reverse transcriptase known as telomerase and DNA polymerase (Figure 1.2b) [4,5].

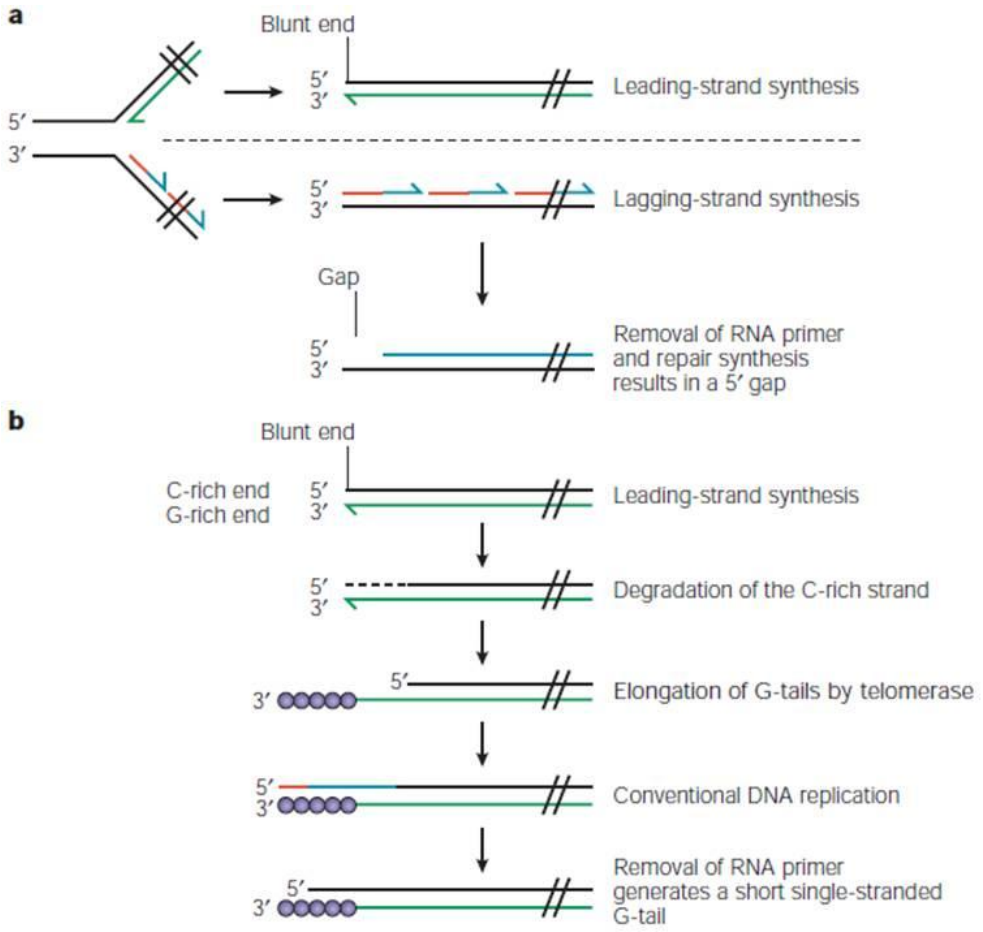

Figure 1.2 End Replication Problem. Telomeres prevent loss of coding DNA with each round of replication due to the end replication problem [6]. DNA polymerase is incapable of fully replicating the 3' end of chromosomes due to the lack of an RNA primer required for the polymerase to bind (a). The ribonucleoprotein telomerase extends G-rich repeats at chromosome termini, facilitating DNA polymerase-mediated extension of these non-coding repeats (b).

2. Telomere Structure

Telomeres are synthesized by the ribonucleoprotein telomerase, a reverse transcriptase minimally comprised of an RNA subunit (TR) and a catalytic protein subunit (TERT). Human telomeres contain approximately 5 – 15 kilo base pairs

of T_2AG_3 repeats [6]. However, the presence of long repeats on chromosome termini alone is insufficient to prevent recognition of the uncapped end by DNA repair mechanisms and induction of senescence or apoptosis [7]. So the chromosome protective function conveyed by telomeres is two-fold: Long, repetitive telomeric sequences provide an alternative for chromosome shortening with each round of DNA replication, and the telomere prevents recognition by DNA repair machinery and induction of senescence/apoptosis in a separate manner. The ability of the telomere to inhibit recognition by DNA repair machinery is integrally connected to the ability of the telomere to form complex structures by binding to several dsDNA binding proteins. This telomeric complex, also known as the "shelterin" complex, is essential in driving the cell's ability to differentiate chromosome ends from dsDNA breaks [8]. In human cells, shelterin includes several proteins that serve to facilitate formation of a T-loop from the telomeric single stranded 3'-overhang [9] (Figure 1.3b).

While a comparison between cells, individuals, and chromosomes reveals that telomeres are somewhat heterogeneous in length, telomeres are maintained within an average range of base pairs with remarkable consistency within species. This homeostasis implies a mechanism that senses telomere length and communicates with telomerase to activate it when telomeric repeat addition is appropriate and prevent it from overextending long telomeres. Several components of shelterin are essential in maintaining this telomere length homeostasis. TRF1, a double stranded telomeric DNA binding protein and shelterin member, inhibits telomerase *in cis* at individual telomeres [10]. TRF1

over-expression allows telomere attrition while expression of a TRF1 dominant negative mutant results in telomere elongation [10].

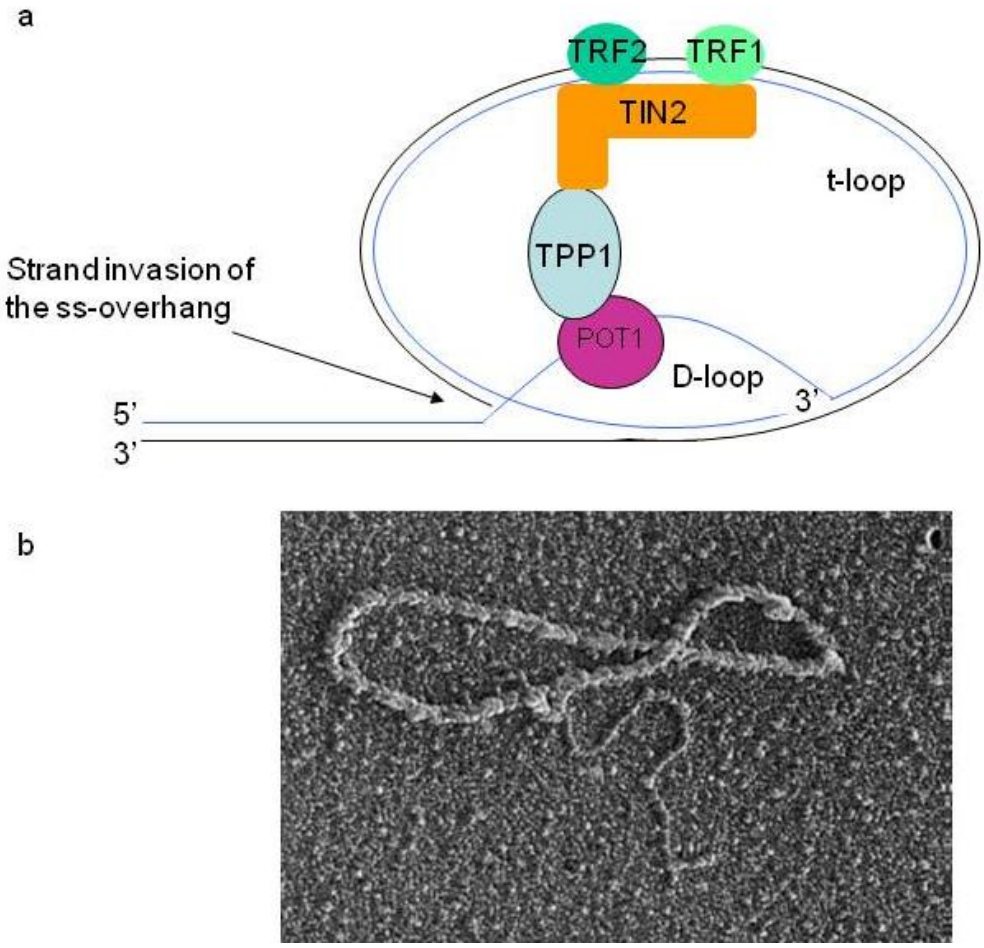

Figure 1.3 Human telomeric DNA requires binding to shelterin proteins to form a T-loop. Formation of a T-loop (A) by binding to shelterin complex proteins prevents recognition of the chromosome termini by cellular DNA repair machinery. B) Electron microscopy of telomeric DNA from HELA cells [9].

In addition, both POT1 and Rap1 have been shown to inhibit telomerase activity by obstructing access of the enzyme to the single-stranded region of the telomeric 3' end and recruitment of co-inhibitory factors, respectively [11,12,13]. Thus telomere structure and maintenance as well as telomerase expression are critical in determining a cell's susceptibility to senescence.

B. Clinical Consequences of Aberrant Telomerase/Telomere Regulation

A number of diseases have been linked to aberrant regulation of telomere maintenance and telomerase activity, and not surprisingly, most of these diseases are characterized by premature aging phenotypes. Dyskeratosis congenita, Werner's syndrome, and congenital aplastic anemia (AA) are all associated with deregulated telomere maintenance or telomerase activity [14] (Figure 1.4). Dyskeratosis congenita (DC) can be caused by a mutation within one of six genes. Four of these genes encode proteins associated with maintaining telomere structure and two encode telomerase subunits [15]. Patients with DC are at increased risk for malignancies, display a number of mucocutaneous abnormalities, and frequently suffer from aplastic anemia during childhood. DC was originally discovered by linking physical symptoms of the affected patients to a mutation in the dyskerin (DKC1) gene [16,17]. DKC1 encodes a protein that is part of the human telomerase holoenzyme complex. Werner syndrome is caused by a mutation in WRN (encoding a helicase), resulting in an increased rate of telomere attrition uncountered by telomerase activity. Patients with Werner syndrome display adult-onset progeroid phenotypes, aging several decades beyond their actual age [18].

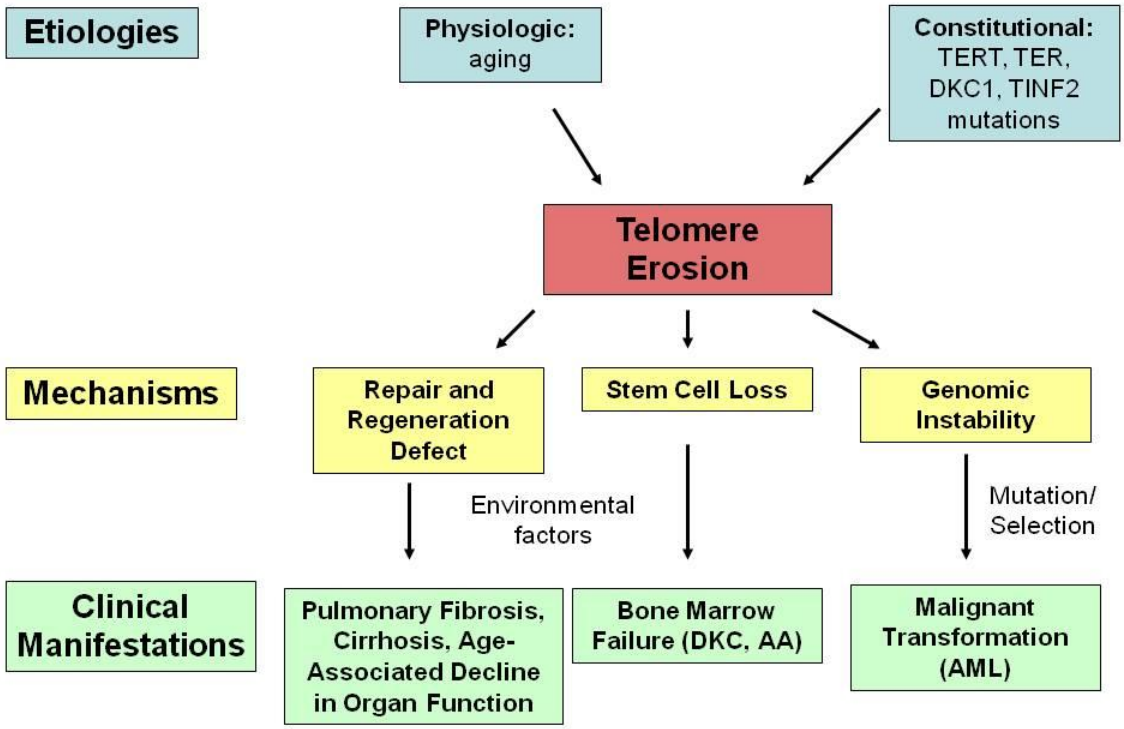

Figure 1.4 Telomere diseases. Deregulation of telomere homeostasis contributes to a number of diseases associated with progeroid phenotypes, including dyskeratosis congenita and Werner's syndrome. Figure adapted from Calado et al [14].

The genetic basis for the influence of telomere and telomerase deregulation in development of cancer is based partly on the induction of DNA repair mechanisms and resultant chromosomal instability caused by non-homologous end-joining or homology-directed repair [19,20]. For instance, evidence in humans reveals that constitutive telomerase mutations result in excessive telomere erosion and chromosome instability in patients with acute

myelogenous leukemia (AML) [21]. This deregulation of telomere homeostasis is a pre-crisis event and presumably contributes to transformation. Finally, a number of non-hematologic diseases have been associated with mutations in the telomerase/telomere pathway, including pulmonary and hepatic fibrosis, although the data for these associations is less extensive [22].

C. Telomerase Structural Biology

Telomerase is a ribonucleoprotein composed of two main subunits, an RNA subunit that serves as template for the synthesis of telomeres (TR) and a protein subunit that contains the catalytic reverse transcriptase activity (TERT). While TERT is highly conserved, sequence and length of TR vary considerably among species [23,24]. The following will provide an overview of TERT and TR structural biology and highlight the challenges impeding a detailed understanding of the impact of TR structure on telomerase activity. A complete understanding of the contribution of TR structure to telomerase activity would facilitate attempts at modulating telomerase activity for anti-tumor and anti-aging drug development.

1. TERT

A comparative sequence analysis of TERT reveals the presence of seven conserved amino acid motifs that have similarity to retroviral reverse transcriptases [25]. In addition, TERT genes contain telomerase-specific regions, such as the N-terminal extension (TEN) and C-terminal extension (CTE) (Figure 1.5a) [26]. The CTE region contains domains that are highly conserved

among vertebrates. In general, the N-terminal and RT domains are involved in RNA binding, while the N and C-terminal parts are involved in DNA binding.

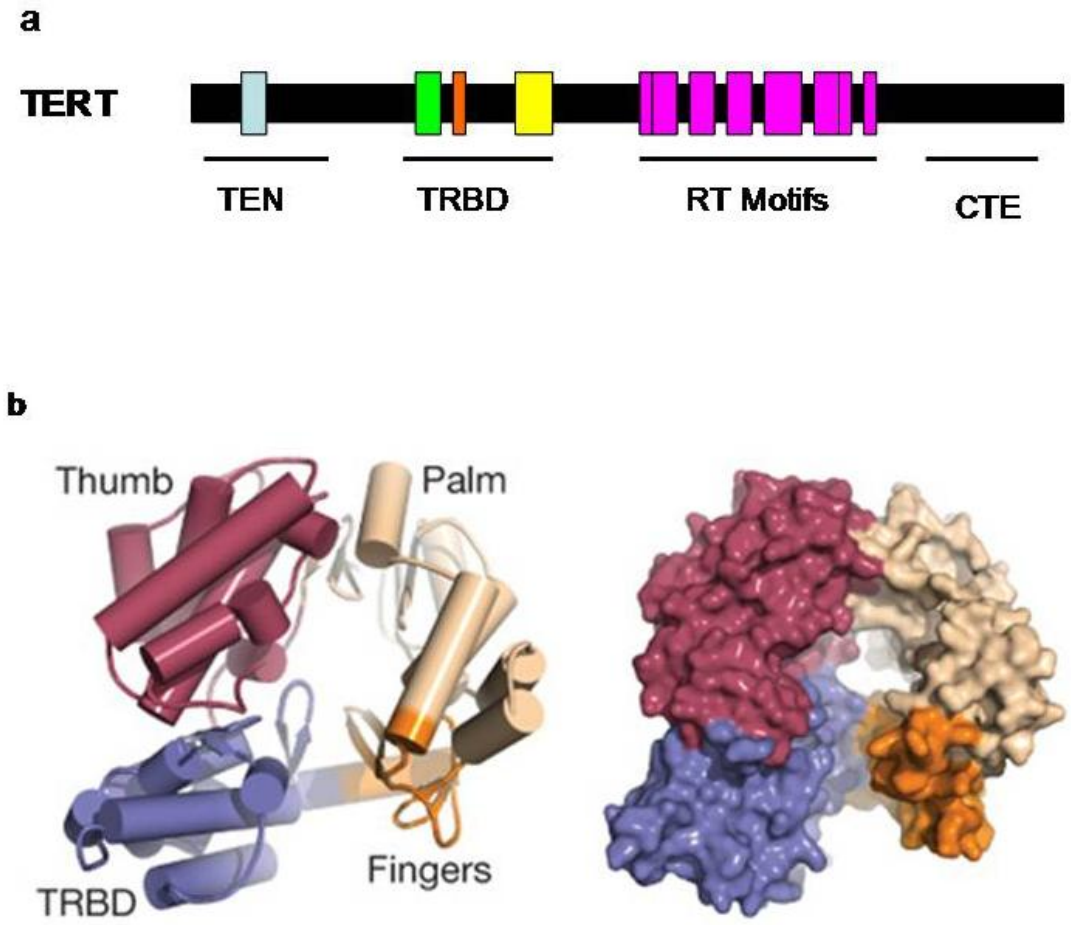

Figure 1.5 Structure of TERT. TERT genes contain seven amino acid motifs that share similarity with retroviral reverse transcriptases (RT). In addition, TERT genes display telomerase-specific motifs, denoted as CTE (C-terminal extension), N terminal-extension (TEN) and a telomerase RNA binding domain (TRBD) (a). Adapted from Sykorova et al [26]. TERT proteins contain a "fingers, palm, and thumb" structure common to other polymerases. Figure from Gillis et al [27] (b).

TERT proteins adopt a conformation referred to as the “fingers, palm, and thumb” structure found in other polymerases (Figure 1.5b). This structural feature is important for type I (nucleotide addition) processivity [28,29]. Type II processivity is specific to telomerase and requires translocation of telomerase for repeat addition of telomeric sequences. Telomerase type II processivity is influenced by two telomerase-specific structural elements, a long insertion within the putative fingers doman (IFD, insertion within fingers domain) and a telomerase-specific domain within the N-terminal extension region [30].

2. TR

Despite the fact that TR genes show very little sequence or length conservation between species, most TRs do share several secondary structural features, based on secondary structure predictions using phylogenetic comparison of sequences and the limited structural information for a few TR domains. This implies an essential role for TR structure in regulating activity of telomerase [31]. A phylogenetic comparison of predicted secondary structures for ciliate and human TRs is shown below (Figure 1.6). Common secondary structural features conserved between human and Tetrahymena TRs (hTR and tTR, respectively) include stem loop IV (also known as the transactivating domain), stem loop II (the template boundary element), and a pseudoknot structure predicted for stem loop III [31].

The focus here will be on analyzing current structural information for tTR, as Tetrahymena thermophila has emerged as a model organism for studying

telomerase. An accurate knowledge of tTR structure will expedite a complete understanding of the contribution of telomerase RNA structure to telomerase activity.

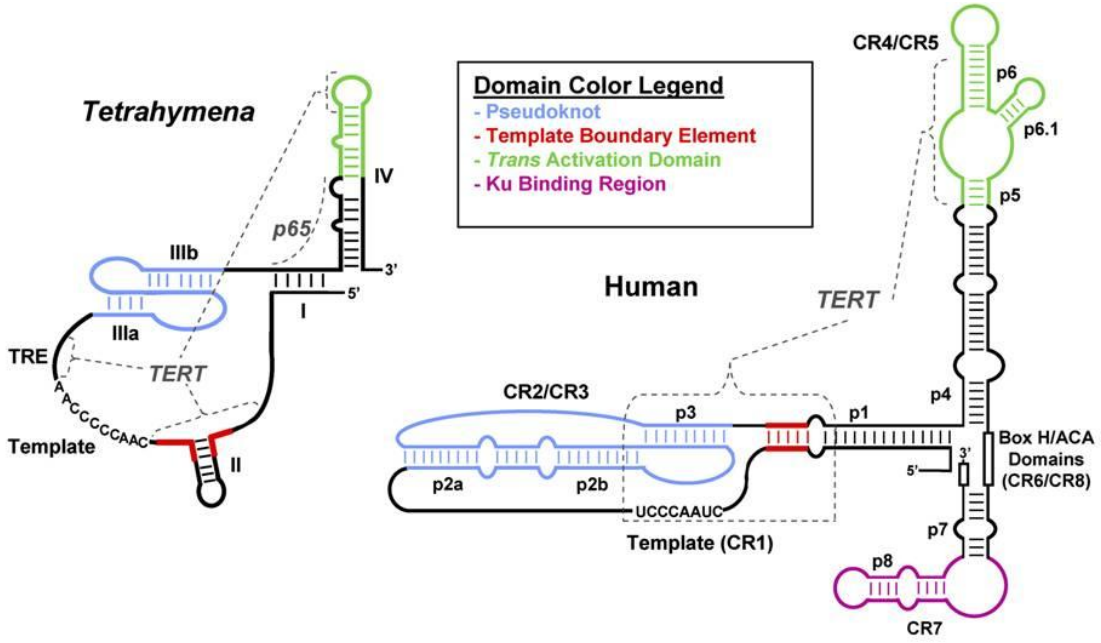

Figure 1.6 Secondary structure models for telomerase RNA. Models for ciliate (Tetrahymena thermophila) and human TR secondary structure are shown. Figure adapted from Chen et al [32].

The size of TR (159 nucleotides for tTR, 451 nt for hTR) presents a formidable barrier to obtaining direct structural evidence for these RNAs via conventional methods. However, the structure of stem II and stem IV of tTR have been solved by NMR [33,34,35] (Figure 1.7). Importantly, the structural information revealed by these NMR studies is in agreement with biochemical studies for these domains [36,37,38]. Biochemical studies reveal that stem loop

II is essential for proper definition of the template boundary, while the distal portion of stem II seems dispensable for telomerase function [39]. Stem loop IV is suggested to be involved in proper pseudoknot formation, telomerase processivity, and TERT binding [36,40,41].

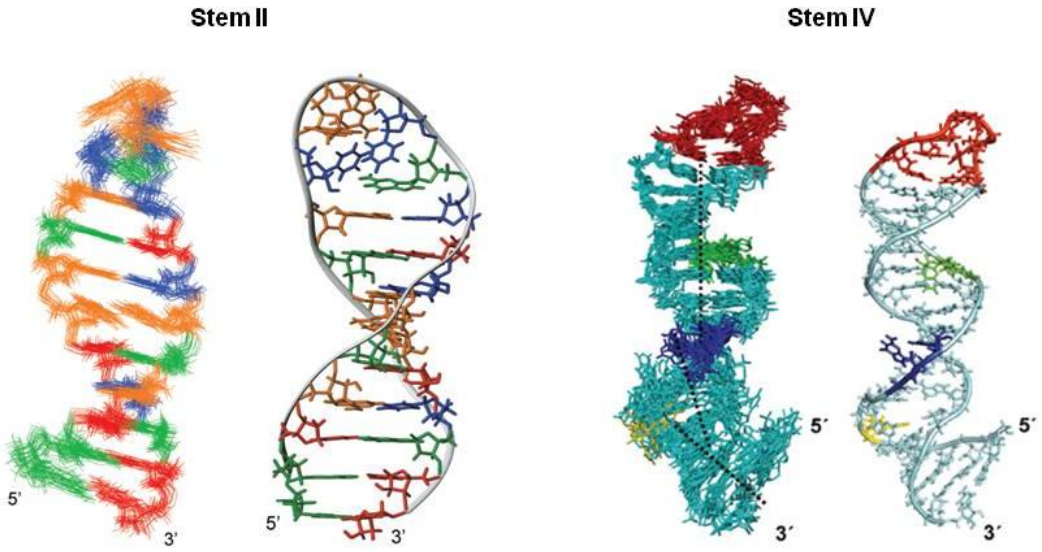

Figure 1.7 tTR Stem II and Stem IV NMR structures. The structures of stem II and IV of tTR have been solved by NMR. Figure adapted from Chen et al and Richards et al [34,35].

Current understanding of the relationship between structure and function of the pseudoknot region of TR is less complete, as construction of an accurate model for the pseudoknot structure has been challenging. AUU base triples are a conserved feature present within the predicted structures of the TR pseudoknot from various species [42,43]. While the in-solution human pseudoknot structure has been resolved by NMR, [43,44] the only evidence contributing to the current

model of tTR is biochemical and phylogenetic in nature. Further, there is no direct evidence of TR structure within in the telomerase complex for either organism. A novel model for tTR secondary structure, based on biochemical evidence generated using a relatively new RNA structure analysis technique (unpublished data, Legassie, Bonifacio, and Jarstfer), predicts dramatic changes in domain III as tTR is assembled into the telomerase complex (Figure 1.8). This model will be validated by studies described in Chapter 2.

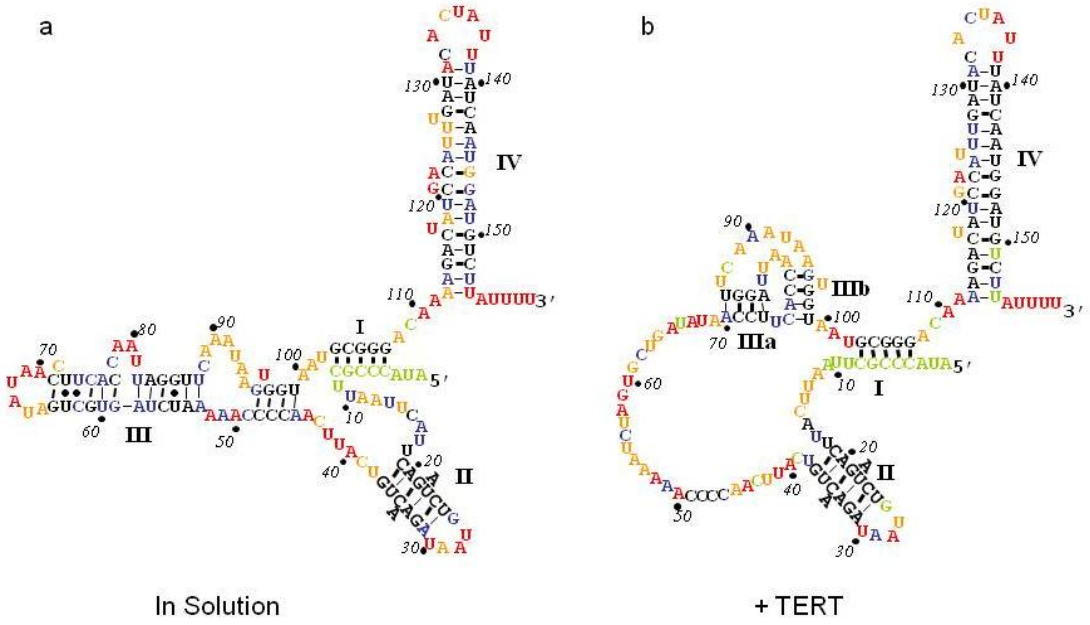

Figure 1.8 Novel Model for tTR Secondary Structure. These models for tTR secondary structure are based on data using a new RNA structure analysis technique (Legassie, Bonifacio, Jarstfer, unpublished work). This new model differs from the currently accepted model for tTR secondary structure by predicting a conformational change in domain III of tTR upon assembly into the telomerase complex. The models are depicted in a color scheme indicating flexibility of each nucleotide, as revealed by the RNA structure analysis experiments. Most to least flexible is indicated by red, orange, blue, and black. Green indicates lack of sufficient data for those nucleotides.

II. The Contribution of Senescence to Aging and Tumorigenesis

Aging is a multietiological phenomenon that occurs at both cellular and organismal levels, and the extent to which factors affecting cellular aging contribute to organismal aging remains unclear. Several theories of aging exist, but can basically be classified into two groups attributing aging to either extrinsic (environmental exposure related) or intrinsic (programmed genetic changes) factors. An emerging consensus view supports a combination of both extrinsic and intrinsic contributors as relevant to organismal aging; however the extent to which specific factors from each pathway contribute to aging is still debated. A brief summary of two of the major contributors from the extrinsic and intrinsic pathways of aging follows in order to facilitate a better appreciation for how senescence might complement these pathways (Figure 1.9).

Reactive oxygen species (ROS), stemming from extrinsic sources such as UV exposure or internally generated by the mitochondria during cell stress, contribute to aging at the cellular level by causing damage to nucleic acids, proteins, and lipids [45]. In turn, this affects aging at the organismal level by compromising the function of tissues. The potential environmental sources capable of engendering increased ROS production are endless and countered by the body's antioxidant store designed to neutralize the reactive species. Potentiating the insult inflicted by increased ROS production during aging is the waning efficiency of antioxidant enzymes [45,46,47,48,49].

In addition to accumulation of environmental insults with age, recent work suggests a role for epigenetics in contributing to cellular and organismal aging. Age-associated chromatin remodeling can occur in a stochastic or programmed

manner, and thus perhaps satisfies both extrinsic and intrinsic pathways of aging [50]. Specifically, evidence supports an age-related change in methylation of PCGTs (targets of polycomb group proteins) in multiple cell types, including human embryonic stem cells that do not undergo senescence [51,52]. This is significant because repression of PCGTs is associated with the most common

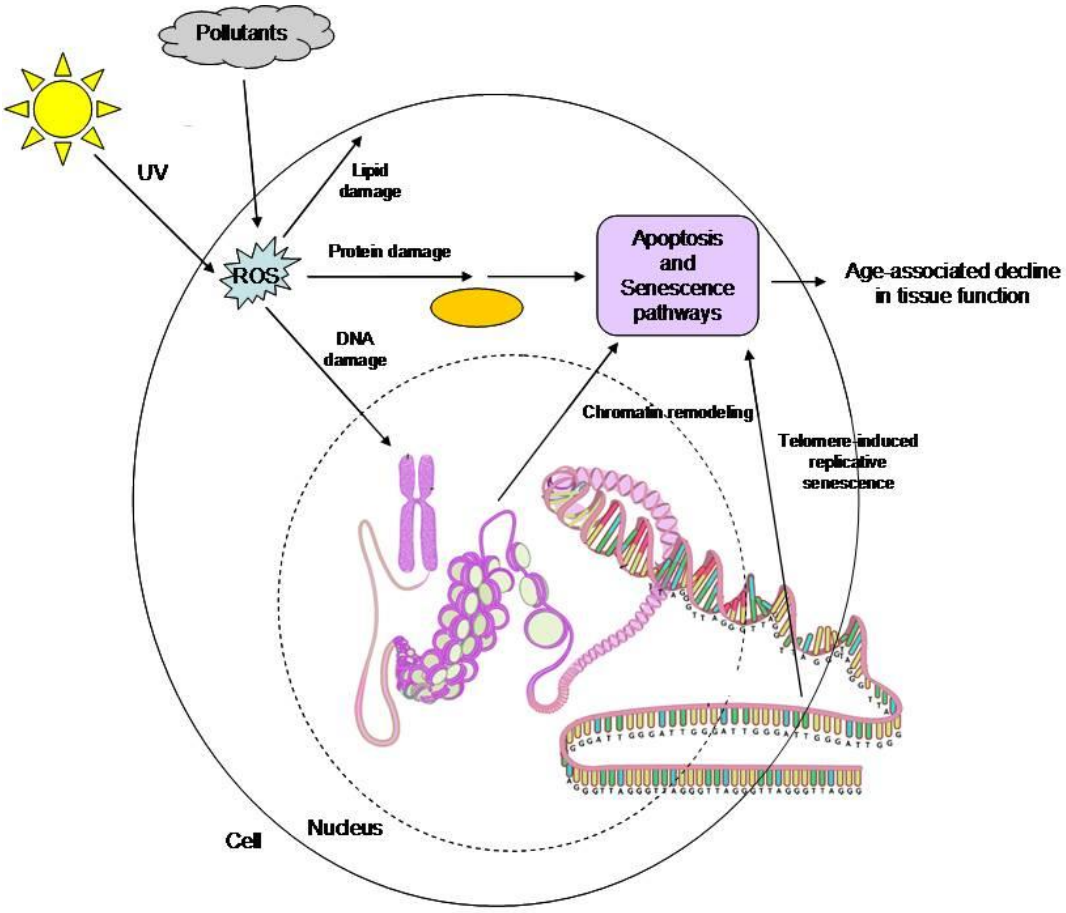

Figure 1.9 Extrinsic and intrinsic contributions to aging. One of the major mechanisms of environmental exposure mediated aging is via induction of ROS pathways. Chromatin remodeling affecting expression of proliferation and lifespan-associated genes affects aging. Telomere attrition due to prolonged cell proliferation in the absence of telomerase induces replicative senescence.

age-related disease – cancer [53]. The functional hypothesis is that repression of PCGTs that occurs with aging forces various cell types to become more “stem” in nature (a clear shift towards tumorigenesis for a somatic cell line) since regulated expression of various PCGTs is required to allow embryonic stem cell differentiation and expansion. The effects of age-associated chromatin remodeling are not limited to altered expression of PCGTs, but also include alterations in expression of other genes and non-coding RNAs. For example, microRNAs (miRNAs), 21-23 nucleotide non-coding RNAs that repress the expression of target mRNAs, are regulated by epigenetic changes associated with aging [54].

As previously mentioned, the initial discovery of replicative senescence in 1956 spawned a theory of aging called the Replicative Senescence Theory of Aging [45]. Although replicative senescence is intrinsic in origin, senescence can be induced by multiple stimuli, including extrinsic and blended factors like oncogene expression and DNA damage. In the early years of an organism’s life, senescence induction due to events that damage DNA or oncogene expression may be beneficial to the organism by preventing further proliferation of cells that bear unstable genomic changes. However, senescence reduces the number of cycling cells in a tissue, clearly limiting the regenerative capacity of aging human tissues. Thus, senescence is an example of antagonistic pleiotropism [55], a process that performs a beneficial (tumor suppressor) function early in life and contributes to decline of the organism later in life. The extent to which

senescence is associated with or causative of cellular and/or organismal aging is highly debated.

A. Evidence disparaging of a causal relationship between senescence and aging:

The major manifestations of aging and age-related decline in humans are most commonly noted in post-mitotic tissues (muscles, brain, and kidneys), which should not be sensitive to telomere length [56]. In addition, murine fibroblasts (which in contrast to human fibroblasts express telomerase) have a very short lifespan in culture compared to human fibroblasts despite having exceptionally long telomeres. Thus replicative senescence doesn't seem to play a predominant role in the aging of cultured murine cells. Additionally, Mollica et al noted a lack of correlation between leukocyte telomere length and hematopoietic reserve in aging woman [57], suggesting that replicative senescence is likely uncoupled from decline in hematopoietic function associated with age .

B. Evidence In support of a causal relationship between senescence and aging:

Recent data reveals that tissue stem cells (progenitor cells) of aging humans are enriched for senescent cells [58]. In contrast, embryonic stem cells and germline cells (which express higher levels of telomerase compared to progenitor cells) do not senesce despite extended proliferation. This implies that replicative senescence may contribute to the attenuated ability of progenitor cells to replenish the accumulating cell population bearing the DNA damage

associated with aging [59]. The concept of progenitor cell senescence may also help address the previously stated concerns of Longo et al [56]. Perhaps the failing efficiency of progenitor cells in post-mitotic tissues resulting in age-related phenotypes is more apparent than decline in function of gastrointestinal or hematopoietic cells due to the relatively low turn-over of kidney and muscle cells.

III. Senescence and Tumorigenesis

The role of senescence in tumorigenesis is less ambiguous than the previously discussed role in aging. As earlier indicated, replicative senescence represents a checkpoint in the cell cycle intended to prevent further proliferation of cells whose telomeres are insufficient to prevent loss of genomic content due to the end replication problem. Further, telomerase (which is essential in specifying whether a cell is capable of senescing), is expressed in 90% of all cancers. In those cancers where telomerase is not active, there are alternative mechanisms of maintaining telomere length [60], suggesting again the importance of telomere length in determining mortality.

Other types of senescence, including DNA damage-induced and oncogene-induced, serve a similar function of repressing proliferation of cells with unstable genomic changes. Transformation of normal human fibroblasts with Ras results in accumulation of p53 and p16 and induction of senescence [61]. In order for an oncogene such as Ras to initiate tumorigenesis, p53 and Rb (two of the three known critical pathways for senescence) must also be inhibited. Restoration of p53 in mice with p53-depleted tumors induced senescence that

resulted in tumor clearance [62]. Indeed, mutations of effectors within the p53 and Rb pathways are present in the majority of, if not all, human cancers. Thus repression of critical senescence pathways [63] and prevention of replicative senescence induction (via telomerase expression) account for two of the molecular changes observed in almost all human tumor formation. Contrary to the tumor suppressive characteristics of senescence, a study with human fibroblasts and epithelial cells revealed that induction of the senescence associated secretory phenotype (SASP), marked by robust cytokine signaling, conveyed malignant phenotypes to nearby pre-malignant and malignant cells [64]. Likewise, although inactivation of Pten (phosphatase and tensin homolog, a tumor suppressor that inhibits Akt/PKB signaling) is a frequent mutation in tumors, acute Pten inactivation results in accumulation of $p19^{ARF}$ and p53, triggering cellular senescence [65]. This again harkens to the notion of senescence as an example of antagonistic pleiotropy.

IV. Molecular Details of Senescence Pathways

Despite the fact that senescence can be induced by various stimuli, current evidence reveals the engagement of only a few critical pathways in all instances: the p53, Rb, and Skp2 pathways [63,66,67]. In fact, in most cases human cells that have impaired p53 and Rb pathways are refractory to senescence-inducing stimuli [61,67]. The complete molecular details governing induction and maintenance of senescence through these pathways remain to be

discerned; however, a summary of the current evidence for the role of each pathway in senescence follows.

p53 is a tumor suppressor protein that elicits a senescence or cell death response in answer to various stimuli, including DNA damage, activation of oncogenes, and hypoxia [68]. In the setting of replicative senescence, p53 functions by recognizing critically short telomeres as DNA damage and responds by engaging the cyclin-dependent-kinase-inhibitor p21. p21 inhibits the CDK2/cyclin E complex required by the cell for G1/S transition. As the telomeres of human fibroblasts approach senescence, they acquire DNA damage foci that include the proteins p53BP1 and phosphorylated ataxia telangiectasia mutated kinase (ATM) [69,70]. ATM phosphorylates and activates p53 (Figure 1.10).

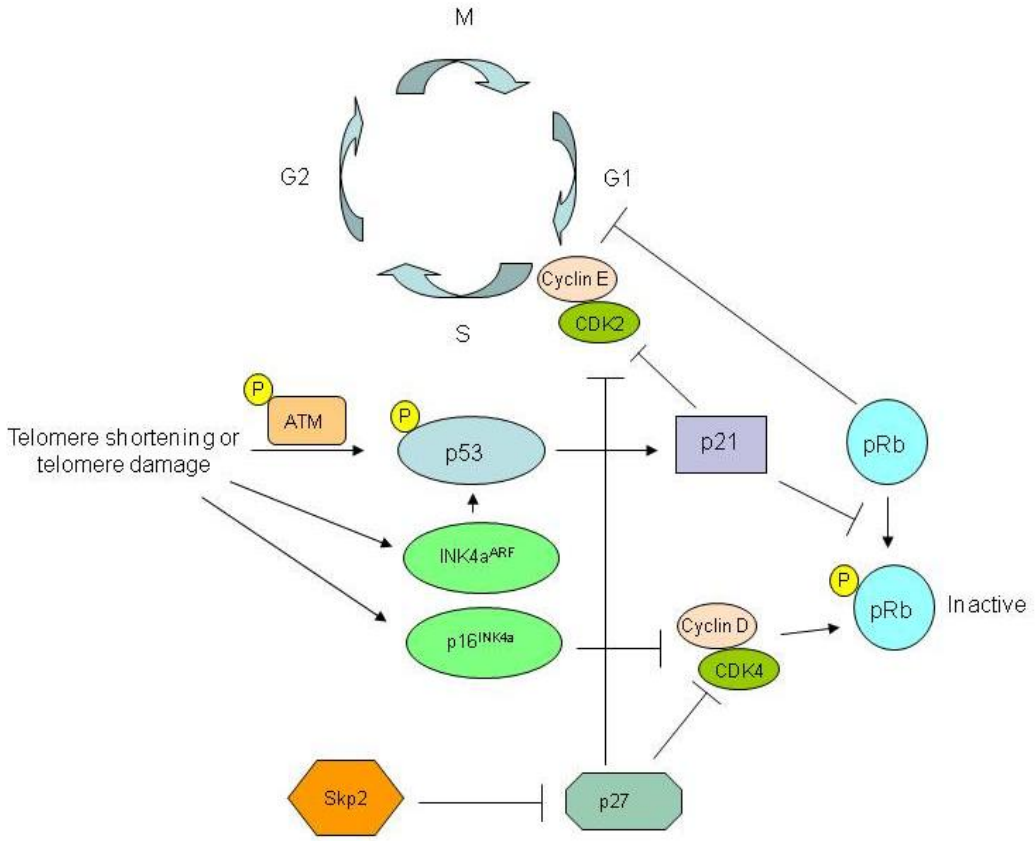

Figure 1.10 Critical Pathways of Senescence. The pathways critical to establishing and maintaining senescence growth arrest are shown. These include p53, pRb, p21 and Skp2 pathways.

Despite the critical role of p53 in conveying senescence, inactivation of either p53 or pRb independently results in senescence of most human cell types [71,72]. This indicates the potential for the pRb pathway to function separately in initiating senescence in addition to the engagement of pRb via the p53 pathway. p16 is up-regulated significantly during telomere shortening and DNA damage-induced senescence in most human cells [73,74]. p16 inhibits the cyclin D1/CDK4 complex that keeps pRb in an inactive (hypophosphorylated) state.

Thus p16 up-regulation during telomere or DNA damage-induced senescence activates pRb, enforcing a G1/S arrest independent of the p53 pathway.

Until very recently, all evidence pointed to the requirement for activation of either the p53 or pRb pathways for induction of senescence in human cells. New evidence reveals that inactivation of Skp2, an E3-ubiquitin ligase targeting p27, induces senescence in a p53 and pRb-independent manner [75]. The most interesting facet of this discovery is the fact that Skp2 inactivation alone is insufficient to induce senescence. However, in the setting of a combination of oncogenic stress (Ras signaling) and tumor suppressor ($p19^{ARF}$ and p53) inactivation, Skp2 inactivation induces senescence and inhibits the ability of Ras to cause transformation [33].

While it is abundantly clear that p53 and pRb are important for initiating senescence growth arrest, the requirements for maintaining growth arrest via these pathways are less straightforward. Recent work reveals that senescence induced by p53 activation in cell lines lacking p16 expression, such as human foreskin fibroblasts, can be reversed by p53 inactivation (in contrast to the previously accepted idea that all senescence is irreversible) [76]. However the vast majority of human cells express both p53 and p16 and in this case the authors hypothesize that once senescence-induced p16 is expressed, hypophosphorylated pRb establishes a permanently repressive chromatin state that continues to inhibit proliferation even if pRb is subsequently inactivated (Figure 1.11).

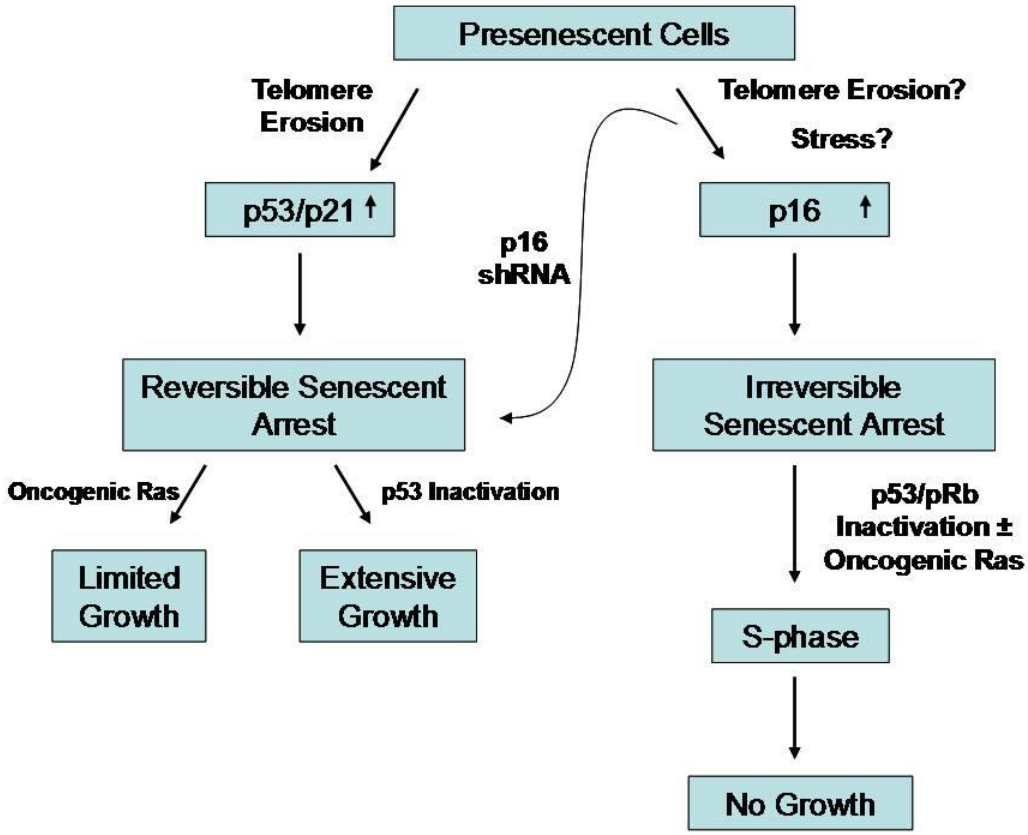

Figure 1.11 p16 maintains permanence of senescence growth arrest. Although both p53 and p16 are capable of inducing senescence growth arrest, Rb activation by p16 results in an irreversible growth arrest in contrast to the reversible arrest established by direct p53 activation. Figure from Beausejour et al [76].

V. MiRNA Role in Regulation of Cell Proliferation/Senescence Pathways

A. MiRNA Overview

For the most part, the discussion of critical pathways that regulate senescence has been centered around changes that occur at gene and protein levels. However, this focus is just beginning to broaden and include investigation into the influence of small non-coding RNAs, particularly microRNAs (miRNA), in

senescence. In 1998, Andrew Fire and Craig Mello (2009 Nobel laureates) discovered a non-coding RNA species, now known as RNA interference or RNAi, that could alter the expression of target mRNAs at the post-transcriptional level [77]. MicroRNA, an endogenous example of RNAi, has emerged over the last decade as a non-coding RNA pathway with capacity to influence expression of ≥ 60% of the human genome. MiRNAs can reside within introns of protein-coding genes, or can originate from their own genes in otherwise non-coding portions of the genome. MiRNAs are transcribed by RNA polymerases pol II or pol III into long precursor transcripts called primary miRNA (pri-miRNA). These precursors contain a characteristic hairpin and are cleaved within the nucleus to generate a shorter precursor miRNA. These short (60-70 nt) hairpin precursors, called pre-miRNA, are generated by an RNase III enzyme called Drosha. Pre-miRNAs are then exported out of the nucleus by Exportin-5 and Ran-GTP. In the cytoplasm, pre-miRNAs are recognized by another RNase III enzyme called Dicer that cleaves the pre-miRNA into the mature ds miRNA. One strand of the ds miRNA duplex that is the mature miRNA (the complimentary strand is referred to as miRNA*) is loaded into the RISC complex which facilitates binding to a complementary sequence in a target mRNA. Although the majority of studies suggest miRNAs bind to sites within the 3'UTR of the target mRNA, recent evidence also suggests the capability of miRNAs to bind at exonic sites within the open reading frame of the target mRNAs and the 5'-UTR [78,79,80,81]. Once loaded into the RISC complex, the miRNA directs repression of a target mRNA

by one of two methods: translational repression or degradation of the mRNA. (Figure 1.12)

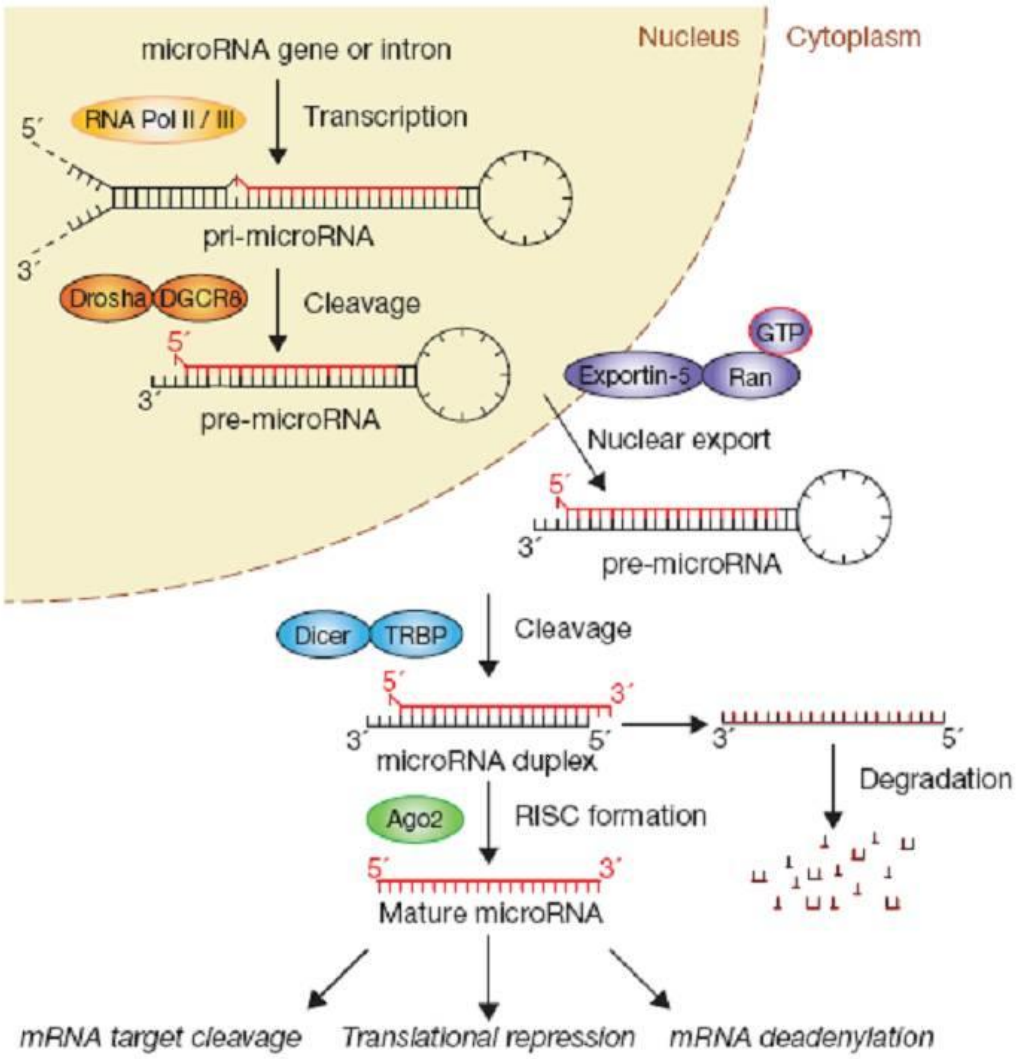

Figure 1.12 MiRNA Biogenesis and Mechanism. MiRNAs are short non-coding RNA sequences that bind to complementary sequences within target mRNAs and attenuate the expression of the target mRNA by either translational repression or mRNA degradation. Figure from Winter et al [82].

The prevailing theory regarding which method is used is as follows: The higher the degree of complementarity between bases 2-8 of the miRNA and the target mRNA sequence (usually perfect complementarity is required), the more likely mRNA degradation will be employed. When imperfect complementarity exists, it is more likely that the miRNA will cause translational repression of the target mRNA [83]. In plants it is more common for the miRNAs to display high target complementarity and direct mRNA cleavage, whereas the opposite is true for humans (it is more common for miRNAs to direct translational repression of their targets) [84].

B. MiRNA Role in Proliferation, Growth Arrest, and Lifespan Determination – Implications for Senescence

There is significant literature precedence indicating the ability of miRNAs to influence aging phenotypes in mice and *C.elegans* [85,86]. In addition, there is a wealth of evidence indicating a role for miRNA in regulating pathways critical to senescence. For example, miR-34a appears to be a downstream effector in the p53 pathway [87,88,89,90]. Induction of miR-34a expression in human colon cancer cells resulted in senescent-like growth arrest characterized by down-regulation of the E2F pathway and up-regulation of the p53 pathway [91]. In general, miRNAs trend towards up-regulation during aging [85]. In 2009, Maes et al demonstrated that miRNAs associated with reversible and irreversible growth arrest states (including replicative senescence, stress-induced premature senescence, and quiescence) were up-regulated in a step-wise manner over time [92]. Recent evidence reveals that the miR-290 cluster, which includes 8

polycistronic miRNAs, is down-regulated in Dicer-1 deficient mice and associated with increased telomere elongation and recombination [93]. Retinoblastoma-like 2 protein (Rbl-2) was validated as a target for the miR-290 cluster in these Dicer1-deficient mice. Rbl-2 inhibits expression of several DNA methylation proteins, resulting in hypomethylation of subtelomeric regions and telomere-elongation phenotypes [93]. Thus an increasing and convincing body of evidence suggests that miRNAs have an important role in aging and regulating the tumor-suppressive barrier known as senescence. However, current knowledge of which miRNAs are involved in regulating senescence is incomplete and based on piecemeal reports of specific miRNAs affecting senescence pathways. Work within this thesis will reveal the first comprehensive report of miRNAs whose expression is differentially regulated during replicative senescence of human foreskin fibroblasts. Further, experiments described herein will begin to delineate novel senescence-regulatory pathways in human foreskin fibroblasts controlled by the miRNAs we identify as involved in senescence. Finally, work performed under the auspices of this thesis will reveal a connection between telomerase expression and expression of miRNAs involved in senescence and aging.

Specific Aims of this Research

I. (Chapter II) Validate a novel model predicting a dynamic conformational change upon telomerase assembly for domain III of Tetrahymena thermophila telomerase RNA (tTR).

II. (Chapter III) Identify miRNAs involved in regulating senescence and miRNAs affected by expression of hTERT in human foreskin fibroblasts

III. (Chapter IV) Elucidate the Role of miRNAs and TERT in Proliferation/Inflammation Pathways

Chapter 2. Validate a novel model for the secondary structure of Tetrahymena thermophila telomerase RNA (tTER)

I. Introduction

Telomerase is a ribonucleoprotein reverse transcriptase that plays a critical role in pathways governing aging [94], lifespan [95,96], and tumorigenesis [97,98]. Recent work [99,100] as well as preliminary evidence described in subsequent chapters within this dissertation, suggests that telomerase influences cellular mortality by several independent mechanisms. However, the most widely appreciated role of telomerase in regulating mortality is its role in telomere maintenance and extension. Despite an evolutionarily conserved role for the telomerase complex in maintaining telomeres across multiple kingdoms, including metazoans, plants [101], and fungi [102], current understanding of the contribution of telomerase structure to telomerase function remains incomplete. Although there is a requirement for species-specific accessory proteins to obtain telomerase activity in vivo, an active telomerase complex can be reconstituted in vitro by expression of the catalytic subunit (TERT) and an RNA subunit (TR), which represents the minimal RNP complex. The sequence and length of TERT shows substantial evolutionary conservation between organisms. TERT contains RT domains homologous to those found in other reverse transcriptases [26,103]. While TR sequence and length vary considerably among species,

several secondary structural elements are highly conserved, implying a critical role for TR structure in facilitating telomerase activity [23,31]. Tetrahymena thermophila has emerged as a model organism for studying telomerase structure and function. The current model of tTR secondary structure (Figure 2.1) is based on phylogenetic and mutational analyses, and supported by NMR data depicting solution structures of domains II [33] and IV [34,35].

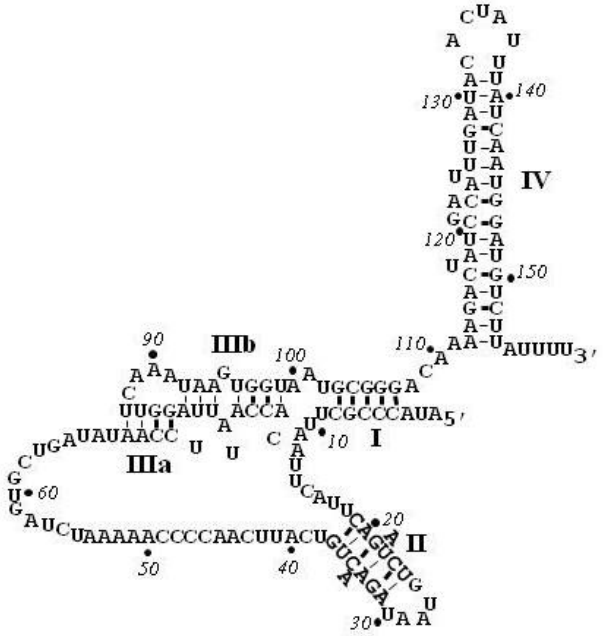

Figure 2.1 Current model for tTR secondary structure. The currently accepted model for tTR secondary structure is based on phylogenetic comparisons, mutational analyses indicating the importance of certain structures (like the pseudoknot) for telomerase activity, and very limited footprinting data.

Although the current model for tTR secondary structure fits well with published biochemical evidence, we believe (based on unpublished data from Legassie, Bonifacio, and Jarstfer) this model is insufficient to describe a conformational change in tTR upon assembly into the telomerase complex. We propose a novel model to describe tTR secondary structure (Figure 2.2).

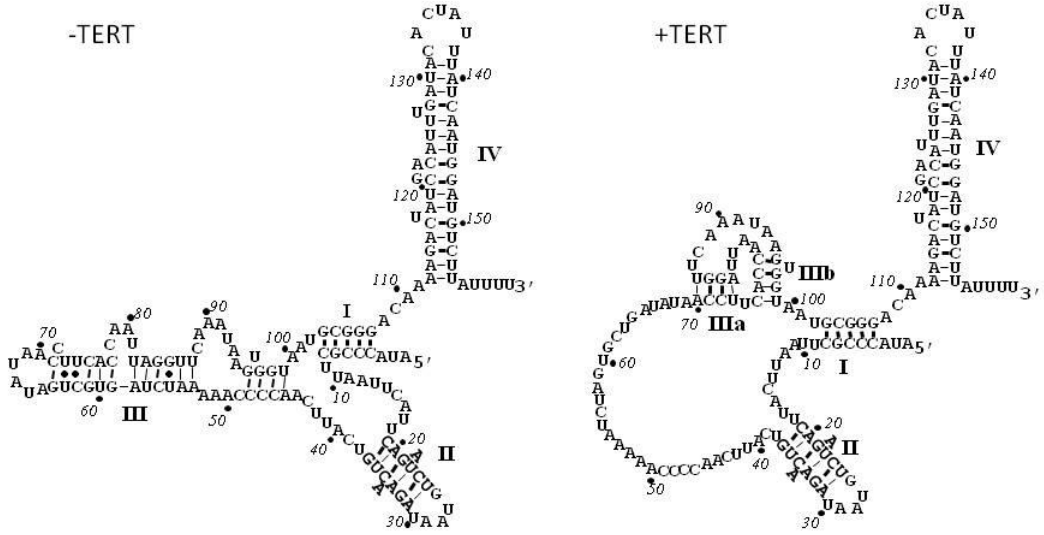

Figure 2.2 Proposed model for tTR secondary structure. The models shown above were derived based on SHAPE footprinting data. This model differs from the currently accepted model primarily in the region of stem III. Based on unpublished data, we believe tTR does not form a pseudoknot or triplet interactions in-solution. These interactions are formed when tTR is in complex with tTERT.

The evidence upon which we developed our model for tTR secondary structure was rendered via a highly sensitive footprinting technique called Selective 2' Hydroxyl Acylation Analyzed by Primer Extension (SHAPE) [104]. SHAPE is a quantitative structure analysis technique that offers an advantage over other footprinting techniques because it can detect with equal sensitivity the flexibility of all four nucleotides in a given RNA. SHAPE footprinting is designed based on the premise that unpaired RNA residues are more conformationally flexible than those that are base-paired. A conformationally flexible nucleotide can sample different conformations, thus making it more likely that the flexible nucleotide will at any given time be in a reactive conformation susceptible to 2'-hydroxyl acylation by the hydroxyl selective acylating reagent *N*-methyl isatoic anhydride (NMIA).

Evidence will be presented in this chapter to validate this novel model for tTR secondary structure that reveals dynamic changes between the in-solution and in-complex forms and an essential contribution of this shift in tTR conformation to telomerase activity. We used SHAPE (Selective 2'-Hydroxyl Acylation analyzed by Primer Extension) footprinting to interrogate this dynamic model for tTR secondary structure by introducing 2 mutations that would singly interrupt predicted pseudoknot interactions and restore interactions essential for pseudoknot formation when present together in tTR. An accurate model for tTR structure will engender an understanding of TR structure contribution to telomerase activity and facilitate attempts to utilize telomerase as an anti-cancer and anti-aging therapeutic target.

II. Results

A. SHAPE of In-Solution tTR Mutants

To interrogate the potential for tTR stem III to form a pseudoknot in-solution, we introduced two mutations to stem III – MS1 and MS2, designed to singly interrupt base-pairing essential to pseudoknot formation in in-solution tTR(Figure 2.3). The compensatory mutant MS1-2, which contains both mutations, should assume an in-solution secondary structure similar to that of wild type tTR if a pseudoknot is present. In contrast, if a pseudoknot is not formed in WT, in-solution tTR, the compensatory mutant will assume a secondary structure different from that of wild type tTR.

To probe the effects of MS1 and MS2 mutations on tTR secondary structure, we analyzed the mutant tTR RNAs with SHAPE [104]. SHAPE is a quantitative RNA structure analysis technique that detects flexibility of each nucleotide in a given RNA to infer likelihood of that nucleotide being base paired. An example of a SHAPE sequencing gel is shown in figure Figure 2.4.

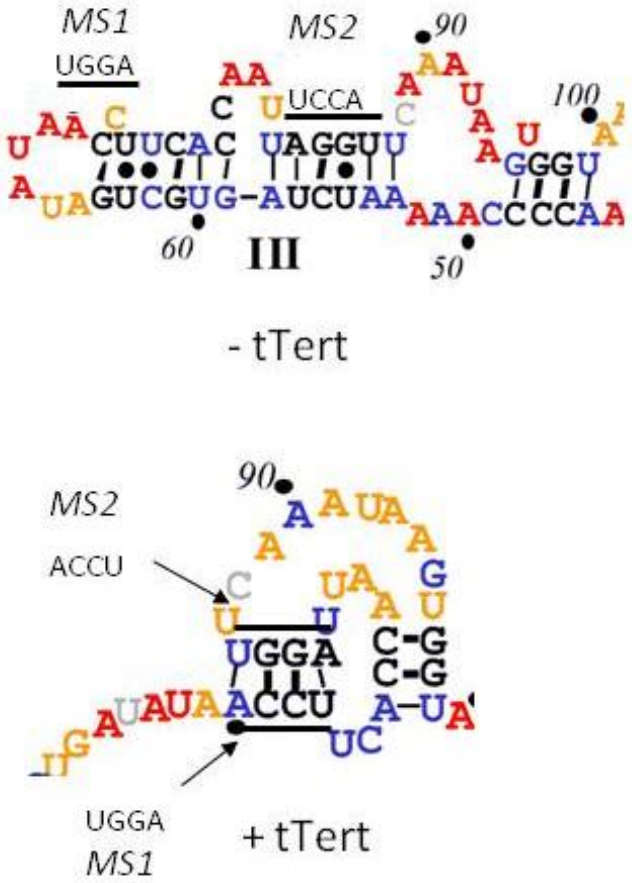

Figure 2.3 tTR stem III mutants. Two mutants, MS1 and MS2, were designed to interrupt base-pairing essential to pseudoknot formation by stem III of tTR. We hypothesize that tTR is incapable of forming a pseudoknot in-solution, but upon assembly into the telomerase complex forms triplets and a complete pseudoknot. The mutations are shown in this figure depicting a stem loop for stem III for in-solution tTR and a pseudoknot for in-complex tTR. Nucleotide bases are colored according to their conformational flexibility as indicated by previous experiments (unpublished, Legassie, Bonifacio, and Jarstfer). Most flexible to least flexible are colored as follows: red, yellow, blue, black. Gray indicates insufficient data for that nucleotide.

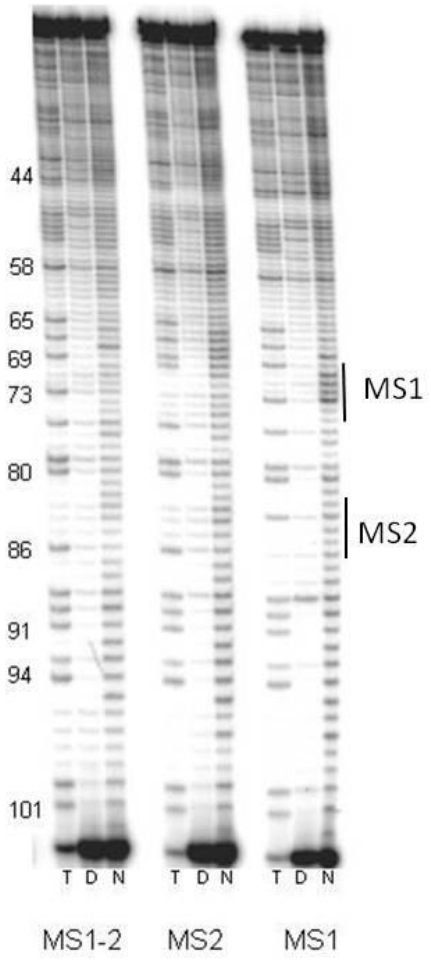

Figure 2.4 SHAPE footprinting gel of tTR mutants. MS1, MS2, and MS1-2 tTR mutants were subjected to SHAPE footprinting with an internally-binding primer to provide high resolution data on the flexibility of nucleotides in Stem III. Nucleotide position in tTR is indicated on the left of the gel and tTR mutants are annotated on the right-hand side. T, D, and N indicate ddT ladder, DMSO control lane, and NMIA hit lanes, respectively.

SHAPE experiments with MS1 RNA (a) reveal increased flexibility for nucleotide regions 61-64, 74-76 compared to WT tTR (Figure 2.5d). This is consistent with the hypothesis that the MS1 mutation affects base-pairing between these two regions of stem III. MS2 SHAPE results (Figure 2.5b) reveal

increased flexibility in nucleotides 51-55, 58-59, 71-76, and 81-89. There is also a decrease in flexibility of the region 92-94 compared to WT. These changes are consistent with the ability of MS2 to force regional unfolding by destabilizing base-pairing interactions at the base of stem III. SHAPE results for MS1-2 RNA (Figure 2.5c) reveal increased flexibility for nucleotides 53-55, 58-62, 72, 76, 83-84, 86 compared to WT. These results are consistent with the potential for MS1-2 to significantly alter the ability of stem III to form a stem-loop or pseudoknot.

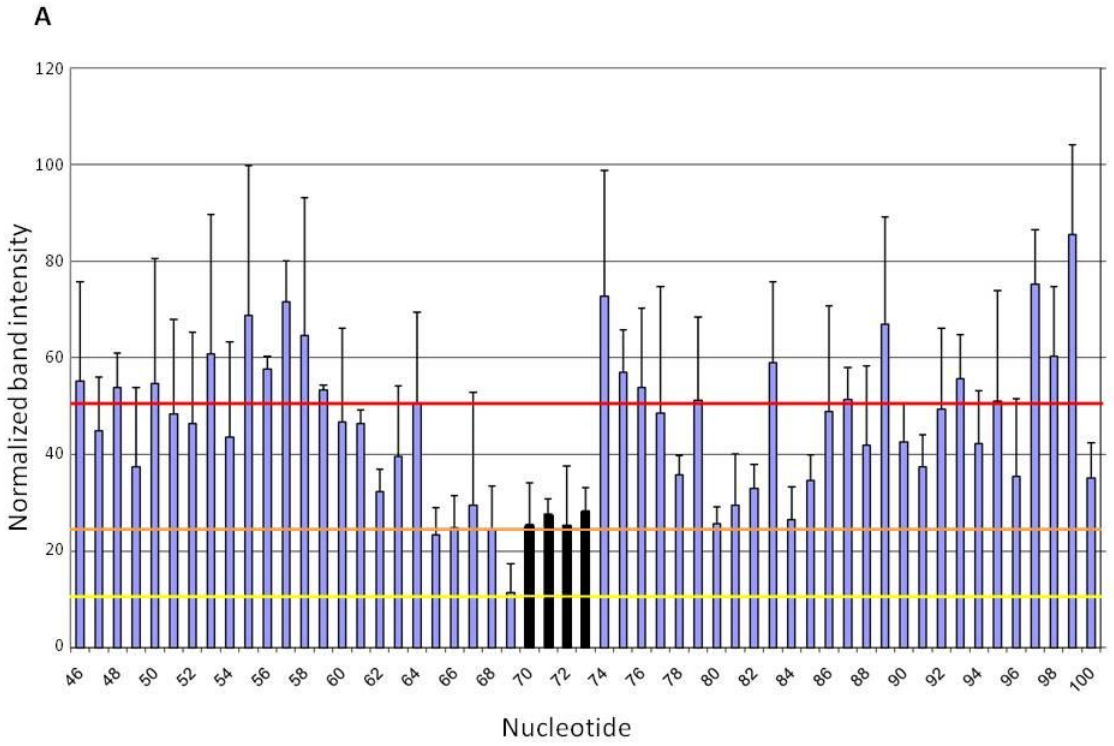

B

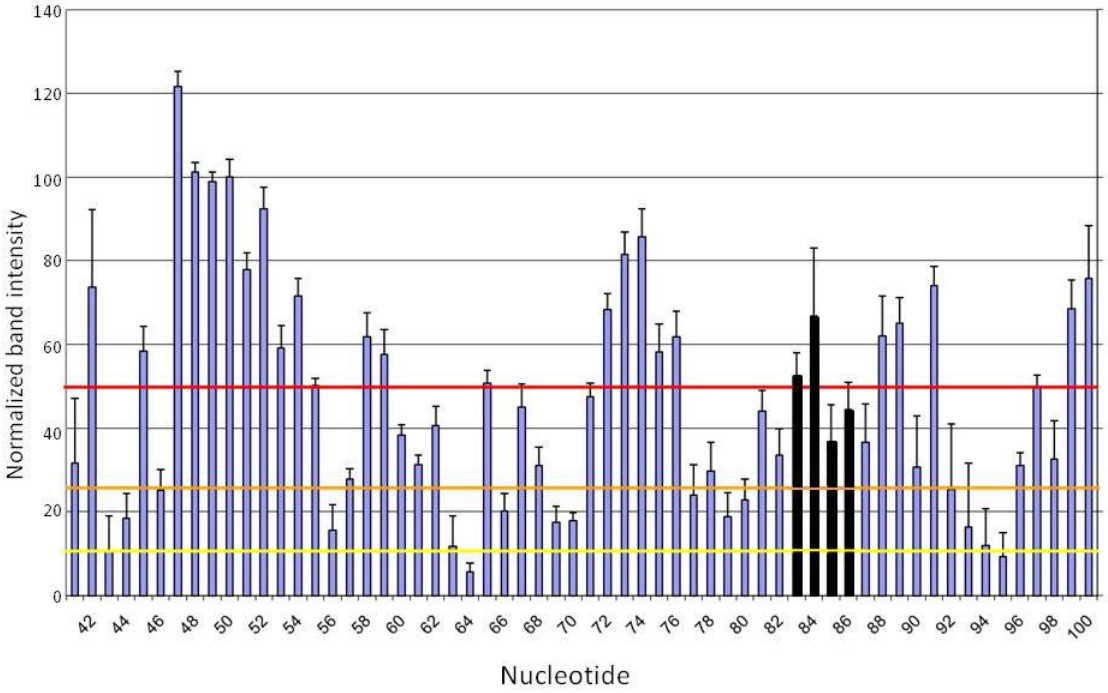
Normalized band intensity
0
20
40
60
80
100
120
140
42 44 46 48 50 52 54 56 58 60 62 64 66 68 70 72 74 76 78 80 82 84 86 88 90 92 94 96 98 100
Nucleotide

C

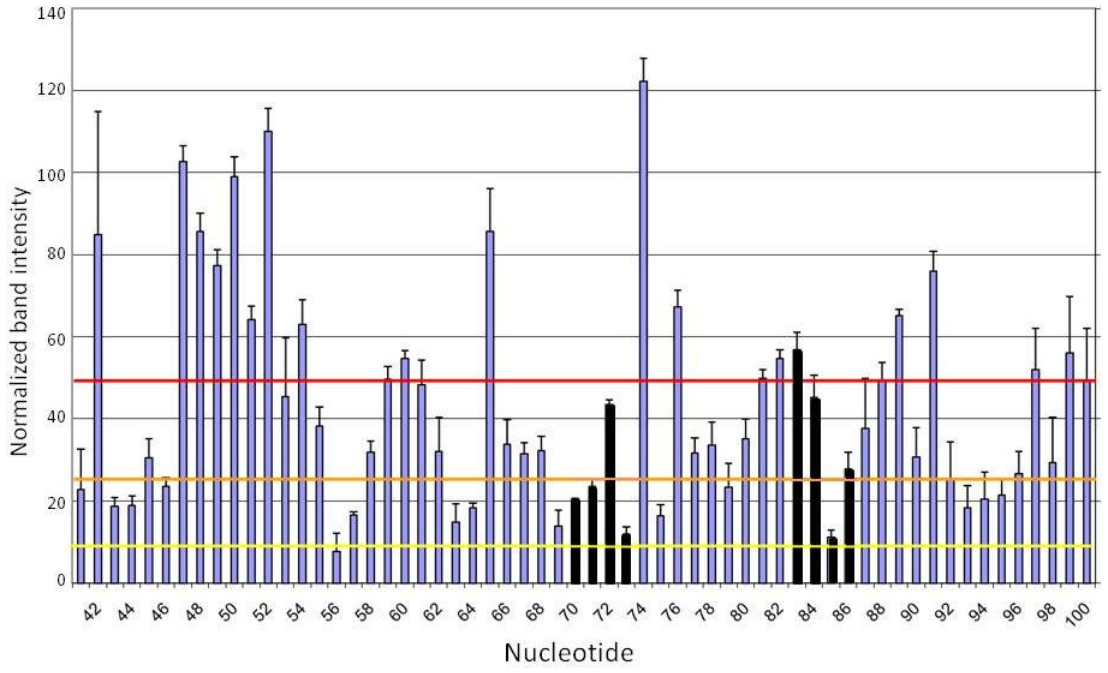
Normalized band intensity
0
20
40
60
80
100
120
140
42 44 46 48 50 52 54 56 58 60 62 64 66 68 70 72 74 76 78 80 82 84 86 88 90 92 94 96 98 100
Nucleotide

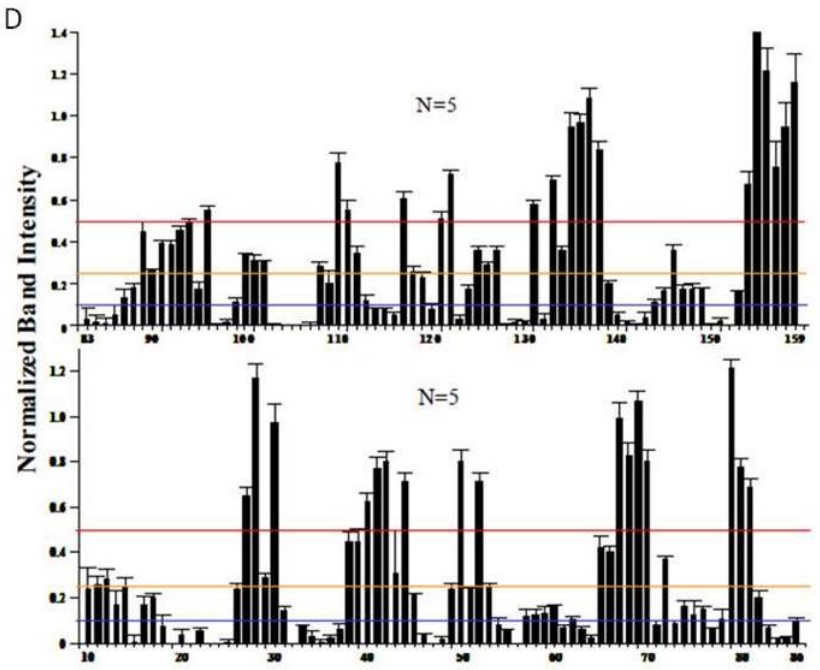

Figure 2.5 In-solution SHAPE profiles of tTR mutants. Flexibility of each nucleotide for in-solution tTR RNAs a) MS1, b) MS2, c) MS1-2, and d) WT tTR (courtesy of Jason Legassie) was probed by SHAPE. The normalized hit frequency for each nucleotide is represented in the graph. Mutated regions of tTR are highlighted with black bars in a, b, and c.

B. tTR Pseudoknot Mutations Impact Telomerase Activity

To determine whether the conformational changes conferred by MS1 and MS2 mutations within the pseudoknot region of tTR impact telomerase activity, we reconstituted telomerase bearing the MS1 and MS2 mutations using an in vitro rabbit reticulocyte lysate expression system and tested the activity of the telomerase complexes with the direct telomerase assay [105]. As expected since the tTR mutants were designed to interrupt base-pairing essential to pseudoknot formation, the single mutants MS1 and MS2 gave rise to telomerase

complexes with substantially impaired activity, whereas the compensatory mutant MS1-2 showed processive elongation of the telomeric primer with only slightly reduced activity compared to wild type (Figure 2.6).

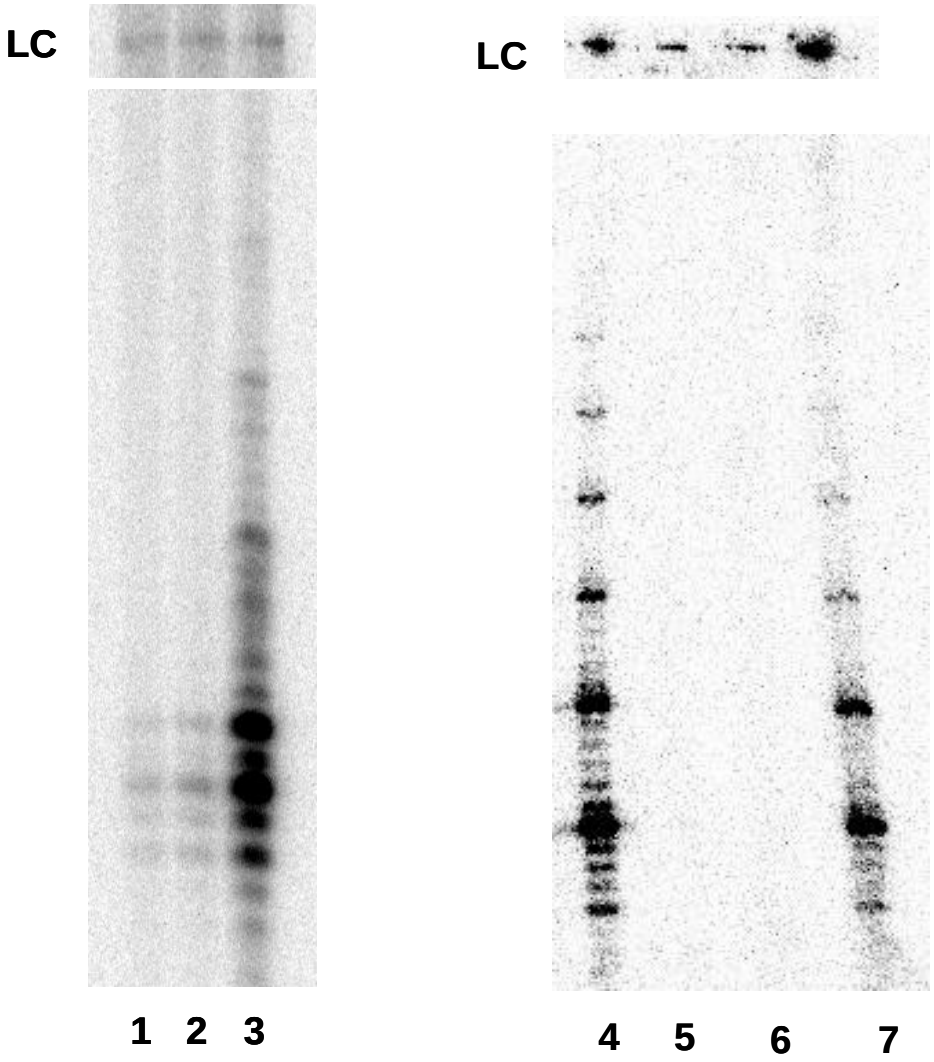

Figure 2.6 MS1-2 compensatory mutant restores telomerase activity. Lanes 1-3 represent MS1, MS2, and MS1-2 telomerase extension assays from crude reticulocyte lysate, respectively. Lanes 4-7 represent WT, MS1, MS2, and MS1-2 telomerase extension assay results using immunopurified telomerase complexes. Lanes 4-7 courtesy of Ryan Hallett and Brian Bower.

III. Discussion

Although telomerase RNA sequence and length varies considerably among species, phylogenetic comparisons reveal the conservation of several secondary structural features. This implies that TR structure may play an essential role in permitting telomerase function. Tetrahymena, a ciliated protozoan, has emerged as a model organism for studying TR structure and function. The currently accepted model for tTR secondary structure is based on phylogenetic analyses [42,106], NMR structures for domains II [33] and IV [34,35], and mutational analyses for other tTR domains [38]. Although this model fits well with biochemical evidence for tTR structure in the telomerase complex, we believe, based on SHAPE data for in-solution tTR (unpublished work, Legassie, Bonifacio, and Jarstfer) that this model is insufficient to describe the structure of tTR in-solution and a conformational change in tTR associated with telomerase assembly. Based on this data, we have proposed a novel model for tTR secondary structure (Figure 2.7). Our model for tTR secondary structure predicts dramatic changes in tTR conformation as it shifts from the in-solution to in-complex form. Specifically, this model differs from the currently accepted model for tTR conformation by indicating a lack of triplet interactions and pseudoknot formation for in-solution tTR. We hypothesize that tTR undergoes a dramatic shift in conformation of domain III to allow pseudoknot formation in the telomerase complex. Evidence from tTR mutational analyses and subsequent SHAPE experiments in this chapter confirm that the secondary structure for tTR domain III undergoes this shift as tTR is assembled into the telomerase complex.

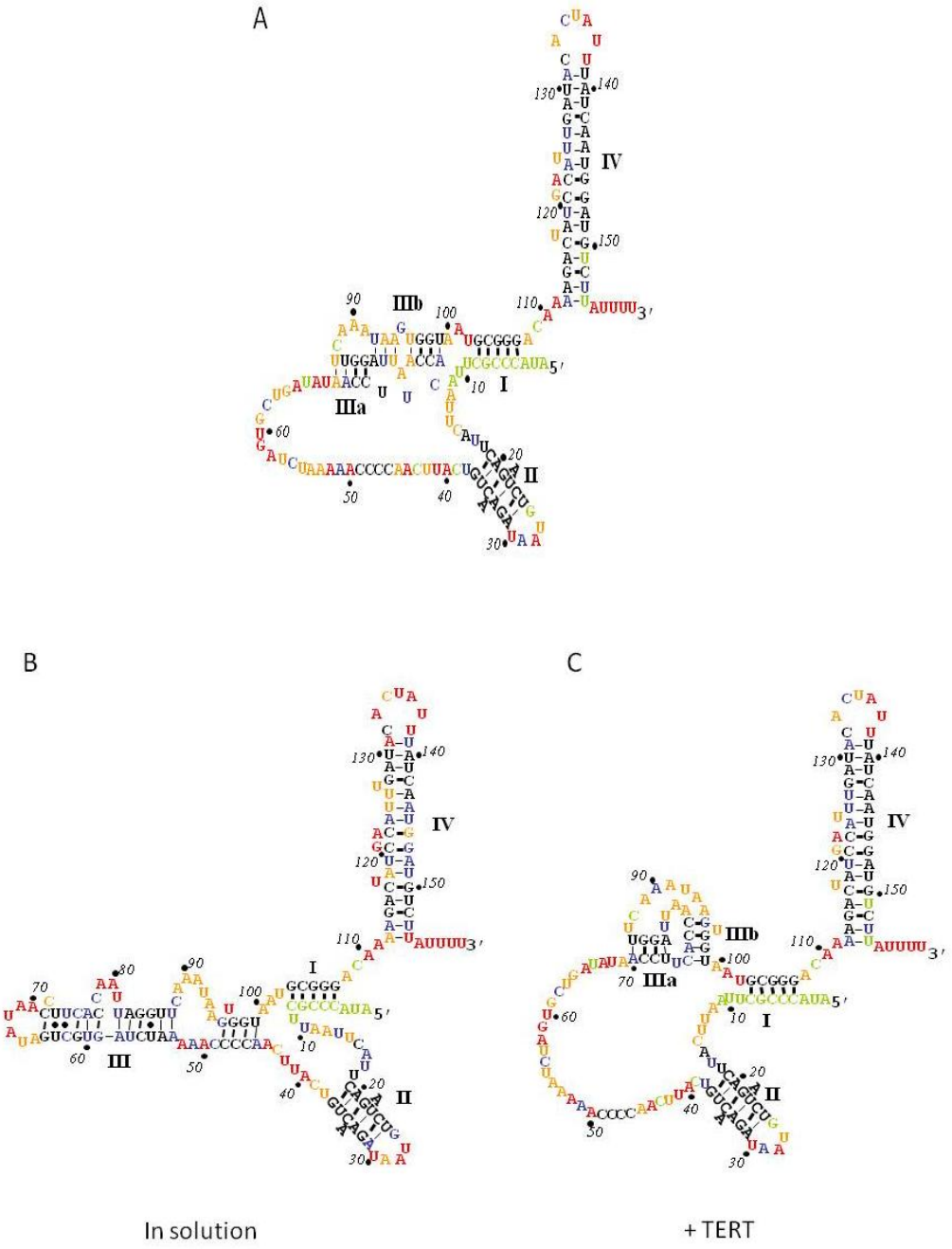

Figure 2.7 Models for tTR secondary structure. The currently accepted model (A) for tTR secondary structure depicts domain III as a pseudoknot. Unpublished SHAPE data (courtesy of Jason Legassie), is consistent with a dynamic model for tTR shown in (B) and (C). These SHAPE results indicate the likelihood for tTR domain III to form a stem loop in-solution, and the formation of a pseudoknot complete with base-triplet interactions upon assembly into the telomerase complex. Models are colored based on SHAPE reactivity of each nt as follows: red > yellow > blue > green > black. Gray indicates lack of sufficient data.

To validate this new model depicting a dynamic secondary structure for domain III of tTR, I created the domain III mutants MS1, MS2, and the compensatory mutant MS1-2, which contains both mutations (Figure 2.3). If our hypothesis regarding tTR secondary structure is correct, the in-solution single mutants MS1 and MS2 and compensatory mutant MS1-2, should yield altered RNA flexibility profiles compared to wild type. Whereas, if domain III of in-solution tTR is capable of forming a pseudoknot, the compensatory MS1-2 mutant should yield an in-solution SHAPE profile similar to that of wild type tTR. As expected, the single mutants MS1 and MS2 yielded SHAPE profiles with increased flexibility in the domain III region (Figure 2.5). Importantly, the compensatory mutant MS1-2 yielded an in-solution SHAPE profile revealing altered flexibility of domain III compared to wild type tTR. If a pseudoknot was present in tTR in-solution, one would expect the in-solution SHAPE profile of MS1-2 RNA to mimic that of WT tTR. It is well established that that the triple helix resulting from pseudoknot formation is essential to telomerase activity in humans and yeast [107]. It is also clear that disruption of pseudoknot base-pairing in tTR prevents assembly of an active telomerase complex in vivo [108]. Thus although a pseudoknot conformation for domain III of tTR is essential for telomerase activity, presumably it does not form in solution, and assumption of this pseudoknot conformation is an event that occurs during assembly of the telomerase complex.

To confirm that the structure assumed by the MS1-2 mutant is biologically relevant, telomerase was assembled in vitro with MS1-2 RNA and the ability of

this mutant telomerase to extend a telomeric primer was measured with the direct telomerase assay. One would anticipate that MS1 and MS2 mutant RNAs (singly) should result in an inactive telomerase complex when assembled with TERT by disrupting pseudoknot formation. Likewise, the compensatory mutant MS1-2 should restore telomerase activity by facilitating interactions crucial for pseudoknot formation. Consistent with these expectations, MS1 and MS2 RNAs resulted in inactive telomerase complexes, whereas telomerase assembled with MS1-2 RNA showed only slightly reduced activity compared to WT telomerase (Figure 2.6).

IV. Future Directions

SHAPE of tTR mutants MS1, MS2, and MS1-2 in the telomerase complex is in progress and will be completed by future graduate students using the constructs that I designed. The results of these experiments will help define the details of tTR secondary structure in the telomerase complex. Preliminary results (experiments performed within the Jarstfer lab using these tTR mutant constructs) indicate a SHAPE profile for MS1-2 in-complex RNA similar to that of in-complex WT tTR. In addition, constraints from SHAPE data (provided by Jason Legassie, PhD) are being combined with other biochemical data for tTR to develop a model for tTR using *in silico* approaches. These experiments will clarify details of in-solution and in-complex tTR secondary structure.

V. Methods

A. Site-directed mutagenesis and transformation to create tTR mutants.

tTR mutants were created by PCR site-directed mutagenesis from the pTet-telo vector that encodes WT tTR modified with a 5' hammerhead ribozyme sequence (HH-tTR). Primers used to create tTR mutants MS1, MS2, and MS1-2 are shown in table 2.1. The 5' and 3' primers are designed to have 5' overlapping complimentary sites along the underlined portions. Site-directed mutagenesis reactions were designed based on a protocol from Zheng, et al [109]. Mutagenesis reactions contained 1X Pfu buffer (Stratagene), 50 ng HH-tTR plasmid, 125 ng 5'-primer, 125 ng 3'-primer, 1 µl dNTP mix (Stratagene), 2.5 units (1 µl) PfuTurbo DNA polymerase (Stratagene), and ddH_2O to a final volume of 50 µl. Each mutagenesis reaction was subjected to the following thermal cycling parameters: 95 °C for 30 secs, 95 °C for 30 secs, 55 °C for 1 min, 68 °C for 6 min (2 min/kb). The underlined steps were repeated for 18 cycles. Each reaction was treated with 10 units DpnI to get rid of parental HH-tTR DNA at 37 °C for 1 hour. 1 µl of each reaction was used to transform Max efficiency DH5α competent cells (Invitrogen) and 25 µl of each transformation reaction was plated onto LB Amp^+ plates. Mutant tTR plasmids were amplified, isolated by boiling lysis, and precipitated with isopropanol. Mutants were verified by sequencing using pUC19f and pUC19r primers (Table 2.2).

B. Generation of SHAPE-RT constructs

SHAPE constructs were generated by addition of a 3' extension to the mutant tTRs via PCR. This 3' extension is designed to facilitate binding of reverse transcriptase, an essential step of the SHAPE footprinting process. PCR was carried out using primers 5'-tTR+HH and 3'-tTER+3'-Linker (Table 2.2) and standard GoTaq DNA polymerase (Promega) reaction conditions utilizing 1X colorless GoTaq Reaction Buffer (Mg^{2+} free) supplemented with 1.5 mM Mg^{2+}. tTR SHAPE-RT constructs were phenol chloroform extracted and EtOH precipitated. Mutant tTR SHAPE RNA constructs were transcribed with the T7 RNA polymerase kit (Ampliscribe). After transcription, 5' hammerhead cleavage was encouraged (generating the native 5' end for tTR) by addition of 12 mM $MgCl_2$ and incubation at 45 °C for 1 hour. The reaction was then treated with DNase, EtOH precipitated, and resuspended in TE. tTR mutant RNA was resolved by PAGE on a 10% acrylamide, 20 X 20 cm, denaturing gel, isolated by UV, then purified by a modified crush and soak method [105,110], and resuspended in TE.

C. NMIA hit reactions

1 pmol of RNA was snap annealed in ddH_2O by heating to 95 °C for 2 min, then cooling on ice for 5 minutes. Then 1X HIT buffer was added from a 5X stock (5X stock contains 250 mM HEPES (pH 8.0) and 10 mM $MgCl_2$) and the solution was incubated at 30 °C for 5 minutes. RNA modification was initiated by addition of 1 µl NMIA (100 mM in anhydrous DMSO) or 1 µl DMSO as control. This solution was tapped gently to mix then incubated at 30 °C for 90

minutes. Each HIT reaction including DMSO controls was then immediately quenched by addition of 80 µl H_2O, 4 µl of 5M NaCl, and 200 µg/ml glycogen, then EtOH precipitated and resuspended in 10 µl of TE (pH 8). Half of each HIT reaction (5 µl) was archived for later use in -80 °C.

D. Superscript III reverse transcriptase reaction

NMIA modifications on tTR mutants were mapped by annealing 5'-[^{32}P]-labeled conRT or C103 primer to the RNA with the following thermal cycler parameters: 95 °C for 1 min, 65 °C for 5 min, and 35 °C for 10 min. Then 2 µl of 5X First-Strand Buffer (Invitrogen) reverse transcription buffer, 0.5 µl 100 mM DTT, and 0.5 µl 10 mM dNTP mix was added to each RNA solution. One half of the total thymidine in the dNTP mixtures used for ddT reactions was ddTTP. Then 3 µl SHAPE buffer (2 µl 5X FSB, 0.5 µl 100 mM DTT, 0.5 µl 10 mM dNTP mix) or ddT buffer (containing dNTP mix that is supplemented with ddTTP) was added to each primer/NMIA-RNA solution and this was heated at 50 °C for 1 min. 1 µl of Superscript III Reverse Transcriptase (Invitrogen) was aded to each solution, tapped to mix, then the solution was incubated at 50 °C for exactly 4 minutes. Immediately following this incubation, 10 µl 400 mM NaOH was added to each reaction to degrade the RNA, and the samples were incubated at 95 °C for 5 minutes to inactivate the reverse transcriptase. Each solution was then neutralized and prepared for preciptaion by the addition of 14.5 µl Quencher solution (10 µl 400 mM HCl, 3.5 µl sodium acetate, and 1 µl 5 mg/ml glycogen per reaction). Reactions were EtOH precipitated, washed in 70% EtOH, then resuspended in 5 µl formamide

denaturing loading buffer (80% formamide, 0.5X TBE, 4 mM EDTA pH 8, 0.01% bromophenol blue and cyanol blue dyes).

E. Sequencing gel electrophoresis

2.5µl of the radiolabled extension products from step 4 were resolved on a 40 cm X 40 cm denaturing, 8% acrylamide gel (29:1 acrylamide: bisacrylamide/7M urea, 90 mM Tris/borate, 2 mM EDTA) at 2000 volts (70 watts) for approximately 1.5 hours. The gel was dried at 80 °C for 45 minutes on filter paper, then exposed to a phosphorscreen overnight before imaging on a Storm 860 PhosphorImager (Molecular Dynamics). Gel images were visualized on ImageQuant 5.1.

F. SAFA data analysis

Individual band intensities of NMIA and DMSO lanes were integrated using the program SAFA [111]. SAFA utilizes Lorentzian curve integration to determine band densities with a high degree of accuracy. Hit intensities were normalized in the following way. Band intensity was corrected for background by subtracting away the density of the corresponding band in the DMSO control lane. Band intensities were then ranked in descending order, and the top 2% of intensities by value were thrown out. The values representing the next 3-8% were averaged and this average was set to 100%. All other intensities were divided by this average and multiplied by 100 to give a hit frequency percentile ranging 1-100.

G. In vitro reconstitution of telomerase

tTERT was translated and assembled with tTER using a TNT Coupled Reticulocyte Lysate Systems kit (Promega). In brief, each 50 µl reaction contained 1µg pET-28a-tTERT, 75 ng tTER (or tTER mutant RNA), 25 µl rabbit reticulocyte lysate (RRL), and 34 pmole of [^{35}S]-methionine (1175 Ci/mmol (Perkin-Elmer) plus other reaction components specified in the kit. Retic reactions were incubated at 30 °C for 90 min.

H. Telomerase Assay to test effect of tTER mutations on activity

Each 20 µl telomerase assembly reaction contained 10 µl of crude RRL reaction, 1X telo buffer (50 mM Tris pH 8.3, 1.25 mM $MgCl_2$, 5 mM DTT), 0.33 µM [α-^{32}P]-dGTP (3000Ci/mmol), 2 µM telomeric p5 primer (Table 2.2), 100 µM dTTP, and 10 µM dGTP. Reactions were incubated at 30 °C for 1 hour. Proteins were removed from the reaction by phenol/chloroform/isoamyl alcohol extraction and radio-labeled primer extension products were recovered by EtOH precipitation with 0.4M ammonium acetate, 100 µg/ml glycogen, and a 5'-[^{32}P]-labeled 100 nt oligonucleotide as counter ion, carrier, and loading control, respectively. Extension products were resuspended in 3 µl TE, combined with 3 µl 2X denaturing loading buffer and resolved by PAGE on an 8% acrylamide, denaturing, 0.4 mm thick, 40 X 40 cm sequencing gel run at 70 watts for 1 hour. Gels were transferred to filter paper, dried for 1 hour at 80 °C, and exposed to a phosphor screen overnight. Phosphor screens were imaged using a Storm 860 PhosphorImager (Molecular Dynamics) and ImageQuant 5.1 software.

Table 2.1 Primers used to create tTR mutants via site-directed mutagenesis.

	5’ primer	3’ primer
MS1	**CTAATTGGTATCCATATATCAGCA CTAGATTTTTGG**	**GCTGATATATGGATACCAATTAGGTTCA AATAAG**
MS2	**CACTTATTTGATGGAAATTGGTAA GGTTATATCAG**	**TACCAATTTCCATCAAATAAGTGGTAAT GCGG**
MS1-2	**CTTATTTGATGGAAATTGGTATCC ATATATCAGCACTAGATTT**	**GCTGATATATGGATACCAATTTCCATCA AATAAGTGGTAATGCG**

Table 2.2 Primers used for tTR SHAPE project.

Primer name	Sequence
pUC19f	GTAAAACGACGGCCAGT
pUC19r	AACAGCTATGACCATG
5’-tTR+HH	TCTAATACGACTCACTATAGGG
3’-tTER+3’-Linker	GAACCGGACCGAAGCCCGATTTGGATCCGGCGAACCGGATC GAAAAATAAGACATCCATTG
conRT	GAACCGGACCGAAGCCCG
C103	GATAGTCTTTTGTCCCGC
p5	GTTGGGGTTGGGGTTGG

Chapter 3. Identify miRNAs involved in regulating senescence and miRNAs affected by expression of hTERT

Adapted from: Bonifacio, L. and M. B. Jarstfer, *MiRNA Profile Associated with Replicative Senescence, Extended Cell Culture, and Ectopic Telomerase Expression in Human Foreskin Fibroblasts*. Accepted in PlosOne, 2010.

I. Introduction

Senescence is a cellular state characterized by loss of replicative potential and continued metabolic activity that appears to function as a tumor suppressor mechanism but also contributes to aging. Several diverse stimuli including DNA damage, oncogene expression, and telomere attrition can lead to senescence. Even though diverse stresses are capable of inducing senescence, p53, Rb, and more recently Skp2 have been identified as critical pathways common to initiation, execution and maintenance of senescence-associated growth arrest [63,67,75]. Highlighting the importance of p53 in senescence and the role of senescence as a barrier against tumorigenesis, restoration of p53 activity in p53-depleted tumors can cause activation of senescence and tumor regression [62]. These critical pathways of senescence are controlled by a complex network that

regulates chromatin remodeling, proliferation arrest, cell remodeling, activation of the senescence associated secretory pathway, and inhibition of apoptosis [63]. While major effectors of these critical pathways have been identified, a complete understanding of this molecular network is still limited.

Accumulating evidence suggests a role for miRNAs in conveying senescence. MiRNAs are small, 19-23 nucleotide non-coding RNAs that repress the expression of target genes by either preventing translation of the target mRNA or causing its degradation. Recent work by Maes et al [92] compared the miRNA profile of replicative senescence, premature senescence, and serum-starved cells in WI-38 fibroblasts. In this chapter, the miRNA profile for replicative senescence in human BJ fibroblasts is presented and compared to the miRNA expression profile of BJ fibroblasts immortalized by the stable transfection of the catalytic subunit of human telomerase (hTERT). In contrast to WI-38 fibroblasts, BJ fibroblasts express negligible amounts of p16. A comparison of the miRNA profile observed in BJ cells to that observed in WI-38 cells suggests a p16-independent senescence-associated function for several miRNAs that were differentially expressed in both cell lines. In addition, the ability of several miRNAs to specifically affect senescence-induced growth arrest in BJ cells is demonstrated by comparing their expression to that observed in late passage immortalized BJ cells and wild type (WT) contact-inhibited quiescent BJ cells.

Importantly, the observation that several miRNAs are down-regulated over time in BJ-hTERT cells (in contrast to their up-regulation during senescence of

WT cells) and one miRNA is up-regulated in late-passage BJ-hTERT cells (in contrast to down-regulation during senescence) suggests that TERT can affect regulation of senescence associated miRNAs. Finally, despite an abundance of evidence linking miR-34a to senescence [112], evidence in this chapter reveals that it is up-regulated similarly in senescent and late passage BJ-hTERT cells. This may imply that programmed changes in miRNA expression associated with aging independent of senescence can regulate miR-34a expression, at least in BJ fibroblasts.

II. Results

A. Characterization of senescence and extended-passage WT and immortalized BJ cells

BJ fibroblasts were passaged to approximately 50 population doublings before population doubling time and morphologic changes indicated senescence in the WT cell line, and senescence was confirmed by beta-galactosidase staining (Figure 3.1a, b). While the WT fibroblasts grew more slowly as they approached senescence, the immortalized BJ fibroblasts maintained a consistent population doubling time regardless of their passage age. Senescent wild type BJ cells were notably larger and flattened with increased lamellipodia compared to their early passage counterparts. The morphologic changes noted in the WT

cell line during senescence were absent in the immortalized late-passage BJ cells (Figure 3.1c, d).

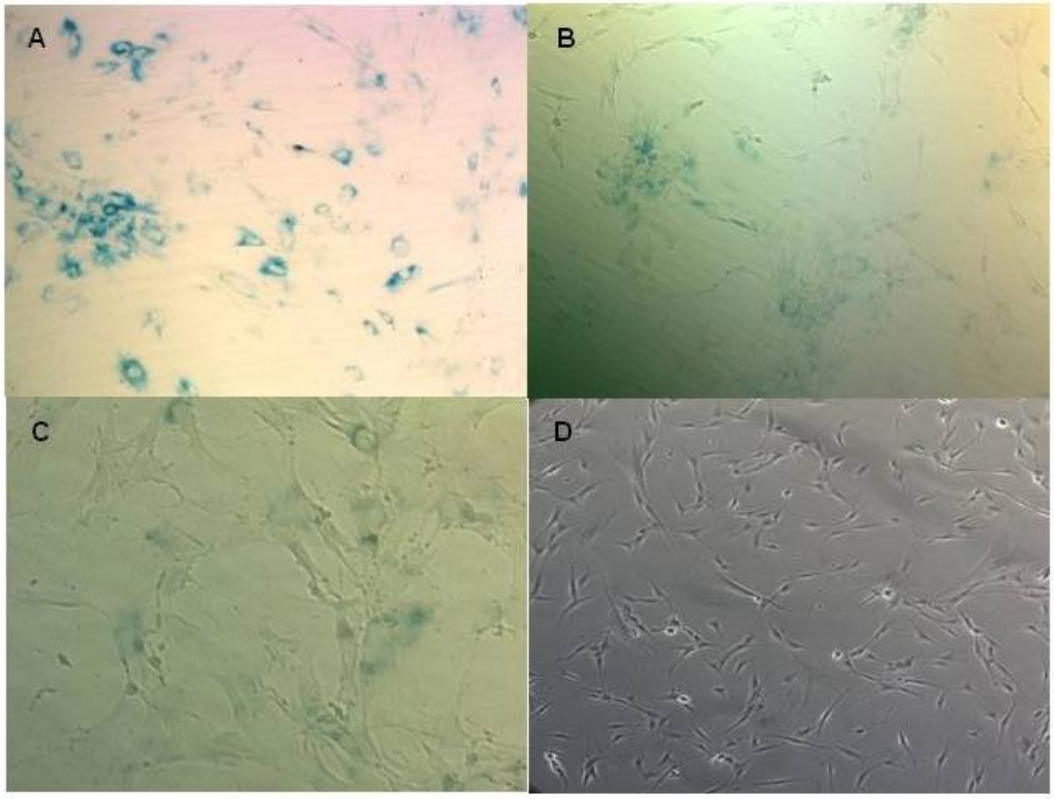

Figure 3.1 Beta-galactosidase staining in senescent WT and late passage immortalized cells. Beta-galactosidase staining is shown as blue cells in senescent WT culture (A) and is absent in the late-passage immortalized BJ cells (B). Senescent BJ fibroblasts (C) are flattened and enlarged compared to early passage WT BJs. Late-passage BJ-hTERT cells (D) do not display senescence-associated morphologic changes.

B. MiRNA profile of senescence in BJ fibroblasts

To identify those miRNAs that are differentially expressed during replicative senescence of BJ fibroblasts, a miRNA microarray platform was utilized that probes for expression of 470 human miRNAs and 64 human viral miRNAs, based on the Sanger miRNA database version 9.1. Microarray results

reveal 83 miRNAs whose expression changed during senescence by more than 1 standard deviation compared to the mean expression of each miRNA in early passage WT fibroblasts (Figure 3.2). Since each total RNA sample was arrayed in duplicate, one of the duplicate signals for a given miRNA must have indicated a change in expression of more than 1 standard deviation from the mean early passage signal for that miRNA to be identified as differentially expressed during senescence. To assist in parsing out those miRNAs that were changed during senescence due to a direct and specific senescence association, the array data from senescent BJ cells and BJ-hTERT cells that were passaged for an equal length of time was compared and contrasted (Figure 3.3).

The microarray results corroborate suggested senescence-associated roles for several miRNAs. The miR-424-503 polycistron as well as miRs-450, 542-3p and 542-5p, which are all within 7kb of the 424-503 polycistron, are significantly up-regulated in senescent BJ cells. This correlates well with previously published evidence indicating that miR-424 and 503 induce G1 arrest when over-expressed in human THP-1 cells by targeting several cell-cycle regulators [112]. Data from the microarray described here also reiterate the senescence associated up-regulation of miR-373* and miR-663 and down-regulation of miR-197 observed in WI-38 cells [92], although less is known about the targets of these miRNAs.

The expression of several miRNAs that appear to be regulated during senescence was validated with quantitative real-time PCR (RT-PCR). MiRNAs for the validation experiment were chosen based on the significance of the

microarray results and published evidence suggesting a role for the selected miRNAs in senescence. RT-PCR data confirm the differential expression of several miRNAs during senescence for which considerable published evidence suggests a role in regulating senescence or proliferation-associated pathways, including miR-34a [113,114,115] and miR-146a [116,117] (Table 3.1).

The senescence-associated expression of several miRNAs with less abundant evidence for senescence-associated function was also validated. This is the first data to reveal that expression of miR-155, a proto-oncogenic miRNA [118,119], is regulated during replicative senescence, consistent with the observed down-regulation in one study of aged WI-38 cells [120] and in aging in humans [121]. MiR-155 was ten-fold down-regulated during senescence of WT BJ fibroblasts. MiR-10b (a miRNA tied to invasion and metastasis in several cancer types) [122,123], and miR-143 and miR-145 (polycistronic miRNAs that are down-regulated in tumors) [124] were also among the most significantly up-regulated (approximately 7-fold, 3.5-fold, and 3.5-fold, respectively) miRNAs during senescence.

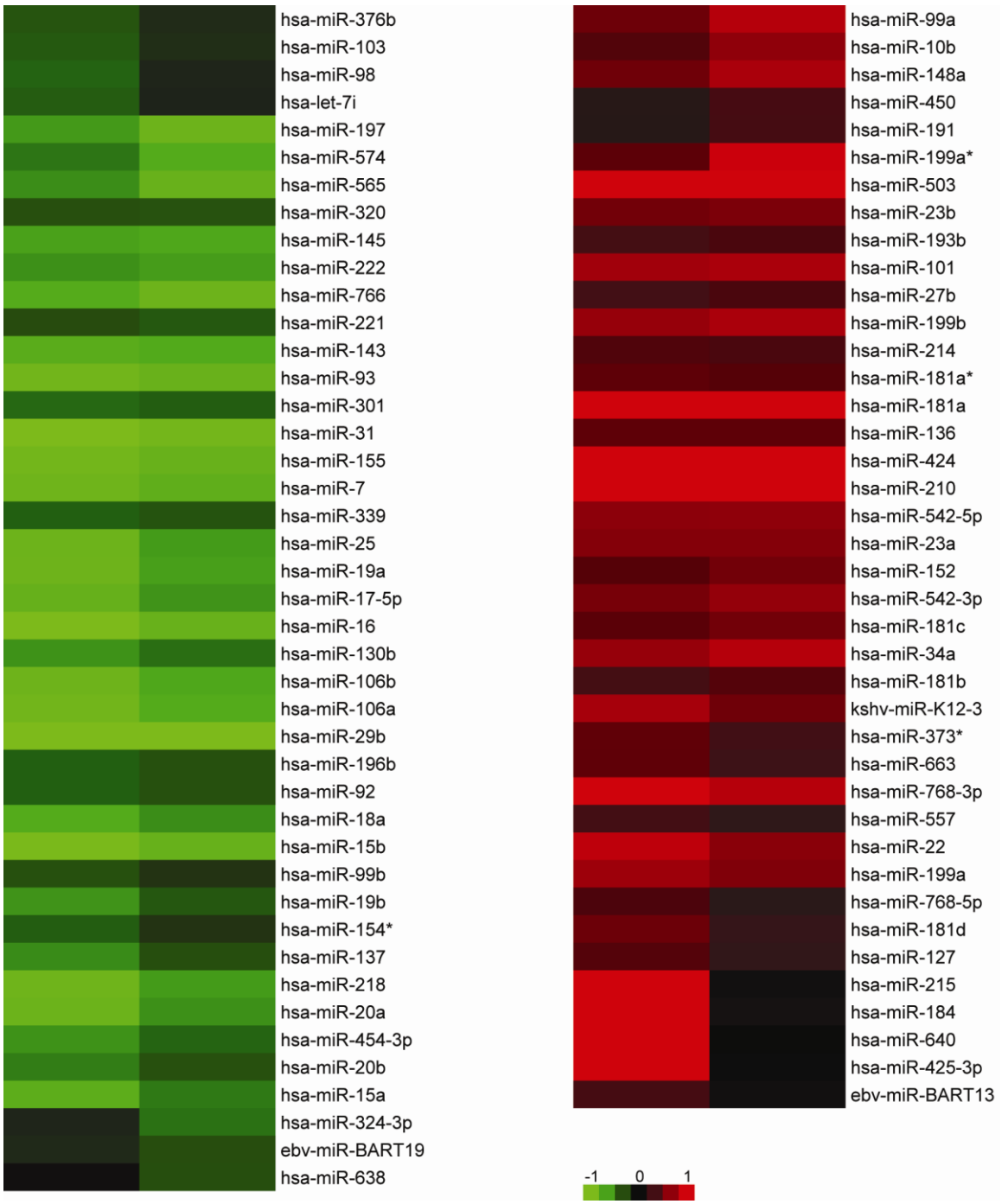

Figure 3.2 MiRNAs differentially expressed during replicative senescence in BJ fibroblasts. 83 miRNAs were differentially expressed (changed by more than 1 SD from the mean expression in early passage) during senescence. Array results are depicted for each duplicate (1 duplicate is represented by each column in the heatmap) of the senescent BJ RNA sample relative to expression in early passage BJ WT cells.

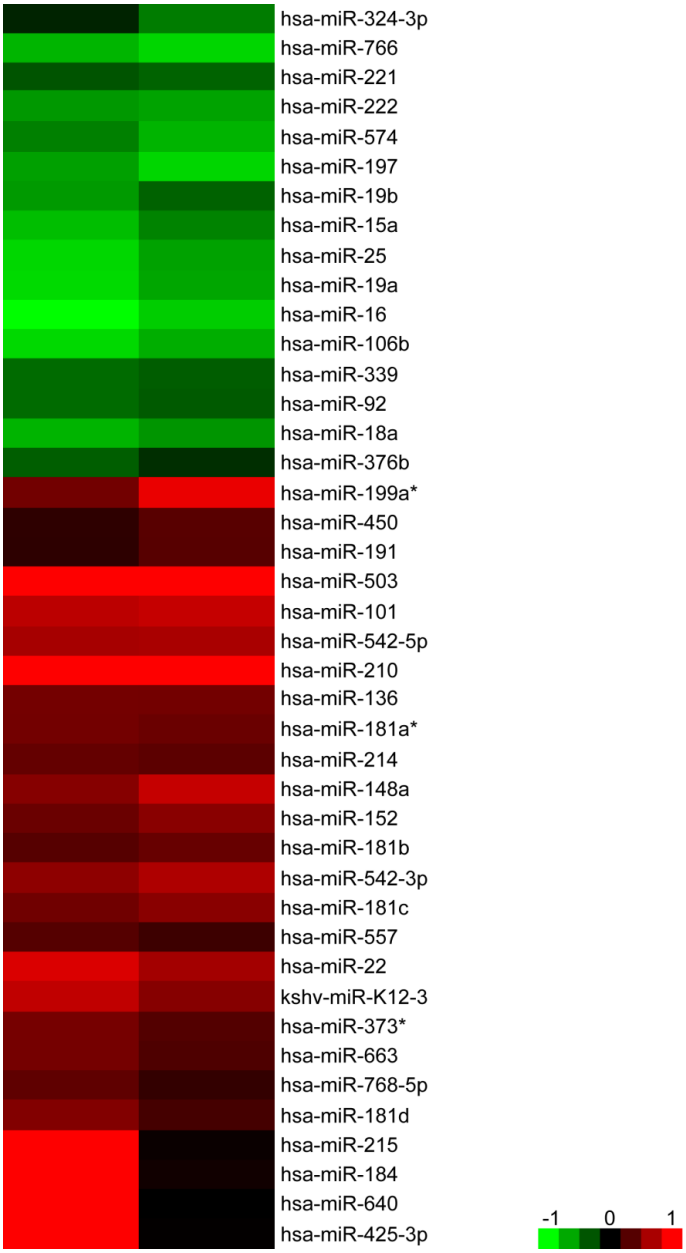

Figure 3.3 MiRNAs regulated in a senescence-specific manner in BJ fibroblasts. Senescence-associated miRNAs that are not differentially regulated in late passage BJ-hTERT cells. Array results are depicted for each duplicate of the senescent BJ RNA sample

MiRNA	Senescent WT BJ fibroblasts*	Early passage BJ-hTERT cells*	Late passage BJ-hTERT cells*	Early passage quiescent WT BJ cells*
Let7c	0.3	0.8	0.7	0.7¥
10b	7.0¥	0.6	13.4¥	4.4¥
19a	1.5	3.3	3.5	1.5¥
21	0.4	1.9	2.3	0.7
23a	3.4¥	1.3	0.9	2.3¥
26a	2.9¥	1.1	1.2	2.1¥
34a	2.6¥	0.9	2.2¥	1.3¥
143	3.6	0.3	0.1	n.d.
145	3.4	0.3	0.1	1
146a	3.4¥	4.9¥	55.4¥	2.1
155	0.1	1	3.2	n.d.
199a-3p	3.2	1.4	1.7	2.2¥
542-5p	3.6¥	1.5	2.3	1.5

Table 3.1 RT-PCR validation of miRNA expression in senescent and quiescent BJ cells and late-passage BJ-hTERT cells. Values reflect average expression (experiments performed in triplicate) relative to the average expression of each miRNA in early passage WT cells. The expression of each miRNA was normalized to that of U6 RNA. Late passage in the wild type cell line indicates senescent cells. *Values reflect expression relative to that in early passage BJ WT cells (set equal to 1). ¥ Denotes statistically significant values relative to 95% confidence interval for experiments in early passage BJ WT cells. n.d. means not detected.

C. Expression of senescence-associated miRNAs during quiescence

In order to determine if the miRNAs validated as being differentially expressed during replicative senescence are associated specifically with replicative senescence pathways or more broadly associated with cell cycle arrest, real-time PCR was used to reveal expression levels of selected miRNAs in early passage, quiescent BJ fibroblasts. For this application, RNA was isolated from BJ WT cells that were population doubling 7 and maintained in a confluent, contact inhibited state for 3 days. Of the miRNAs identified as regulated during senescence and validated with RT-PCR, 6 were confirmed to be up-regulated in senescence and either unchanged or down-regulated (in the case of miR-143) in quiescent cells (Table 3.1). MiR-146a is up-regulated 3.4-fold during replicative senescence and lacks a significant change in expression during quiescence. MiR-145, which is approximately 3.5-fold up-regulated during senescence, is undetected in the quiescent samples. The expression of its polycistronic counterpart, miR-143, is unchanged during quiescence relative to expression in early passage cells. MiR-23a, a miRNA capable of inducing apoptosis in HEK cells [125], is 3.4-fold up-regulated during senescence and shows no change during quiescence. Three of the miRNAs screened for expression during quiescence were up-regulated during both senescence and quiescence (miR-199a-3p, miR-26a, and miR-10b) and one was down-regulated in both senescent and quiescent samples (miR-155).

D. MiRNA profile of extended passage immortalized BJ fibroblasts

To determine if changes in the miRNA footprint of senescent cells were related to extended cell culturing, a BJ cell line (BJ-hTERT) rendered immortal by the stable ectopic expression of hTERT, the telomerase catalytic subunit, was utilized. BJ-hTERT cells experienced the same cell culture conditions as the WT cells and were only differentiated from the WT cell line by the expression of hTERT. RNA from BJ-hTERT cells was used to reveal effects of long term cell culture and the expression of telomerase on miRNA expression. The expression of a few miRNAs increased significantly over time in the immortalized cell line in contrast to a small increase or a decrease over time in the wild type BJ cells (Figure 3.4). One of the most significant examples of this is hsa-miR-155, an oncogenic miRNA [118]. MiR-155 was expressed at similar levels in early passage WT and immortalized BJ fibroblasts soon after transfection (Table 3.1). However, miR-155 levels increased approximately three-fold in the late passage BJ-hTERT cells whereas in senescent WT cells miR-155 decreased ten-fold relative to early passage WT cells. In addition, miR-146a increased 10-fold in the late passage immortalized cell line when compared to the early passage immortalized cells, whereas it increased only 3.4-fold in senescent WT cells. MiR-146a levels were also higher in early passage BJ-hTERT cells compared to the early passage WT cells. Finally, whereas miR-143 and miR-145 were significantly up-regulated in senescent BJ cells, these miRNAs were down-regulated approximately 2 and 3-fold respectively in late-passage BJ-hTERT cells.

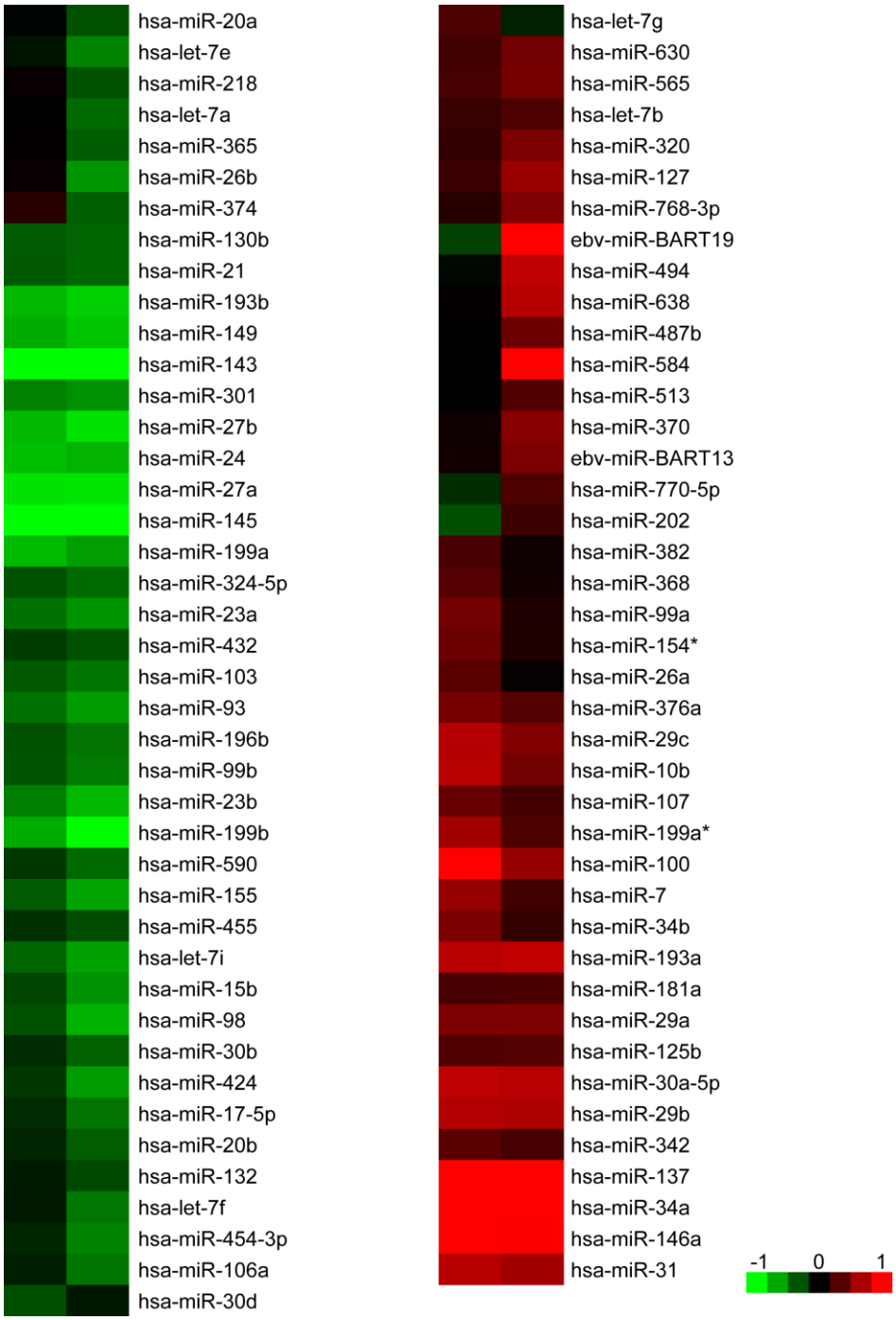

Figure 3.4 MiRNAs whose expression changed over time in BJ-hTERT cells. 83 miRNAs were differentially expressed (changed by more than 1 SD from the mean expression in early passage) during extended culturing of BJ-hTERT cells. Array results are depicted for each duplicate of the late passage BJ-hTERT RNA sample relative to expression in early passage BJ-hTERT cells.

III. Discussion

Senescence is the result of complex input from several pathways. Recent direct and indirect data indicate a role for miRNAs in regulating senescence [92,116,126,127]. In this chapter, an investigation of the roles for miRNAs in senescence was initiated by examining replicative senescence in BJ fibroblasts. Replicative senescence requires significant exposure to cell culture conditions, which potentially influences miRNA expression independently of senescence. For example, recent work reveals an age-related increase in DNA methylation in multiple cell types, including telomerase positive stem cells [52,128]. Further, this hyper-methylation of was shown to be present in both primary cell lines and extended-passage cell culture [51]. This data suggests the potential for programmed genetic changes to contribute to cellular aging independent from senescence. To differentiate the impact of extended culture on the miRNA profile from changes in miRNA expression related specifically to senescence, the expression of miRNAs in late passage immortalized BJ-hTERT cells and senescent WT BJ fibroblasts were compared.

A. MiRNAs with Significant Link to Senescence Pathways

Of the 470 human miRNAs and 64 human viral miRNAs screened, 83 showed differential expression in BJ fibroblasts during replicative senescence. Many of the miRNAs up-regulated in senescent BJ cells, as revealed in the array data, could be plausibly linked to senescence via published data that supports a role for the given miRNAs in a senescence-associated pathway. For example,

the miR-424-503 polycistron, miR-542-5p and 3p, and miR-450, all of which are likely to be part of the same primary transcript [112], are up-regulated significantly in senescent BJ cells. These results are consistent with previous reports showing that miR-424 and miR-503 are capable of inducing G1 arrest in multiple cell types [112,129]. These data also corroborate the up-regulation of miR-373* and miR-663 and down-regulation of miR-197 observed in senescent and quiescent WI-38 cells [92]. While little is known about the pathways regulated by these miRNAs, the fact that these miRNAs are regulated in replicatively senescent BJ cells implies a p16-independent senescence function.

Notably, array and RT-PCR results assisted in identification of a pair of miRNAs with previously characterized roles in cancer cells, but an unclear role in regulating proliferation of normal human cells. MiR-143 and miR-145, both processed from the same primary transcript, are up-regulated approximately 3.5-fold during senescence in WT BJ cells and either show no change or are down-regulated in the quiescent BJ cells. Further, both miRNAs are significantly down-regulated in late-passage BJ-hTERT cells. Together with the reported down regulation of miR-143 and miR-145 in several cancer cells, this suggests that miR-143 and miR-145 have a general role in regulating cellular proliferation and may function as tumor suppressor miRNAs. Consistent with this hypothesis, forced expression of these two miRNAs in cancer cells resulted in decreased growth [130]. In Chapter 4, the ability of miR-143 to influence growth arrest in BJ cells will be examined.

B. MiRNAs Affected by TERT Expression and Extended Cell Culture

Surprisingly, the expression pattern of some miRNAs changed differently overtime in late-passage immortalized BJ cells when compared to the WT senescent BJ cells. MiR-146a, which appears to function in a negative feedback loop to suppress the senescence associated secretory pathway [116] is expressed at 5-fold higher levels in early passage BJ-hTERT cells, relative to early passage WT cells, and undergoes an even more pronounced up-regulation in late passage BJ-hTERT cells (10-fold higher in late passage BJ-hTERT compared to senescent BJ cells). MiR-146a has been shown to down-regulate IRAK1 (part of the IL-1 signaling pathway) in response to inflammatory signaling that occurs during senescence [116]. Another major inflammatory signaler, the Wingless family (Wnt) proteins, participate in pathways controlling differentiation, inflammation, and tumorigenesis [131]. Evidence supports the altered regulation of Wnt genes in cells which have bypassed senescence and undergone transformation. For instance, the Wnt2B gene is in a chromosomal region known to be deleted and rearranged in a variety of cancers [132]. In addition, a recent report revealed that hTERT facilitates Wnt signaling by binding BRG1, a histone remodeling protein that signals through the β-catenin pathway, to affect proliferation and cell survival of progenitor cells [133]. Perhaps ectopic expression of TERT in a somatic cell line such as BJ fibroblasts stimulates robust Wnt and pro-inflammatory signaling causing up-regulation of miR-146a as part of a negative feed-back loop.

Another miRNA exhibiting a significant increase in expression over time in BJ-hTERT cells is miR-155. This is in contrast to a gradual decrease over time in WT BJ cells with an ultimate 10-fold down-regulation at senescence compared to expression during early passage populations. The down-regulation of miR-155 during senescence in BJ cells is consistent with published data indicating its role in promoting tumorigenesis [134]. MiR-155 expression is induced by a number of inflammatory mediators and is directly induced by AP-1 binding within its promoter [135]. AP-1 is a validated suppressor of the hTERT promoter in human cells [136]. It's possible that the over-expression of hTERT in BJ fibroblasts activates a negative feedback pathway that up-regulates AP-1, thereby inducing expression of miR-155. Alternatively, if ectopic expression of hTERT engages the Wnt pathway as has been proposed [133], any number of the resultant up-regulated inflammatory modulators may be involved in the up-regulation of miR-155 in late-passage BJ-hTERT cells.

Although miR-34a has been linked to senescence via numerous publications [87,91,92], we demonstrate up-regulation of miR-34a in late-passage BJ-hTERT cells to a similar degree as that observed in senescent WT cells. Based on the previous observation that miR-34a is more frequently down-regulated in colorectal cancer cells compared to adenomas, in contrast to the frequent down-regulation of miR-143 and miR-145 in both cancer cells and adenomas, it has been implied that miR-143 and miR-145 regulate processes implicated in earlier phases of tumorigenesis [130]. Thus, I postulate that miR-143 and miR-145 are critically involved in regulating the G1/S transition, whereas

miR-34a may have broader roles in regulating stress response, including the stress of long-term cell culture conditions.

By profiling the miRNA expression in early passage and senescent human BJ fibroblasts and comparing this to an immortalized version of these cells that expresses the human catalytic component of telomerase (hTERT) and quiescent samples of early passage WT fibroblasts, the following subsets of miRNAs have been identified: miRNAs whose expression is regulated in the setting of replicative senescence in human fibroblasts devoid of substantial p16 activity and miRNAs whose expression is regulated over time in the presence of enforced hTERT expression. This accounting of miRNAs affected by the ectopic expression of TERT will help fill in the details regarding the relationship between telomerase, replicative senescence, and senescence-independent aging.

IV. Materials and Methods

A. Cell Culture.

Human BJ foreskin fibroblasts (ATCC) were cultured at 37 °C in a 5% CO_2 incubator in MEMα supplemented with 1mM sodium pyruvate, 1.5 g/L sodium bicarbonate, and 10% fetal bovine serum. Replicative senescence was induced by serial passage and was determined by observing an arrest in the growth rate, changes in cell morphology and senescence-associated β-galactosidase staining. HEK 293TS cells were used to generate retrovirus for stable transfection of hTert.

B. Immortalized BJ fibroblasts.

BJ fibroblasts were immortalized by stable transfection with the catalytic subunit of human telomerase (hTERT). First, 250 µl serum-free media was incubated with 30 µl fugene, 3 µg packaging plasmid 467, and 3 µg pBabe-hTERT-hygro plasmid (a generous gift from Dr. Christopher Counter, Duke University) [25] at room temperature for 15 minutes. HEK 293TS cells that were 40-50% confluent were then transfected with this mixture. Twenty four hours after transfection, 5 mls of virus-laden media passed through a 0.45 µm filter was used to infect BJ fibroblasts in the presence of 4 µg/ml polybrene and 3 ml non-selective media. Twenty four hours after infection, the media was changed. Twenty four hours after the media change, the infected cells were split 1:2 and transduced cells were selected for in 100 µg/ml hygromycin. A horizontal spread assay (mock transduction) was conducted to determine that BJ cells were free of contamination by virus-producing HEK cells. Expression of hTERT was verified in the immortalized cells by using the TRAPeze Telomerase Detection kit (Chemicon.)

C. Senescence-associated β-galactosidase staining.

Cell staining was performed using a kit from Cell Signaling Technology with samples grown in a 6-well plate. After removing growth medium from the cells, the cells were washed with PBS and fixed for 15 minutes at room temperature. The cells were then washed twice with PBS and stained with X-gal staining solution overnight at 37 °C following the manufacturer's protocol.

D. MiRNA microarray sample preparation, hybridization, and analysis.

Total RNA was isolated from wild type early passage and senescent cells, as well as immortalized early and late passage cells using mirVana miRNA Isolation kit (Ambion). Sample quality was verified by measuring the ratio of 28S to 18S rRNA (initially by denaturing agarose) and again just before the array analysis using the Agilent 2100 Bioanalyzer. 200 ng total RNA was dephosphorylated with CIP and labeled with pCp-Cy3. Labeled RNA was purified via spin column and hybridized to the Agilent miRNA microarray chip version 1. Details of protocol version 1.5 can be found on www.agilent.com. Mean signal for each probe was quantile normalized and $\log_2$ transformed. Signals that mapped to the same miRNAs were collapsed into individual miRNAs by averaging. Each cell line high passage miRNA array was normalized to its corresponding low passage miRNA array. MiRNAs that differed one standard deviation or more from the their mean expression in early passage WT cells were identified. MiRNAs changing over time (specifically in the WT cell line and not the immortalized cells) were identified by selecting only those miRNAs that differed by more than one standard deviation in the WT BJs but not in the immortalized cells. The array data are MIAME compliant and have been deposited at the GEO database at the NCBI: accession number GSE22134.

E. Quantitative real-time PCR.

Selected miRNA microarray expression results were validated using the miRNA Taqman Assay (Applied Biosystems). PCR experiments were

performed in triplicate using the Applied Biosystems 7500 Real Time PCR instrument and normalized to the expression of U6. 10 ng of total RNA was reverse transcribed using a miRNA-specific primer then 1 µL of RT product was subjected to real-time PCR with a miRNA-specific probe.

Chapter 4. Elucidating the Role of miRNAs and TERT in Proliferation/Inflammation Pathways

I. Introduction

In Chapter 3 the miRNA footprint of replicative senescence in human foreskin (BJ) fibroblasts was defined. Specifically, 83 miRNAs were identified that are differentially expressed during senescence. We showed for the first time that anti-proliferative miRNAs miR-143 and miR-145 are up-regulated significantly and the pro-proliferative miR-155 is significantly down-regulated during replicative senescence. Interestingly, these miRNAs undergo contrasting regulation during extended proliferation in fibroblasts stably expressing ectopic hTERT. Specifically, miR-143 and miR-145 are down-regulated over time in BJ-hTERT cells, while miR-155 is up-regulated over time in these immortalized cells.

MiR-143, located on chromosome 5, is transcribed as part of a primary transcript that also contains miR-145. Both miRNA effectors in this polycistronic transcript are predicted to attenuate the expression of proteins involved in regulating the cell cycle [137,138,139]. In addition, previous evidence revealed that tumor growth is inhibited by enforced expression of miR-143 [130]. Using *in silico* miRNA target prediction tools, potential targets of miR-143 and miR-145 were identified that would, upon validation, elucidate molecular details regarding the anti-proliferative effects of these miRNAs. Insight into the details of these

miRNA-controlled pathways would clarify the link between regulation of senescence and tumorigenesis. Experiments aimed towards validation of a potential target of miR-143 involved in regulating cell cycle and senescence-induced growth arrest will be described in this chapter.

MiR-155 has well established pro-proliferative roles in various cell types and recent evidence suggests a role for this miRNA in sensing inflammatory signaling and initiating anti-inflammatory pathways as well [134,135]. In Chapter 3, it was revealed that miR-155 is down-regulated during senescence and surprisingly undergoes robust up-regulation during extended cell culture in BJ-hTERT cells. Evidence is accumulating to support the ability of telomerase to confer pro-proliferative effects upon a cell by pathways separate from those involved in telomerase extension of telomeres [99]. In this chapter, possible mechanisms for TERT-mediated regulation of proliferation and inflammatory pathways by influencing expression of miR-143, 145, and 155 will be presented as well as preliminary evidence towards characterizing these hypotheses.

II. Results

A. Senescence-associated miR-143 induces cell cycle arrest in WT BJ cells

To determine whether miR-143 is sufficient to modulate the proliferative ability of BJ fibroblasts, as opposed to the possibility of it being up-regulated independently of cell cycle arrest, we transfected young BJ cells with miR-143 mimic and observed effects on proliferation with the sulforhodamine B (SRB)

assay. MiR-143 inhibited the proliferation of young BJ cells in a dose-dependent manner. At a concentration of 60 nM, miR-143 inhibited proliferation to a degree comparable to growth inhibition caused by serum starvation (Figure 4.1). Analysis by one-way ANOVA suggests that inhibition of cell growth in cells transfected with miR-143 mimic is not statistically different from the inhibition caused by serum starvation, but produces a statistically significant difference in cell proliferation compared to untransfected cells.

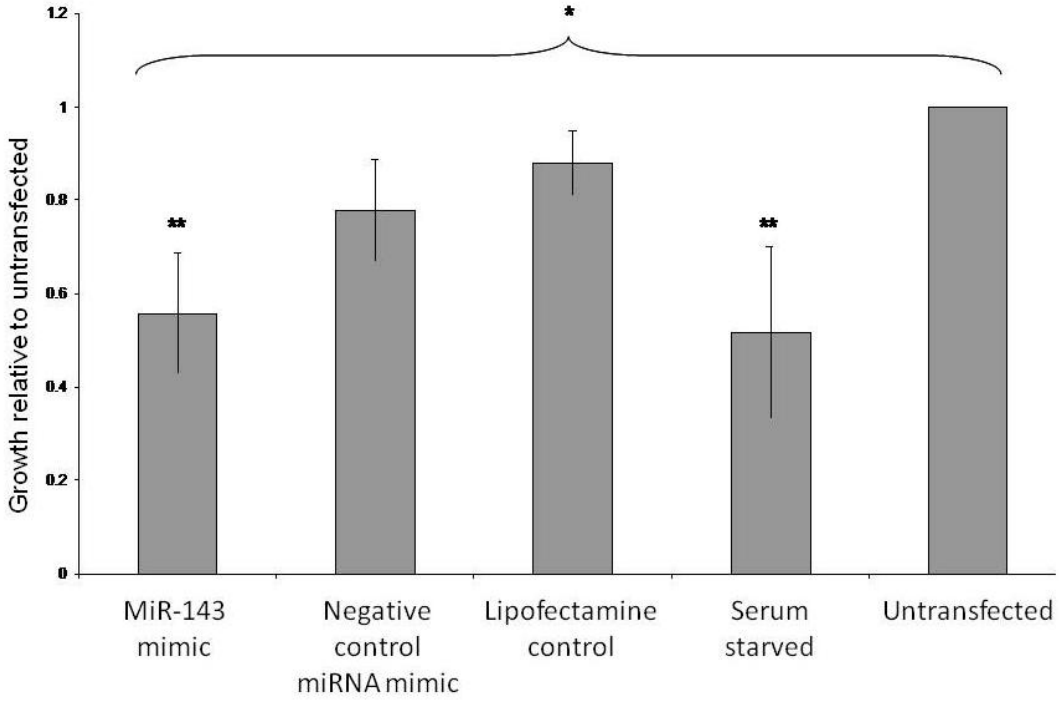

Figure 4.1 MiR-143 represses cell growth similarly to serum starvation. Transient transfection with miR-143 mimic repressed cell growth in WT BJ cells to a similar extent as serum starvation. Cell proliferation 72 hours after transfection was assessed by the sulforhodamine B assay and is shown here relative to untransfected cells (set to 1). *A statistically significant difference in the variance between denoted groups is observed via one-way ANOVA. **Denotes lack of statistically significant difference between indicated groups. Cell population of serum starved sample is equal to biomass of cells at time of transfection, indicating serum starvation causes complete inhibition of growth (data not shown).

To determine the nature of miR-143 induced growth arrest, early passage BJ WT cells were transiently transfected with 60 nM miR-143 mimic. 48 hours after transfection, the cells were stained for senescence associated β-galactosidase (SA β-gal) activity. β-gal activity is normally only observed at low pH's, however in senescent cells it can be observed at pH 6 due to increased activity of the lysosomal enzyme in these cells. The increased SA β-gal activity

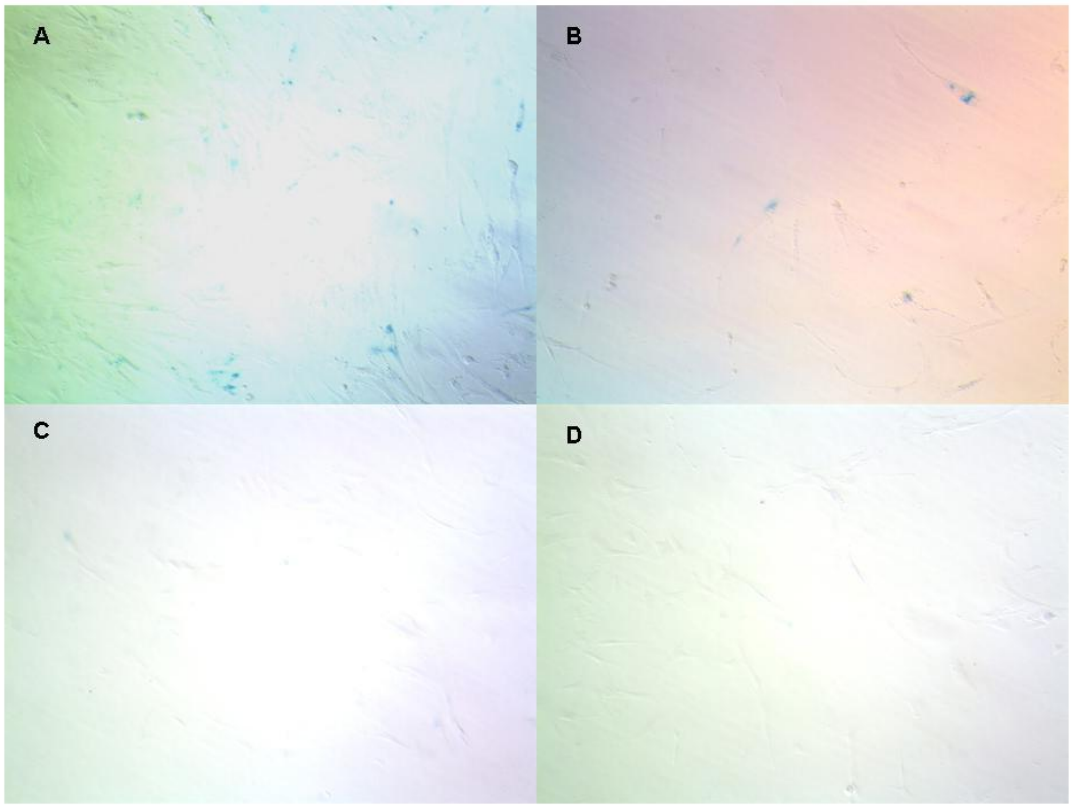

Figure 4.2 Early passage BJ cells transfected with miR-143 mimic have increased β-galactosidase activity. Early passage BJ fibroblasts were transfected with miR-143 mimic and stained for β-galactosidase activity (A and B). Cells positive for β-galactosidase activity appear blue. Untransfected early passage BJ cells are shown as a control (C and D).

observed in miR-143 transfected cells compared to untransfected cells (Figure 4.2) and an arrest of proliferation suggest that senescence is induced in young WT BJ fibroblasts by over-expressing miR-143.

B. MiR-143 Target Prediction

Although others have shown that miR-143 can inhibit proliferation of cancer cells and demonstrated the down-regulation of miR-143 and polycistronic counterpart miR-145 in tumors [130], the proliferation and survival pathways regulated by these miRNAs in non-transformed cells remain elusive. *In silico* miRNA target prediction algorithms TargetScan [140], Microcosm, and Pictar-Vert [137,138,139] were used to identify potential targets of miR-143 and miR-145 germane to regulation of proliferation and senescence in BJ fibroblasts. Validated targets of miR-143 known to affect cell cycle include DNA methyltransferase (DNMT3a) [141] and KRAS [142]. Likewise, miR-145 has been shown to affect cell growth by regulating expression of insulin receptor substrate-1 (IRS-1) [143,144], cyclin D1 and eIF4E [145]. One particularly intriguing (and currently unvalidated) predicted target of miR-143, cell division control 6 (CDC6), is a licensing factor for origins of DNA replication and is thus essential for entry into S phase [146]. One site within the CDC6 3'UTR that is predicted to bind miR-143 is conserved among 3 species – *H. sapiens, M. mulatta, and C. familaris*. This site bears near perfect complementarity to the miR-143 seed sequence with the exception of two G-U wobbles, the most common and highly conserved non-canonical base pair in RNA [147]. All current online miRNA target prediction algorithms incorporate a requirement for

evolutionary conservation and are restricted to searches within the 3'UTR of mRNA sequences. This is likely based on the fact that the first miRNAs discovered interacted with their targets via recognition of sites within their 3'UTR [148,149]. However, more recent data has indicated the ability of miRNAs to regulate target gene expression by interaction with regions within the coding sequence and 5'UTR of target mRNAs [150]. Another site bearing perfect complementarity to the miR-143 seed sequence was discovered by manually scanning within the CDC6 coding region sequence; this potential miRNA-complimentary sequence resides in an exon 374 nucleotides upstream from the start of the 3'UTR (Figure 4.3).

Data from recent work also supports the notion that miRNA recognition elements that are not conserved across species can regulate expression of their mRNAs [151]. Based on these concepts, a new miRNA-target prediction algorithm was developed named rna22. Rna22 differs from all other miRNA-target prediction algorithms used in this study in that it does not constrain prediction of potential MREs to the 3'UTR and does not enforce a requirement for cross-species conservation of MREs. Using rna22, an additional one potential miR-143 miRNA recognition element (MRE) is identified within the CDC6 3'UTR plus one additional MRE in the open reading frame (ORF) [152].

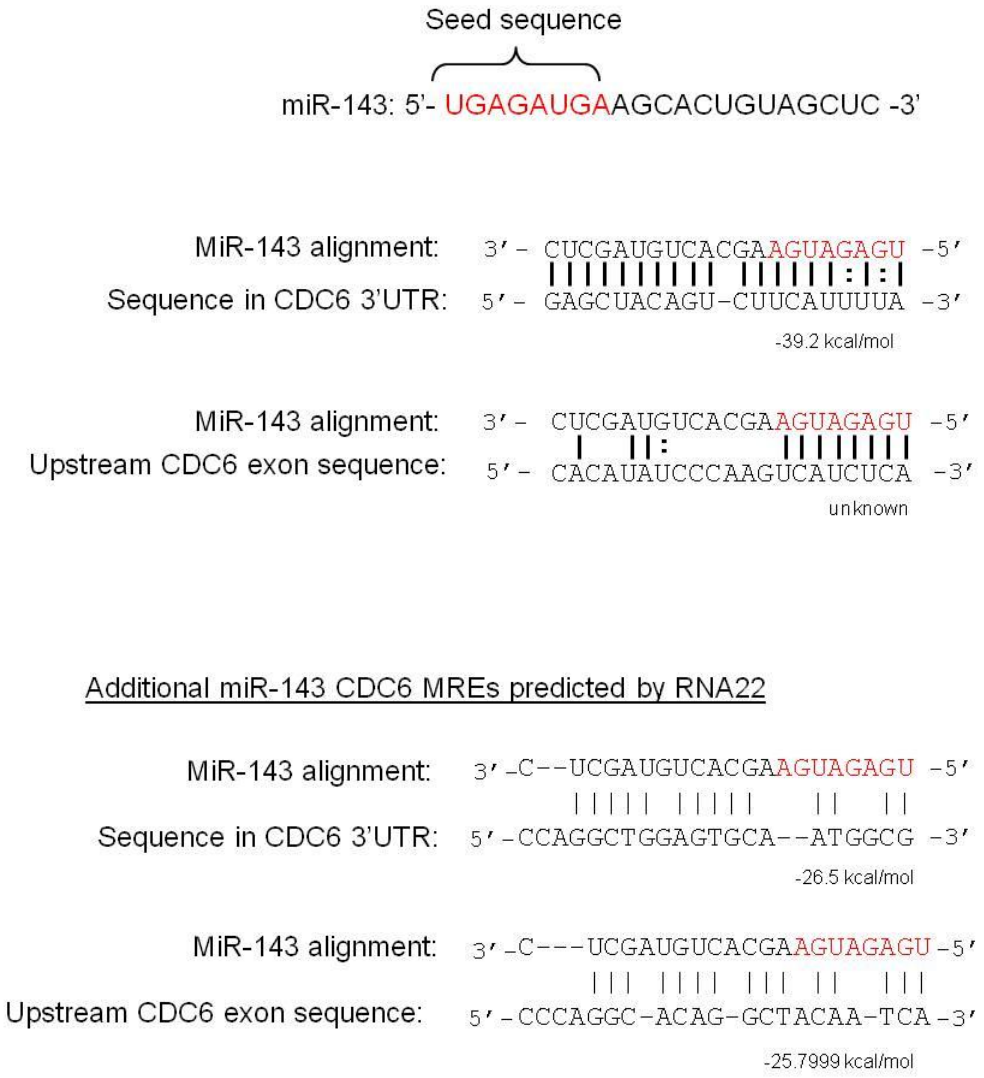

Figure 4.3 MiR-143 CDC6 predicted alignment. MiRNA target prediction algorithm TargetScan identifies a site within the CDC6 3'UTR with extensive complementarity to miR-143. A site within the CDC6 coding region that bears complete complementarity to the miR-143 seed sequence was also identified by manual scanning. RNA22, a new target prediction algorithm, predicts two additional miR-143 MREs within CDC6.

C. MiR-143 does not inhibit growth of NHF1-hTERT cells expressing mutant CDC6

To assess the requirement for miR-143 recognition and regulation of CDC6 to inhibit proliferation, SRB assays were performed with NHF1 cells stably expressing hTERT and a modified CDC6 construct lacking the 3'UTR (CDC6Δ).

Another variation of this cell line bearing mutation of three CDC6 serine residues to aspartic acid (mutations that render CDC6 resistant to degradation by APC [153]) was also included in these assays (CDC6ΔS3D). Ectopic miR-143 expression did not affect proliferation of NHF1 CDC6Δ or the CDC6ΔS3D cells. However, miR-143 over-expression also had no impact on proliferation in NHF1-hTERT cells expressing only endogenous CDC6 (Figure 4.4).

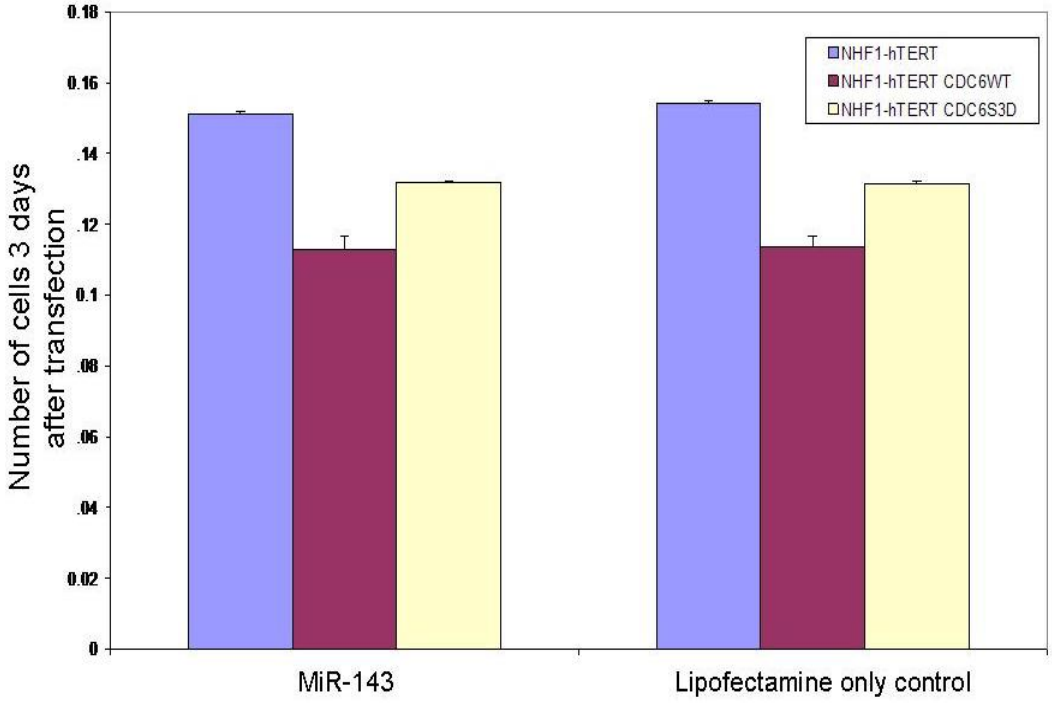

Figure 4.4 CDC6 3'UTR influence on miR-143 induced growth arrest. Transient transfection of miR-143 mimic did not induce growth arrest in cells overexpressing a mutant CDC6 lacking the 3'UTR (CDC6Δ) or a constitutively active version of this mutant (CDC6ΔS3D).

D. Ectopic TERT expression prevents miR-143 induced growth arrest

I previously observed that ectopic expression of TERT in BJ cells impacts miRNA expression. Specifically, in BJ-hTERT cells, miR-143 and miR-145 are

significantly down-regulated over time as opposed to the up-regulation observed during senescence of WT cells. Also, it should be noted that ectopic miR-143 expression in immortalized NHF1 cells that stably express a truncated form of CDC6 lacking the 3'UTR had no effect on proliferation (Figure 4.4).

In order to determine whether the observation that TERT interferes with miR-143 induced growth arrest was cell type specific (to the NHF1 cells), BJ-hTERT cells were transfected with miR-143 and the effects on proliferation were determined by the SRB assay. MiR-143 over-expression in BJ-hTERT cells had no impact on proliferation compared to untransfected cells (Figure 4.5).

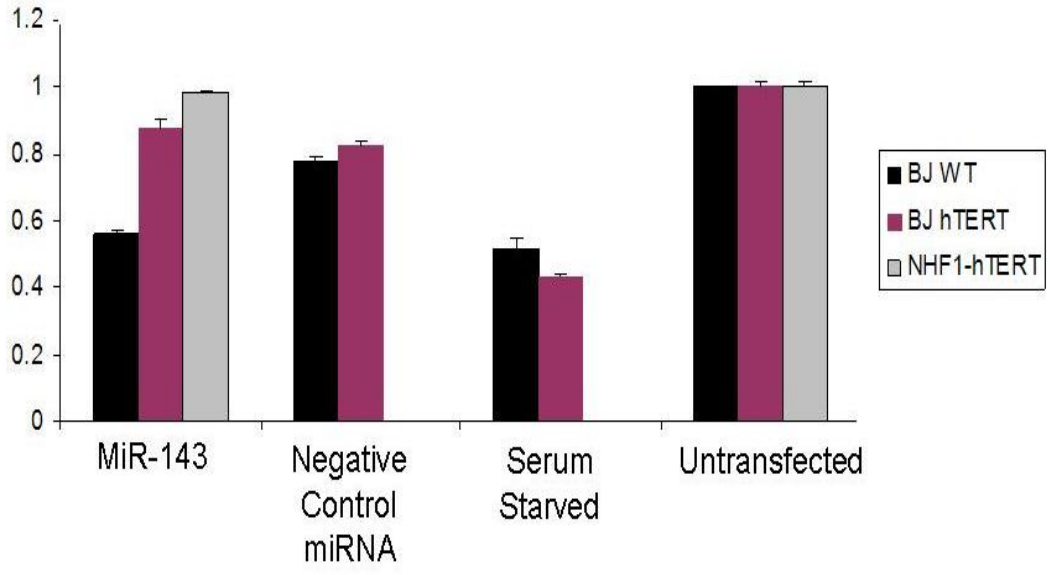

Figure 4.5 MiR-143 does not induce growth arrest in cells expressing ectopic TERT. Transient transfection with miR-143 mimics did not induce growth arrest in BJ or NHF1 cells that stably transfected with hTERT. Results were obtained by SRB.

E. TERT effect on CDC6 expression

To determine whether CDC6 levels are regulated in cells in response to the altered miRNA expression profile associated with senescence and TERT expression, western blotting was used to reveal CDC6 protein levels in early and late passage WT BJ cells, BJ cells with control pBabe vector (lacking the hTERT insert), and BJ-hTERT cells (Figure 4.6). No significant difference in CDC6 expression between the samples representing early and late passage BJ cells was observed. However, CDC6 levels were higher in BJ-hTERT cells (both early and late passage samples) compared to BJ WT cells.

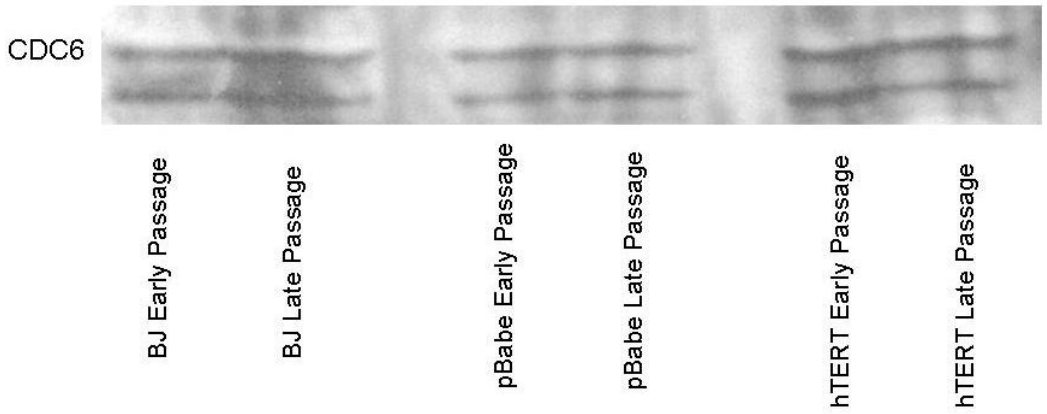

Figure 4.6 CDC6 levels in cells with varied miR-143 expression. CDC6 levels were obtained by western blotting in early and late passage BJ cells. Cell lines shown include BJ WT, BJ cells stably expressing the pBabe vector, and BJ cells stably expressing hTERT. BJ Late passage and pBabe Late Passage cells indicate senescent populations.

F. MiR-145 is predicted to regulate expression of genes in the CDC6 pathway

Although gross differences in the level of endogenous CDC6 were not detected in senescent WT BJ fibroblasts (compared to early passage BJ cells), it is still possible that miR-143 might attenuate CDC6 expression causing a biologically relevant phenotype. MiR-143 and miR-145 are polycistronic miRNAs that are part of the same pri-miRNA precursor. One might predict, based on this fact, that miR-143 and miR-145 should target proteins within the same pathway since they will be coordinately regulated at the transcriptional level. Using TargetScan miRNA-target prediction algorithm [140], several potential targets for miR-145 that function within the cell cycle and/or CDC6 pathways were identified, including E2F3, Skp1, and Cyclin D2.

III. Discussion

It is well established that miRNAs can have a profound impact on cellular proliferation and differentiation [154,155,156,157]. Less established is the role of miRNAs in regulating important cellular checkpoints such as the G1/S and G2/M transitions. An essential role for miRNAs in regulation of these transitions is implied by the observations that miRNAs are generally down-regulated in tumors, and Ras-induced senescence is prevented by ectopic expression of a set of miRNAs that inhibit p21 [158]. In addition, several miRNAs have been identified that are differentially expressed during replicative senescence of WI-38 cells [92]

and human mesenchymal stem cells [159] and in aging human mononuclear cells [160] .

The level of telomerase expression is a key factor in determining the propensity of a specific cell type to senesce in a physiological setting. This effect is partly explained by the fact that prevention of telomere attrition by telomerase inhibits DNA-damage induced senescence. However, accumulating evidence also suggests a role for telomerase in promoting proliferation through pathways separate from telomerase action at the telomere [96,99,100]. To date, no data explains how the pro-proliferative properties of telomerase may contribute to regulation of senescence.

Our initial studies revealed that two polycistronic anti-proliferative miRNAs, miR-143 and miR-145, and the proto-oncogenic miR-155 undergo regulated changes in expression during replicative senescence of BJ fibroblasts. Although data exists to support a role for these miRNAs as tumor suppressors [130,145] and oncomir, respectively, the mechanism by which these miRNAs regulate cell proliferation and their role in regulating proliferation in non-transformed cells remains to be defined. We present evidence herein to support the ability of TERT to affect expression of these senescence-associated and pro-proliferative miRNAs and preliminary results from experiments designed to elucidate the molecular details of proliferation pathways controlled by miR-143.

A. Ectopic miR-143 induces senescence in BJ WT but not BJ-hTERT cells

Although many miRNAs are regulated during senescence, it was previously unclear whether any one specific miRNA is sufficient for induction of senescence. Our previous experiments characterized the regulation of miR-143 and polycistronic partner miR-145 during senescence in a cell line that is p16-deficient, implying a strong probability for the requirement of p53-mediated pathways in conveyance of replicative senescence. It has been previously shown that p53 enhances the maturation of mirR-143 and miR-145 in human diploid fibroblasts (WI-38 and TIG3 cell lines) in response to DNA damage [161]. It is also established that ectopic introduction of miR-143 into tumor cells results in decreased proliferation and tumor regression. In order to determine whether miR-143 is capable of inducing senescence in fibroblasts, we transiently transfected early passage BJ WT and BJ-hTERT cells with miR-143 mimic. Introduction of miR-143 into early passage BJ WT cells resulted in complete growth arrest (similar to serum starvation) and increased SA β-gal activity (Figures 4.1 and 4.2). Notably, however, the transfected cells did not show a distinct shift towards senescence-associated morphology (larger, flattened cells with increased blebbing). In addition, while SA-β-gal was increased in cells expressing ectopic miR-143 mimic, it wasn't as prolific as that seen in WT BJ senescent cells. This could potentially be explained by an examination of experimental timing and the time required for full induction of senescence. Here, cells were stained 48 hours after transfection with miR-143 mimic. We suggest that perhaps the conglomerate of senescence-associated changes that occur within a cell (including membrane remodeling, differential protein expression, and

full induction of senescence-associated inflammatory signaling) may require greater than 48 hours from the first stimulus to senesce for easiest detection. Another possible reason for relatively slow induction of the senescence phenotype after transfecting with miR-143 is the possibility that miR-143 targets essential for inducing senescence may have long half-lives within the cell.

Interestingly, introduction of miR-143 mimic into BJ-hTERT cells did not induce any discernable phenotypic changes or growth arrest (Figure 4.5). Our initial array and RT-PCR studies (chapter 3) revealed that endogenous mature miR-143 is expressed at significantly lower levels in early and late passage BJ-hTERT cells (5 and 10-fold lower, respectively) compared to early passage BJ WT cells. The ability of TERT to prevent miR-143 induced growth arrest is not cell type specific, as we observed similar effects in NHF1 cells. One hypothesis is that TERT may up-regulate a target of miR-143 that is essential for inducing senescence growth arrest. Alternatively, TERT may alter expression of other proteins capable of impacting miR-143/miR-145 expression. If a miR-143 target is up-regulated in BJ-hTERT cells, this target may function in a negative feedback fashion to inhibit miR-143 expression, explaining the endogenous down-regulation of miR-143 in immortalized cells.

B. Potential TERT/miR-143 mediated proliferation pathways

Using *in silico* miRNA target prediction algorithms, cell division cycle 6, or CDC6, was identified as a potential target of miR-143. Initial studies were focused on validation of this miRNA-target pair for several reasons. First, CDC6 is key mediator of a cell's ability to enter S phase [162,163], and senescent cells

are unable to make this G1/S transition in the absence of oncogenic signaling. Target prediction algorithms were also used to predict proliferation-associated targets for miR-145. Theoretically, miR-145 should inhibit the expression of proteins relevant to the pathways regulated by miR-143, since the two miRNAs are transcribed coordinately as part of the same pri-miRNA. Several proteins were identified whose transcripts are predicted to be targeted by miR-145 that function within the CDC6 pathway. Specifically, miR-145 is predicted to target E2F3, a prominent transcription factor that is responsible for expression of CDC6 [164,165]. Skp1, also predicted to be targeted by miR-145, is part of the SCF-ubiquitin ligase complex responsible for degrading p27 via direct phosphorylation by cyclin E-CDK2. The cyclin E-CDK2 complex is recruited to origins of DNA replication by CDC6 [166,167]. Finally, cyclin D2, a component of the complex that phosphorylates and inactivates pRB leading to E2F transcription factor activation, is predicted to be a target of miR-145.

To explore the ability of miR-143 to affect CDC6 expression, the levels of endogenous CDC6 in early and late passage BJ WT and BJ-hTERT cells were first examined using western blotting. MiR-143 and miR-145 levels are approximately 3.5-fold higher in senescent WT cells, and thus one would expect that CDC6 levels would be lower in senescent cells if it is a miR-143 target. Unfortunately, there was no detectable difference in CDC6 levels between early and late passage WT cells using this approach. However, there are several caveats to using this type of approach to validate a miRNA-target relationship that support the need for using additional methods to test this relationship. First,

although senescent cell lysates were derived from a cell population that was senescent as a whole, the population is actually heterogenous since we did not sort cells. Second, it isn't clear to what extent miRNAs can regulate expression of their targets singly or require co-recognition by other miRNAs to realize significant target attenuation producing phenotypic changes. Also, *ex vivo* biochemical assays utilizing reporter vectors generate an average 30-50% reduction in expression of a target miRNA after transfection with miRNA mimics. These systems are often optimized for detection by incorporation of multiple copies of the MRE (miRNA recognition element) within the reporter construct. Such a relatively modest attenuation in target expression in an optimized setting may translate into a difficult to discern target reduction in unaltered cells where the chance for crosstalk between complex cellular pathways exists. To evaluate the potential miRNA-target relationship between miR-143 and CDC6 additional experiments will be needed.

Another interesting result from initial experiments was the observation that while miR-155 is down-regulated significantly (10-fold) during senescence, it is up-regulated significantly over time in BJ-hTERT cells. MiR-155 is a pro-proliferative, proto-oncogenic [119,134,168] miRNA whose expression is induced by inflammation [169,170]. Suppressor of cytokine signaling 1 (SOCS1) is a validated target of miR-155 relevant to miR-155 induced oncogenesis [169]. In addition, it has been shown that SOCS family enzymes are essential for fibroblast ability to undergo G1 arrest [171,172]. However, this is the first evidence of miR-155 regulation as a result of TERT expression. Based on this

result and the ability of TERT to influence miR-143 mediated growth arrest during senescence, I hypothesize that TERT expression in a somatic, post-mitotic cell line influences expression of various proliferation-associated miRNAs, potentially via inflammatory signaling including Wnt and/or AP-1 (Figure 4.7).

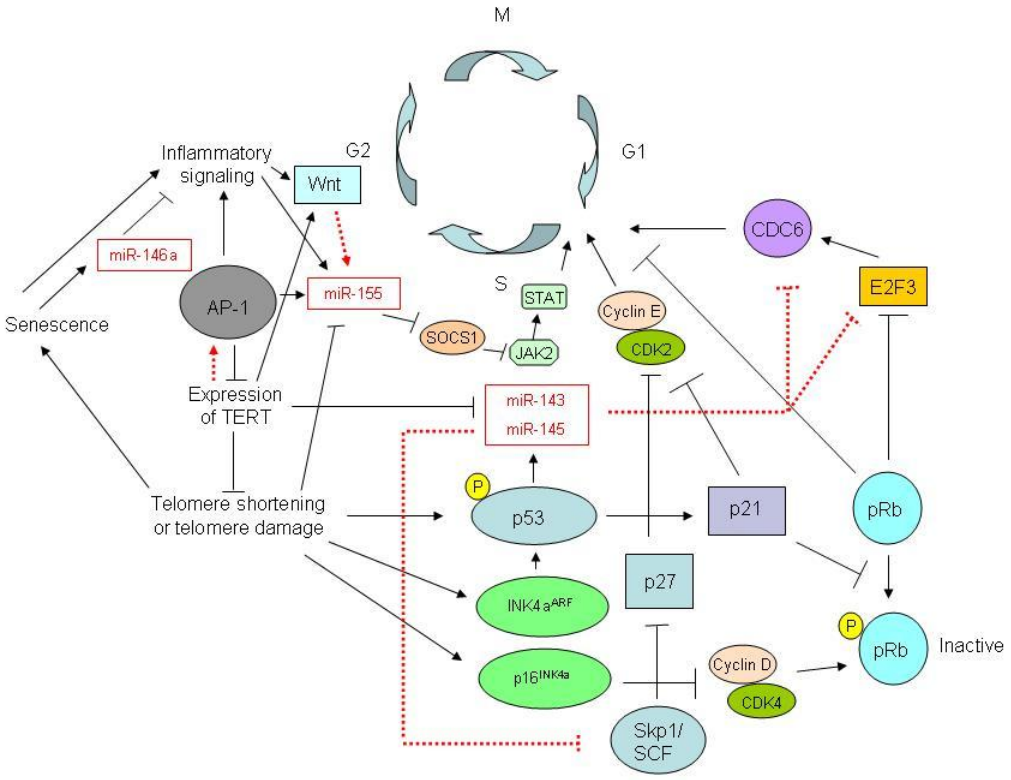

Figure 4.7 TERT affects expression of miRNAs mediating senescence and proliferation. Hypotheses based on data from experiments described in this chapter are indicated by red lines. Known relationships between pathway effectors are denoted with black lines.

IV. Future Directions for miR-143 CDC6 miRNA-target validation and revealing TERT effects on senescence and tumorigenesis-associated miRNA expression

I have designed a reporter construct to reveal the ability of miR-143 to regulate CDC6 expression via recognition of the predicted CDC6 3'UTR MRE. The construct bears two copies of the purported CDC6 3'UTR MRE in the 3'UTR of the firefly luciferase gene. To discern how TERT affects miR-143 and miR-145 expression, one should test the effects of expressing a catalytically inert TERT on miRNA expression and measure levels of pri-, pre-, and mature miR-143 and miR-145 in BJ-hTERT cells. Additionally, it would be interesting to incorporate various cell lines into these experiments to determine to what extent these pathways can be generalized or are cell type specific.

V. Methods

A. Cell Culture.

Human BJ foreskin fibroblasts (ATCC) were cultured at 37 °C in a 5% CO_2 incubator in MEMα supplemented with 1mM sodium pyruvate, 1.5 g/L sodium bicarbonate, and 10% fetal bovine serum. NHF1-hTERT, NHF1-hTERT CDC6Δ, and NHF1-hTERT CDC6ΔS3D cells (gifts from the Jean Cook lab at UNC-CH) were cultured in DMEM supplemented with 10% FBS and 2mM glutamine.

B. Transient transfection with miRNA mimics and SRB assay.

BJ WT cells at population doubling number 5 or early passage NHF1 cells were transfected with 60nM miR-143 mimic or negative control miRNA mimic (Dharmacon miRIDIAN mimics) for 6 hours in Opti-MEMI in the presence of

3µg/ml Lipofectamine 2000. After 6 hours, media was changed to normal BJ or NHF1 media without antibiotic. The sulforhodamine B assay was utilized as described in detail in Kirtikara et al [173] to determine effects of miR-143 on growth of early passage BJ cells. SRB assays were performed 72 hours after transfection. One way ANOVA was used to analyze the significance of variance between cell types from separate experiments, each performed in octuplet.

C. Senescence-associated β-galactosidase staining.

Cell staining was performed using a kit from Cell Signaling Technology with samples grown in a 6-well plate. After removing growth medium from the cells, the cells were washed with PBS and fixed for 15 minutes at room temperature. The cells were then washed twice with PBS and stained with X-gal staining solution overnight at 37 °C following the manufacturer's protocol.

D. miRNA Target Prediction

Online target prediction algorithms TargetScan, Microcosm, and Pictar-Vert were accessed via miRBase to predict targets of miR-143, 145, and 155 [137,138,139]. RNA22, a database useful to predicting "non-canonical" miRNA-target matches, was accessed to assess likelihood of the miR-143/CDC6 target relationship [152]. Also, the coding region sequence of CDC6 was manually scanned for sequences complimentary to the miR-143 seed sequence.

E. Detection of CDC6 levels in cells with varied expression of miR-143

Western blotting was used to detect levels of CDC6 in early and late passage BJ WT, BJ-pBabe, and BJ-hTERT cells. Samples used for western blotting correspond to samples used for miRNA microarray and qRT-PCR studies. Lysis buffer stock (81.7 µl) containing 50 mM Tris-HCl (pH 7.6), 150 mM NaCl, and 1% Triton X-100 was supplemented with 14.3 µl of freshly prepared 7X Protease Inhibitor Cocktail (Roche) and 4 µl of 100X diluted β-mercaptoethanol. Cell pellets were incubated in 20-40 µl of lysis buffer at 4 °C for 30 minutes with rotation. Lysed pellets were then spun at 4 °C for 10 minutes at 13g. Supernatant was collected and aliquotted, and a 10X dilution was used to determine protein concentration by Bradford Assay (Pierce). 40 µg of each cell lysate was resolved on an 8% acrylamide SDS gel. SDS gels were run in 1X TrisGlycine running buffer at 115 volts for approximately 70 minutes. PVDF membrane from Immobilon-P blotting sandwiches (Milipore) was wetted with 100% MeOH for 1 minute, rinsed with water, then soaked with the included filter paper (and two additional pieces of extra thick filter paper) in transfer buffer. Gels were equilibrated in transfer buffer before being assembled into blotting sandwich. Resolved proteins were transferred to PVDF membrane using a BioRad Trans-Blot Semi-Dry Electrophoretic Transfer apparatus at 15 volts for 20 minutes using transfer buffer containing 390 mM glycine, 50 mM Tris base (do not adjust pH), and 20% MeOH. Transfer quality was assessed using Ponceau staining. Post-transfer, PVDF membrane was blocked with 5% milk in TBST (10 mM Tris pH 8.0, 150 mM NaCl, 0.2% Tween 20) for 30 minutes at room temperature (RT). Blots were probed for 2 hours at RT with 1:500 anti-CDC6

antibody (Santa Cruz 180.2, sc-9964) then washed three times for 5 minutes each with TBST. Blots were then probed with 1:1000 ECL peroxidase anti-mouse antibody (Amersham, NA931VS) to detect CDC6 and 1:2000 to detect β -actin for 1 hour at RT before being rinsed another three times with TBST. ECL Plus reagent (Pierce) was used to detect secondary antibody. Blots were stripped with 50 mM glycine (pH 2.4), 0.5 M NaCl, and 0.1% Igepal for 15 minutes at RT, rinsed once with H_2O, then "equilibrated" with 1-2 quick washes in PBS before probing for β-actin (Santa Cruz, sc-47778).

F. Construction of a dual luciferase reporter vector to validate miR-143/CDC6 miRNA target pair

The dual luciferase miRNA-target expression vector pmirGLO (Promega) was modified for these experiments. A construct was designed to validate the ability of miR-143 to regulate expression of CDC6 via recognition of the predicted (via TargetScan) target sequence in the 3'UTR of CDC6.

1. Oligomers

Single-stranded DNA oligos were obtained from IDT and annealed to create dsDNA bearing two copies of the predicted miR-143 seed recognition element from the CDC6 3'UTR. The oligos are designed to facilitate ligation into the pmirGLO vector by XbaI and SacI such that successful ligation will obliterate the XbaI recognition site. Oligo sequences are shown (nucleotides representing CDC6 3'UTR miR-143 seed complement are underlined):

5'-CAGAGCTACAGTCTTCATTTTAGTGCTTAGAGCTACAGTCTT

CATTTTAGTGCTTG-3’ and 5’-CTAGCAAGCACTAAAATGAAGAC

TGTAGCTCTAAGCACTAAAATGAAGACTGTAGCTCTGAGCT-3’

2. Annealing to create vector insert

The oligos shown above were each diluted to 1 µg/µl in Tris-EDTA (pH 7.6). 2 µg of each oligo was annealed in 46 µl Oligo Annealing Buffer (Promega) by heating to 90 °C for 3 minutes then transferring to a 37 °C water bath for 15 minutes.

3. Digestion of pmirGLO vector

5 µg pmirGLO vector was digested with 100 units XbaI (NEB) overnight at 37 °C in Buffer #4 (NEB) then heat inactivated at 95 °C for 3 minutes before digestion with 100 units SacI (NEB) for 5 hours at 37 °C. Both digestions were performed in the presence of and 100 µg/ml bovine serum albumin (BSA). SacI was heat inactivated then the digested plasmid was treated with shrimp alkaline phosphatase (SAP, Roche) at 37 °C for 1 hour to prevent religation. Proteins were removed from the solution by phenol/chloroform extraction. Linearized vector was concentrated by EtOH precipitation and resuspended in TE.

4. Ligation and Transformation

Four ligation reactions were assembled with varying amounts of cDNA (0 ng, 4 ng, 10 ng, and 50 ng). Ligation reactions contained 50 ng linearized pmirGLO, 1 µl of 10X T4 DNA ligase buffer (containing ATP), 10 units bacteriophage T4 DNA ligase, cDNA, and H_2O to a final volume of 10 µl and were completed at room temperature for 30 minutes. 1 µl of ligation reaction was used to transform

JM109 cells (Promega) and transformed cells were grown overnight on Amp plates. 10 colonies were used to inoculate 2-3 ml starter cultures from which the pmirGLO vector was purified using QiaPrep Spin Miniprep (Qiagen). Purified vectors were screened for successful ligation by digestion with XbaI and NotI in buffer #3 (NEB) overnight at 37 °C. Resolution of a successfully ligated vector should yield 1 product on an agarose gel since NotI cleaves at position 93 in the pmirGLO vector and ligation of the insert obliterated the XbaI cleavage site. This construct was designed to be used with the Dual-GLO Luciferase Assay System (Promega).

References

1. Hayflick L (1965) The Limited in Vitro Lifetime of Human Diploid Cell Strains. Exp Cell Res 37: 614-636.

2. Watson JD (1972) Origin of concatemeric T7 DNA. Nat New Biol 239: 197-201.

3. Van Zant G, Liang Y (2003) The role of stem cells in aging. Exp Hematol 31: 659-672.

4. Wellinger RJ, Ethier K, Labrecque P, Zakian VA (1996) Evidence for a new step in telomere maintenance. Cell 85: 423-433.

5. Dionne I, Wellinger RJ (1996) Cell cycle-regulated generation of single-stranded G-rich DNA in the absence of telomerase. Proc Natl Acad Sci U S A 93: 13902-13907.

6. Vega LR, Mateyak MK, Zakian VA (2003) Getting to the end: telomerase access in yeast and humans. Nat Rev Mol Cell Biol 4: 948-959.

7. Karlseder J, Broccoli D, Dai Y, Hardy S, de Lange T (1999) p53- and ATM-dependent apoptosis induced by telomeres lacking TRF2. Science 283: 1321-1325.

8. McClintock B (1941) The Stability of Broken Ends of Chromosomes in Zea Mays. Genetics 26: 234-282.

9. Griffith JD, Comeau L, Rosenfield S, Stansel RM, Bianchi A, et al. (1999) Mammalian telomeres end in a large duplex loop. Cell 97: 503-514.

10. van Steensel B, de Lange T (1997) Control of telomere length by the human telomeric protein TRF1. Nature 385: 740-743.

11. Wotton D, Shore D (1997) A novel Rap1p-interacting factor, Rif2p, cooperates with Rif1p to regulate telomere length in Saccharomyces cerevisiae. Genes Dev 11: 748-760.

12. Kelleher C, Kurth I, Lingner J (2005) Human protection of telomeres 1 (POT1) is a negative regulator of telomerase activity in vitro. Mol Cell Biol 25: 808-818.

13. Hardy CF, Sussel L, Shore D (1992) A RAP1-interacting protein involved in transcriptional silencing and telomere length regulation. Genes Dev 6: 801-814.

14. Calado RT, Young NS (2008) Telomere maintenance and human bone marrow failure. Blood 111: 4446-4455.

15. Kirwan M, Dokal I (2009) Dyskeratosis congenita, stem cells and telomeres. Biochim Biophys Acta 1792: 371-379.

16. Heiss NS, Knight SW, Vulliamy TJ, Klauck SM, Wiemann S, et al. (1998) X-linked dyskeratosis congenita is caused by mutations in a highly conserved gene with putative nucleolar functions. Nat Genet 19: 32-38.

17. Knight SW, Heiss NS, Vulliamy TJ, Greschner S, Stavrides G, et al. (1999) X-linked dyskeratosis congenita is predominantly caused by missense mutations in the DKC1 gene. Am J Hum Genet 65: 50-58.

18. Crabbe L, Verdun RE, Haggblom CI, Karlseder J (2004) Defective telomere lagging strand synthesis in cells lacking WRN helicase activity. Science 306: 1951-1953.

19. De Lange T (2005) Telomere-related genome instability in cancer. Cold Spring Harb Symp Quant Biol 70: 197-204.

20. de Lange T (2002) Protection of mammalian telomeres. Oncogene 21: 532-540.

21. Calado RT, Regal JA, Hills M, Yewdell WT, Dalmazzo LF, et al. (2009) Constitutional hypomorphic telomerase mutations in patients with acute myeloid leukemia. Proc Natl Acad Sci U S A 106: 1187-1192.

22. Tsakiri KD, Cronkhite JT, Kuan PJ, Xing C, Raghu G, et al. (2007) Adult-onset pulmonary fibrosis caused by mutations in telomerase. Proc Natl Acad Sci U S A 104: 7552-7557.

23. Chen J-L, Blasco MA, Greider CW (2000) Secondary structure of vertebrate telomerase RNA. Cell 100: 503-514.

24. Zappulla DC, Goodrich K, Cech TR (2005) A miniature yeast telomerase RNA functions in vivo and reconstitutes activity in vitro. Nat Struct Mol Biol 12: 1072-1077.

25. Lingner J, Hughes TR, Shevchenko A, Mann M, Lundblad V, et al. (1997) Reverse transcriptase motifs in the catalytic subunit of telomerase. Science 276: 561-567.

26. Sykorova E, Fajkus J (2009) Structure-function relationships in telomerase genes. Biol Cell 101: 375-392, 371 p following 392.

27. Gillis AJ, Schuller AP, Skordalakes E (2008) Structure of the Tribolium castaneum telomerase catalytic subunit TERT. Nature 455: 633-637.

28. Peng Y, Mian IS, Lue NF (2001) Analysis of telomerase processivity: mechanistic similarity to HIV-1 reverse transcriptase and role in telomere maintenance. Molecular Cell 7: 1201-1211.

29. Huard S, Moriarty TJ, Autexier C (2003) The C terminus of the human telomerase reverse transcriptase is a determinant of enzyme processivity. Nucleic Acids Res 31: 4059-4070.

30. Lue NF (2004) Adding to the ends: what makes telomerase processive and how important is it? Bioessays 26: 955-962.

31. Legassie JD, Jarstfer MB (2006) The unmasking of telomerase. Structure 14: 1603-1609.

32. Chen JL, Greider CW (2004) An emerging consensus for telomerase RNA structure. Proc Natl Acad Sci U S A 101: 14683-14684.

33. Richards RJ, Theimer CA, Finger LD, Feigon J (2006) Structure of the Tetrahymena thermophila telomerase RNA helix II template boundary element. Nucleic Acids Res 34: 816-825.

34. Richards RJ, Wu H, Trantirek L, O'Connor C M, Collins K, et al. (2006) Structural study of elements of Tetrahymena telomerase RNA stem-loop IV domain important for function. RNA 12: 1475-1485.

35. Chen Y, Fender J, Legassie JD, Jarstfer MB, Bryan TM, et al. (2006) Structure of stem-loop IV of Tetrahymena telomerase RNA. EMBO J 25: 3156-3166.

36. Sperger JM, Cech TR (2001) A stem-loop of *Tetrahymena* telomerase RNA distant from the template potentiates RNA folding and telomerase activity. Biochemistry 40: 7005-7016.

37. Zaug AJ, Cech TR (1995) Analysis of the Structure of Tetrahymena Nuclear RNAs in vivo: Telomerase RNA, the Self-Splicing rRNA Intron, and U2 snRNA. RNA 1: 363-374.

38. Bhattacharyya A, Blackburn EH (1994) Architecture of telomerase RNA. EMBO J 13: 5721-5731.

39. Lai CK, Miller MC, Collins K (2002) Template boundary definition in Tetrahymena telomerase. Genes Dev 16: 415-420.

40. Lai CK, Miller MC, Collins K (2003) Roles for RNA in telomerase nucleotide and repeat addition processivity. Mol Cell 11: 1673-1683.

41. Mason DX, Goneska E, Greider CW (2003) Stem-loop IV of tetrahymena telomerase RNA stimulates processivity in trans. Mol Cell Biol 23: 5606-5613.

42. Ulyanov NB, Shefer K, James TL, Tzfati Y (2007) Pseudoknot structures with conserved base triples in telomerase RNAs of ciliates. Nucleic Acids Res 35: 6150-6160.

43. Theimer CA, Blois CA, Feigon J (2005) Structure of the human telomerase RNA pseudoknot reveals conserved tertiary interactions essential for function. Mol Cell 17: 671-682.

44. Comolli LR, Smirnov I, Xu L, Blackburn EH, James TL (2002) A molecular switch underlies a human telomerase disease. Proc Natl Acad Sci U S A 99: 16998-17003.

45. Harman D (1956) Aging: a theory based on free radical and radiation chemistry. J Gerontol 11: 298-300.

46. Tian L, Cai Q, Wei H (1998) Alterations of antioxidant enzymes and oxidative damage to macromolecules in different organs of rats during aging. Free Radic Biol Med 24: 1477-1484.

47. Jayakumar T, Thomas PA, Geraldine P (2007) Protective effect of an extract of the oyster mushroom, Pleurotus ostreatus, on antioxidants of major organs of aged rats. Exp Gerontol 42: 183-191.

48. Wong YT, Ruan R, Tay FE (2006) Relationship between levels of oxidative DNA damage, lipid peroxidation and mitochondrial membrane potential in young and old F344 rats. Free Radic Res 40: 393-402.

49. Hamilton ML, Van Remmen H, Drake JA, Yang H, Guo ZM, et al. (2001) Does oxidative damage to DNA increase with age? Proc Natl Acad Sci U S A 98: 10469-10474.

50. Gravina S, Vijg J (2010) Epigenetic factors in aging and longevity. Pflugers Arch 459: 247-258.

51. Meissner A, Mikkelsen TS, Gu H, Wernig M, Hanna J, et al. (2008) Genome-scale DNA methylation maps of pluripotent and differentiated cells. Nature 454: 766-770.

52. Teschendorff AE, Menon U, Gentry-Maharaj A, Ramus SJ, Weisenberger DJ, et al. (2010) Age-dependent DNA methylation of genes that are suppressed in stem cells is a hallmark of cancer. Genome Res 20: 440-446.

53. Ohm JE, McGarvey KM, Yu X, Cheng L, Schuebel KE, et al. (2007) A stem cell-like chromatin pattern may predispose tumor suppressor genes to DNA hypermethylation and heritable silencing. Nat Genet 39: 237-242.

54. Liang R, Bates DJ, Wang E (2009) Epigenetic Control of MicroRNA Expression and Aging. Curr Genomics 10: 184-193.

55. Kirkwood TB, Austad SN (2000) Why do we age? Nature 408: 233-238.

56. Longo DL (2009) Telomere dynamics in aging: much ado about nothing? J Gerontol A Biol Sci Med Sci 64: 963-964.

57. Mollica L, Fleury I, Belisle C, Provost S, Roy DC, et al. (2009) No association between telomere length and blood cell counts in elderly individuals. J Gerontol A Biol Sci Med Sci 64: 965-967.

58. Imanishi T, Tsujioka H, Akasaka T (2010) Endothelial progenitor cell senescence--is there a role for estrogen? Ther Adv Cardiovasc Dis 4: 55-69.

59. Ogden DA, Mickliem HS (1976) The fate of serially transplanted bone marrow cell populations from young and old donors. Transplantation 22: 287-293.

60. Cesare AJ, Reddel RR (2010) Alternative lengthening of telomeres: models, mechanisms and implications. Nat Rev Genet 11: 319-330.

61. Serrano M, Lin AW, McCurrach ME, Beach D, Lowe SW (1997) Oncogenic ras provokes premature cell senescence associated with accumulation of p53 and p16INK4a. Cell 88: 593-602.

62. Xue W, Zender L, Miething C, Dickins RA, Hernando E, et al. (2007) Senescence and tumour clearance is triggered by p53 restoration in murine liver carcinomas. Nature 445: 656-660.

63. Fridman AL, Tainsky MA (2008) Critical pathways in cellular senescence and immortalization revealed by gene expression profiling. Oncogene 27: 5975-5987.

64. Campisi J, Yaswen P (2009) Aging and cancer cell biology, 2009. Aging Cell 8: 221-225.

65. Chen Z, Trotman LC, Shaffer D, Lin HK, Dotan ZA, et al. (2005) Crucial role of p53-dependent cellular senescence in suppression of Pten-deficient tumorigenesis. Nature 436: 725-730.

66. Campisi J, Sedivy J (2009) How does proliferative homeostasis change with age? What causes it and how does it contribute to aging? J Gerontol A Biol Sci Med Sci 64: 164-166.

67. Dimri GP, Itahana K, Acosta M, Campisi J (2000) Regulation of a senescence checkpoint response by the E2F1 transcription factor and p14(ARF) tumor suppressor. Mol Cell Biol 20: 273-285.

68. Krizhanovsky V, Xue W, Zender L, Yon M, Hernando E, et al. (2008) Implications of cellular senescence in tissue damage response, tumor suppression, and stem cell biology. Cold Spring Harb Symp Quant Biol 73: 513-522.

69. Takai H, Smogorzewska A, de Lange T (2003) DNA damage foci at dysfunctional telomeres. Curr Biol 13: 1549-1556.

70. d'Adda di Fagagna F, Reaper PM, Clay-Farrace L, Fiegler H, Carr P, et al. (2003) A DNA damage checkpoint response in telomere-initiated senescence. Nature 426: 194-198.

71. Hara E, Tsurui H, Shinozaki A, Nakada S, Oda K (1991) Cooperative effect of antisense-Rb and antisense-p53 oligomers on the extension of life span in human diploid fibroblasts, TIG-1. Biochem Biophys Res Commun 179: 528-534.

72. Shay JW, Pereira-Smith OM, Wright WE (1991) A role for both RB and p53 in the regulation of human cellular senescence. Exp Cell Res 196: 33-39.

73. Brenner AJ, Stampfer MR, Aldaz CM (1998) Increased p16 expression with first senescence arrest in human mammary epithelial cells and extended growth capacity with p16 inactivation. Oncogene 17: 199-205.

74. Alcorta DA, Xiong Y, Phelps D, Hannon G, Beach D, et al. (1996) Involvement of the cyclin-dependent kinase inhibitor p16 (INK4a) in replicative senescence of normal human fibroblasts. Proc Natl Acad Sci U S A 93: 13742-13747.

75. Lin HK, Chen Z, Wang G, Nardella C, Lee SW, et al. (2010) Skp2 targeting suppresses tumorigenesis by Arf-p53-independent cellular senescence. Nature 464: 374-379.

76. Beausejour CM, Krtolica A, Galimi F, Narita M, Lowe SW, et al. (2003) Reversal of human cellular senescence: roles of the p53 and p16 pathways. EMBO J 22: 4212-4222.

77. Fire A, Xu S, Montgomery MK, Kostas SA, Driver SE, et al. (1998) Potent and specific genetic interference by double-stranded RNA in Caenorhabditis elegans. Nature 391: 806-811.

78. Tay Y, Zhang J, Thomson AM, Lim B, Rigoutsos I (2008) MicroRNAs to Nanog, Oct4 and Sox2 coding regions modulate embryonic stem cell differentiation. Nature 455: 1124-1128.

79. Forman JJ, Legesse-Miller A, Coller HA (2008) A search for conserved sequences in coding regions reveals that the let-7 microRNA targets Dicer within its coding sequence. Proc Natl Acad Sci U S A 105: 14879-14884.

80. Ko HY, Lee DS, Kim S (2009) Noninvasive imaging of microRNA124a-mediated repression of the chromosome 14 ORF 24 gene during neurogenesis. FEBS J 276: 4854-4865.

81. Lee I, Ajay SS, Yook JI, Kim HS, Hong SH, et al. (2009) New class of microRNA targets containing simultaneous 5'-UTR and 3'-UTR interaction sites. Genome Res 19: 1175-1183.

82. Winter J, Jung S, Keller S, Gregory RI, Diederichs S (2009) Many roads to maturity: microRNA biogenesis pathways and their regulation. Nat Cell Biol 11: 228-234.

83. Bartel DP (2004) MicroRNAs: genomics, biogenesis, mechanism, and function. Cell 116: 281-297.

84. Bartel B, Bartel DP (2003) MicroRNAs: at the root of plant development? Plant Physiol 132: 709-717.

85. Maes OC, An J, Sarojini H, Wang E (2008) Murine microRNAs implicated in liver functions and aging process. Mech Ageing Dev 129: 534-541.

86. Ibanez-Ventoso C, Driscoll M (2009) MicroRNAs in C. elegans Aging: Molecular Insurance for Robustness? Curr Genomics 10: 144-153.

87. He L, He X, Lim LP, de Stanchina E, Xuan Z, et al. (2007) A microRNA component of the p53 tumour suppressor network. Nature 447: 1130-1134.

88. Raver-Shapira N, Marciano E, Meiri E, Spector Y, Rosenfeld N, et al. (2007) Transcriptional activation of miR-34a contributes to p53-mediated apoptosis. Mol Cell 26: 731-743.

89. Chang TC, Wentzel EA, Kent OA, Ramachandran K, Mullendore M, et al. (2007) Transactivation of miR-34a by p53 broadly influences gene expression and promotes apoptosis. Mol Cell 26: 745-752.

90. Tarasov V, Jung P, Verdoodt B, Lodygin D, Epanchintsev A, et al. (2007) Differential regulation of microRNAs by p53 revealed by massively parallel sequencing: miR-34a is a p53 target that induces apoptosis and G1-arrest. Cell Cycle 6: 1586-1593.

91. Tazawa H, Tsuchiya N, Izumiya M, Nakagama H (2007) Tumor-suppressive miR-34a induces senescence-like growth arrest through modulation of the E2F pathway in human colon cancer cells. Proc Natl Acad Sci U S A 104: 15472-15477.

92. Maes OC, Sarojini H, Wang E (2009) Stepwise up-regulation of MicroRNA expression levels from replicating to reversible and irreversible growth arrest states in WI-38 human fibroblasts. J Cell Physiol.

93. Benetti R, Gonzalo S, Jaco I, Munoz P, Gonzalez S, et al. (2008) A mammalian microRNA cluster controls DNA methylation and telomere recombination via Rbl2-dependent regulation of DNA methyltransferases. Nat Struct Mol Biol 15: 998.

94. Sahin E, Depinho RA (2010) Linking functional decline of telomeres, mitochondria and stem cells during ageing. Nature 464: 520-528.

95. Zimmermann S, Martens UM (2008) Telomeres, senescence, and hematopoietic stem cells. Cell Tissue Res 331: 79-90.

96. Mattson MP, Fu W, Zhang P (2001) Emerging roles for telomerase in regulating cell differentiation and survival: a neuroscientist's perspective. Mech Ageing Dev 122: 659-671.

97. Belgiovine C, Chiodi I, Mondello C (2008) Telomerase: cellular immortalization and neoplastic transformation. Multiple functions of a multifaceted complex. Cytogenet Genome Res 122: 255-262.

98. Artandi SE, DePinho RA (2010) Telomeres and telomerase in cancer. Carcinogenesis 31: 9-18.

99. Blasco MA (2002) Telomerase beyond telomeres. Nat Rev Cancer 2: 627-633.

100. Beliveau A, Yaswen P (2007) Soothing the watchman: telomerase reduces the p53-dependent cellular stress response. Cell Cycle 6: 1284-1287.

101. Watson JM, Riha K (2010) Telomeres, Aging, and Plants: From Weeds to Methuselah - A Mini-Review. Gerontology.

102. Linger BR, Price CM (2009) Conservation of telomere protein complexes: shuffling through evolution. Crit Rev Biochem Mol Biol 44: 434-446.

103. Autexier C, Lue NF (2006) The Structure and Function of Telomerase Reverse Transcriptase. Annu Rev Biochem 75: 493-517.

104. Wilkinson KA, Merino EJ, Weeks KM (2006) Selective 2'-hydroxyl acylation analyzed by primer extension (SHAPE): quantitative RNA structure analysis at single nucleotide resolution. Nat Protoc 1: 1610-1616.

105. Legassie JD, Jarstfer MB (2005) Telomerase as a DNA-dependent DNA polymerase. Biochemistry 44: 14191-14201.

106. Romero DP, Blackburn EH (1991) A conserved secondary structure for telomerase RNA. Cell 67: 343-353.

107. Qiao F, Cech TR (2008) Triple-helix structure in telomerase RNA contributes to catalysis. Nat Struct Mol Biol 15: 634-640.

108. Gilley D, Blackburn EH (1999) The telomerase RNA pseudoknot is critical for the stable assembly of a catalytically active ribonucleoprotein. Proceedings of the National Academy of Science USA 96: 6621-6625.

109. Zheng L, Baumann U, Reymond JL (2004) An efficient one-step site-directed and site-saturation mutagenesis protocol. Nucleic Acids Res 32: e115.

110. Maxam AM, Gilbert W (1977) A new method for sequencing DNA. Proc Natl Acad Sci U S A 74: 560-564.

111. Das R, Laederach A, Pearlman SM, Herschlag D, Altman RB (2005) SAFA: semi-automated footprinting analysis software for high-throughput quantification of nucleic acid footprinting experiments. RNA 11: 344-354.

112. Forrest AR, Kanamori-Katayama M, Tomaru Y, Lassmann T, Ninomiya N, et al. (2010) Induction of microRNAs, mir-155, mir-222, mir-424 and mir-503, promotes monocytic differentiation through combinatorial regulation. Leukemia 24: 460-466.

113. Zhao T, Li J, Chen AF (2010) MicroRNA-34a induces endothelial progenitor cell senescence and impedes its angiogenesis via suppressing silent information regulator 1. Am J Physiol Endocrinol Metab.

114. Fujita K, Mondal AM, Horikawa I, Nguyen GH, Kumamoto K, et al. (2009) p53 isoforms Delta133p53 and p53beta are endogenous regulators of replicative cellular senescence. Nat Cell Biol 11: 1135-1142.

115. Christoffersen NR, Shalgi R, Frankel LB, Leucci E, Lees M, et al. (2010) p53-independent upregulation of miR-34a during oncogene-induced senescence represses MYC. Cell Death Differ 17: 236-245.

116. Bhaumik D, Scott GK, Schokrpur S, Patil CK, Orjalo AV, et al. (2009) MicroRNAs miR-146a/b negatively modulate the senescence-associated inflammatory mediators IL-6 and IL. Aging (Albany NY) 1: 402-411.

117. Li G, Luna C, Qiu J, Epstein DL, Gonzalez P (2010) Modulation of inflammatory markers by miR-146a during replicative senescence in trabecular meshwork cells. Invest Ophthalmol Vis Sci 51: 2976-2985.

118. Costinean S, Zanesi N, Pekarsky Y, Tili E, Volinia S, et al. (2006) Pre-B cell proliferation and lymphoblastic leukemia/high-grade lymphoma in E(mu)-miR155 transgenic mice. Proc Natl Acad Sci U S A 103: 7024-7029.

119. Eis PS, Tam W, Sun L, Chadburn A, Li Z, et al. (2005) Accumulation of miR-155 and BIC RNA in human B cell lymphomas. Proc Natl Acad Sci U S A 102: 3627-3632.

120. Brosh R, Shalgi R, Liran A, Landan G, Korotayev K, et al. (2008) p53-Repressed miRNAs are involved with E2F in a feed-forward loop promoting proliferation. Mol Syst Biol 4: 229.

121. Hooten NN, Abdelmohsen K, Gorospe M, Ejiogu N, Zonderman AB, et al. (2010) Expression Patterns Reveal Differential Expression of Target Genes with Age. PLoS ONE 5: e10724.

122. Ma L, Reinhardt F, Pan E, Soutschek J, Bhat B, et al. (2010) Therapeutic silencing of miR-10b inhibits metastasis in a mouse mammary tumor model. Nat Biotechnol 28: 341-347.

123. Tian Y, Luo A, Cai Y, Su Q, Ding F, et al. (2010) MicroRNA-10b promotes migration and invasion through KLF4 in human esophageal cancer cell lines. J Biol Chem 285: 7986-7994.

124. Akao Y, Nakagawa Y, Hirata I, Iio A, Itoh T, et al. (2010) Role of anti-oncomirs miR-143 and -145 in human colorectal tumors. Cancer Gene Ther 17: 398-408.

125. Chhabra R, Adlakha YK, Hariharan M, Scaria V, Saini N (2009) Upregulation of miR-23a-27a-24-2 cluster induces caspase-dependent and -independent apoptosis in human embryonic kidney cells. PLoS ONE 4: e5848.

126. He X, He L, Hannon GJ (2007) The guardian's little helper: microRNAs in the p53 tumor suppressor network. Cancer Res 67: 11099-11101.

127. Lafferty-Whyte K, Cairney CJ, Jamieson NB, Oien KA, Keith WN (2009) Pathway analysis of senescence-associated miRNA targets reveals common processes to different senescence induction mechanisms. Biochim Biophys Acta 1792: 341-352.

128. Rakyan VK, Down TA, Maslau S, Andrew T, Yang TP, et al. (2010) Human aging-associated DNA hypermethylation occurs preferentially at bivalent chromatin domains. Genome Res 20: 434-439.

129. Liu Q, Fu H, Sun F, Zhang H, Tie Y, et al. (2008) miR-16 family induces cell cycle arrest by regulating multiple cell cycle genes. Nucleic Acids Res 36: 5391-5404.

130. Akao Y, Nakagawa Y, Naoe T (2006) MicroRNAs 143 and 145 are possible common onco-microRNAs in human cancers. Oncol Rep 16: 845-850.

131. Pereira CP, Bachli EB, Schoedon G (2009) The wnt pathway: a macrophage effector molecule that triggers inflammation. Curr Atheroscler Rep 11: 236-242.

132. Katoh M (2002) Molecular cloning and characterization of ST7R (ST7-like, ST7L) on human chromosome 1p13, a novel gene homologous to tumor suppressor gene ST7 on human chromosome 7q31. Int J Oncol 20: 1247-1253.

133. Park JI, Venteicher AS, Hong JY, Choi J, Jun S, et al. (2009) Telomerase modulates Wnt signalling by association with target gene chromatin. Nature 460: 66-72.

134. Faraoni I, Antonetti FR, Cardone J, Bonmassar E (2009) miR-155 gene: a typical multifunctional microRNA. Biochim Biophys Acta 1792: 497-505.

135. Yin Q, Wang X, McBride J, Fewell C, Flemington E (2008) B-cell receptor activation induces BIC/miR-155 expression through a conserved AP-1 element. J Biol Chem 283: 2654-2662.

136. Takakura M, Kyo S, Inoue M, Wright WE, Shay JW (2005) Function of AP-1 in transcription of the telomerase reverse transcriptase gene (TERT) in human and mouse cells. Mol Cell Biol 25: 8037-8043.

137. Griffiths-Jones S (2004) The microRNA Registry. Nucleic Acids Res 32: D109-111.

138. Griffiths-Jones S, Grocock RJ, van Dongen S, Bateman A, Enright AJ (2006) miRBase: microRNA sequences, targets and gene nomenclature. Nucleic Acids Res 34: D140-144.

139. Griffiths-Jones S, Saini HK, van Dongen S, Enright AJ (2008) miRBase: tools for microRNA genomics. Nucleic Acids Res 36: D154-158.

140. Lewis BP, Burge CB, Bartel DP (2005) Conserved seed pairing, often flanked by adenosines, indicates that thousands of human genes are microRNA targets. Cell 120: 15-20.

141. Ng EK, Tsang WP, Ng SS, Jin HC, Yu J, et al. (2009) MicroRNA-143 targets DNA methyltransferases 3A in colorectal cancer. Br J Cancer 101: 699-706.

142. Chen X, Guo X, Zhang H, Xiang Y, Chen J, et al. (2009) Role of miR-143 targeting KRAS in colorectal tumorigenesis. Oncogene 28: 1385-1392.

143. La Rocca G, Badin M, Shi B, Xu SQ, Deangelis T, et al. (2009) Mechanism of growth inhibition by MicroRNA 145: the role of the IGF-I receptor signaling pathway. J Cell Physiol 220: 485-491.

144. Shi B, Sepp-Lorenzino L, Prisco M, Linsley P, deAngelis T, et al. (2007) Micro RNA 145 targets the insulin receptor substrate-1 and inhibits the growth of colon cancer cells. J Biol Chem 282: 32582-32590.

145. Sachdeva M, Mo YY (2010) miR-145-mediated suppression of cell growth, invasion and metastasis. Am J Transl Res 2: 170-180.

146. Pelizon C (2003) Down to the origin: Cdc6 protein and the competence to replicate. Trends Cell Biol 13: 110-113.

147. Xu D, Landon T, Greenbaum NL, Fenley MO (2007) The electrostatic characteristics of G.U wobble base pairs. Nucleic Acids Res 35: 3836-3847.

148. Lee RC, Feinbaum RL, Ambros V (1993) The C. elegans heterochronic gene lin-4 encodes small RNAs with antisense complementarity to lin-14. Cell 75: 843-854.

149. Wightman B, Ha I, Ruvkun G (1993) Posttranscriptional regulation of the heterochronic gene lin-14 by lin-4 mediates temporal pattern formation in C. elegans. Cell 75: 855-862.

150. Qin W, Shi Y, Zhao B, Yao C, Jin L, et al. (2010) miR-24 regulates apoptosis by targeting the open reading frame (ORF) region of FAF1 in cancer cells. PLoS ONE 5: e9429.

151. Rigoutsos I (2009) New tricks for animal microRNAS: targeting of amino acid coding regions at conserved and nonconserved sites. Cancer Res 69: 3245-3248.

152. Miranda KC, Huynh T, Tay Y, Ang YS, Tam WL, et al. (2006) A pattern-based method for the identification of MicroRNA binding sites and their corresponding heteroduplexes. Cell 126: 1203-1217.

153. Hall JR, Kow E, Nevis KR, Lu CK, Luce KS, et al. (2007) Cdc6 stability is regulated by the Huwe1 ubiquitin ligase after DNA damage. Mol Biol Cell 18: 3340-3350.

154. Boehm M, Slack F (2005) A developmental timing microRNA and its target regulate life span in C. elegans. Science 310: 1954-1957.

155. Boehm M, Slack FJ (2006) MicroRNA control of lifespan and metabolism. Cell Cycle 5: 837-840.

156. Thai TH, Calado DP, Casola S, Ansel KM, Xiao C, et al. (2007) Regulation of the germinal center response by microRNA-155. Science 316: 604-608.

157. Liu SP, Fu RH, Yu HH, Li KW, Tsai CH, et al. (2009) MicroRNAs regulation modulated self-renewal and lineage differentiation of stem cells. Cell Transplant 18: 1039-1045.

158. Borgdorff V, Lleonart ME, Bishop CL, Fessart D, Bergin AH, et al. (2010) Multiple microRNAs rescue from Ras-induced senescence by inhibiting p21(Waf1/Cip1). Oncogene 29: 2262-2271.

159. Wagner W, Horn P, Castoldi M, Diehlmann A, Bork S, et al. (2008) Replicative senescence of mesenchymal stem cells: a continuous and organized process. PLoS ONE 3: e2213.

160. Noren Hooten N, Abdelmohsen K, Gorospe M, Ejiogu N, Zonderman AB, et al. (2010) microRNA expression patterns reveal differential expression of target genes with age. PLoS ONE 5: e10724.

161. Suzuki HI, Yamagata K, Sugimoto K, Iwamoto T, Kato S, et al. (2009) Modulation of microRNA processing by p53. Nature 460: 529-533.

162. Duursma A, Agami R (2005) p53-Dependent regulation of Cdc6 protein stability controls cellular proliferation. Mol Cell Biol 25: 6937-6947.

163. Nevis KR, Cordeiro-Stone M, Cook JG (2009) Origin licensing and p53 status regulate Cdk2 activity during G(1). Cell Cycle 8: 1952-1963.

164. Takahashi Y, Rayman JB, Dynlacht BD (2000) Analysis of promoter binding by the E2F and pRB families in vivo: distinct E2F proteins mediate activation and repression. Genes Dev 14: 804-816.

165. Humbert PO, Verona R, Trimarchi JM, Rogers C, Dandapani S, et al. (2000) E2f3 is critical for normal cellular proliferation. Genes Dev 14: 690-703.

166. Furstenthal L, Kaiser BK, Swanson C, Jackson PK (2001) Cyclin E uses Cdc6 as a chromatin-associated receptor required for DNA replication. J Cell Biol 152: 1267-1278.

167. Furstenthal L, Swanson C, Kaiser BK, Eldridge AG, Jackson PK (2001) Triggering ubiquitination of a CDK inhibitor at origins of DNA replication. Nat Cell Biol 3: 715-722.

168. Gueta K, Molotski N, Gerchikov N, Mor E, Savion S, et al. (2010) Teratogen-induced alterations in microRNA-34, microRNA-125b and

microRNA-155 expression: correlation with embryonic p53 genotype and limb phenotype. BMC Dev Biol 10: 20.

169. Jiang S, Zhang HW, Lu MH, He XH, Li Y, et al. (2010) MicroRNA-155 functions as an OncomiR in breast cancer by targeting the suppressor of cytokine signaling 1 gene. Cancer Res 70: 3119-3127.

170. Tili E, Croce CM, Michaille JJ (2009) miR-155: on the crosstalk between inflammation and cancer. Int Rev Immunol 28: 264-284.

171. Sitko JC, Yeh B, Kim M, Zhou H, Takaesu G, et al. (2008) SOCS3 regulates p21 expression and cell cycle arrest in response to DNA damage. Cell Signal 20: 2221-2230.

172. Walz C, Crowley BJ, Hudon HE, Gramlich JL, Neuberg DS, et al. (2006) Activated Jak2 with the V617F point mutation promotes G1/S phase transition. J Biol Chem 281: 18177-18183.

173. Vichai V, Kirtikara K (2006) Sulforhodamine B colorimetric assay for cytotoxicity screening. Nat Protoc 1: 1112-1116.